A STUDY ON THE ULTRASTRUCTURE AND CONTROL OF THE GLADIOLUS RUST PATHOGEN, *UROMYCES TRANSVERSALIS*

by

Johan Francois Ferreira

Submitted in partial fulfilment of the

requirements for the Ph.D. degree

in the

Department of Microbiology and Plant Pathology,

University of Natal

Pietermaritzburg

1988

ABSTRACT

The substomatal vesicle of *Uromyces transversalis* develops in five distinct stages after the formation of a single infection peg in the host plant *Gladiolus* spp. The primary hyphae of the substomatal vesicle orientate at right angles (rather than at acute angles or parallel) to the stomatal slit and the parallel veins of a gladiolus leaf or to those of the non-host, *Zea mays*. The transverse orientation of *Uromyces transversalis* uredia is apparently a genetically controlled phenomenon. The two primary hyphae normally develop asynchronously on opposite sides of the substomatal vesicle, and, after the formation of a haustorium mother cell, secondary hyphae branch off. These subsequently form basal cells each of which give rise to one or more holoblastic protruberances on its distal surface. A septum delimits the protruberance from the basal cell to form a urediospore initial, which in turn elongates and, by septum formation, forms a pedicel and a urediospore. The urediospore is seceded mechanically through the process of schizolysis. The pedicel of a spore thus formed remains on the basal cell and becomes a collar around the next protruberance. The basal layer of the two-layered septum, that delimited the pedicel from the basal cell, grows out to form the wall of the subsequent protruberance, in the process rupturing and laterally displacing the terminal septal layer. A new basipetal septum forms to delimit the subsequent urediospore initial. Therefore, successive urediospores are formed enteroblastically and give rise to a series of basipetal collars.

Cultivars, naturally occurring species and breeding lines of gladiolus were evaluated for rust resistance. The cultivars showed no sign of resistance, whereas the populations of wild species and breeding lines had similar resistance profiles. The species *G. daleni* and *G. tristis* var. *tristis* showed promise for breeding. Infection of these species caused an almost immune, fleck reaction. The resistance of the species *G. daleni* was manifested by the abortion of primary hyphae prior to the formation of the haustorial mother cell. The intercellular hyphae of gladiolus rust only partially adhered to the mesophyll cell of the resistant host. The haustorial apparatus that did form in the mesophyll cells in the

resistance reaction was inhibited at various stages of its development. The rust disease could be controlled chemically by either bitertanol or triadimefon. Triadimefon, however, caused a shortening of the internodes of the flower spike. The early development of *U. transversalis* infection structures in bitertanol-treated leaves was inhibited at, or shortly after, substomatal vesicle development. A number of mature substomatal vesicles with intercellular hyphae, however, did develop in the bitertanol-treated leaf tissue, probably because this fungicide undergoes limited translocation in the gladiolus lamina.

PREFACE

The experimental work described in this thesis was carried out in the the Pathology Section of the Vegetable and Ornamental Plant Research Institute, Pretoria, and the Department of Microbiology and Plant Pathology, University of Natal, Pietermaritzburg, from January 1983 to December 1988, under the supervision of Professor F.H.J. Rijkenberg.

Chapter 1 has been accepted for publication in Canadian Journal of Botany, accordingly the format of this Chapter and subsequent Chapters is that of Canadian Journal of Botany. Since each Chapter has been prepared as for journal submission, some repetition was unavoidable.

I hereby declare that these studies represent original work by the author and have not been submitted in any form to another University. Where use was made of the work of others it has been duly acknowledged in the text.

J.F. FERREIRA

ACKNOWLEDGEMENTS

1. Dr B.H. Boelema, V.O.P.R.I., my mentor, for his continued support and the critical reading of this manuscript, although he claimed to do but his duty.

2. Prof F.H.J. Rijkenberg for the many fruitful discussions when his time was limited, in particular during my stay in the Department, October 1986 to January 1987 and for the critical reading of this manuscript. I could not have wished for a better student / professor relationship.

3. Mr P.C. van der Merwe for the excellent technical assistance, given without reserve, during the long period over which this research was conducted.

4. The electron microscope units at the Plant Protection Research Institute, Pretoria, the Dept. Electron Microscopy, University of Pretoria, The Electron Microscope Unit, University of Natal, Pietermaritzburg, and, in particular, Mr H.J. van Tonder, Prof J. Coetzee and Mr A.G. Bruton.

5. Miss J. Wilkinson for the preparation of the line drawings and species description.

6. Mrs H.D. Johnson for the assisstance with the preparation of the final draft.

7. All others, who, consciously or unconsciously, contributed to this dissertation with their ideas, discussions and support.

8. The Department of Agriculture and Water Supply for the funding of facets GS 2433/19/5/1 and GS 2433/19/5/2, on which this dissertation is based.

Rust never sleeps.

- Neil Young.

Uromyces transversalis (Thümen) Winter nova spec. II. Uredo= Uredo transversalis. III. Uromyces. Acervulis cum iis formae uredinae consociatis plerumque densissime stipatis, minutis, punctiformibus, hemisphaericis v. ellipticis, saepe confluentibus, greges irregulares ve—l (rarius) transvers parum elongatas formantibus, epidermide cinerascente, pustulatim inflata longe tectis velastique. Sporidiis plerumque pyriformibus, rarius rotundatis vel ellipsoideis, apice incrassata, truncata, rotundata, vel conice attenuata, luteo-fuscis, laevibus, 21~31μ longis, 14~19μ crassis. Stipite longo, sed fragili, hyalino vel sursum perparum infuscato. In foliis vivis Tritoniae securigerae Ker. prope Somerset — East, Caput Bonae spei. Leg. Mac Owan.

Winter, G. 1884. Flora 67 : 263.

LIST OF CONTENTS

APPENDIX II :

CHAPTER 1

Development of Infection Structures of *Uromyces transversalis* in Leaves of the Host and a non-Host

ABSTRACT

Substomatal vesicle development of *Uromyces transversalis* on its host, gladiolus, was studied with a scanning electron microscope. Development after penetration occurred in distinct stages; the single infection peg developed into a globose immature substomatal vesicle, which initiated one or two primary hyphae that frequently developed asynchronously. Observed elongated primary hyphae delimited haustorial mother cells. Observations on the orientation of the long axis of the substomatal vesicle in relation to the stomatal slit showed development of the primary hyphae at right angles rather than acute angles or parallel. A similar trend was observed in the substomatal vesicle formed in a non-host, maize.

INTRODUCTION

Scanning electron microscopy has been successfully used for the study of germination behaviour of urediospores (Paliwal and Kim 1974, Staples *et al.* 1983, Staples *et al.* 1985, Wynn 1976). Very little information (Davies and Butler 1986, Hughes and Rijkenberg 1985) is available on the initiation and formation of the substomatal vesicle (SSV) and its subsequent development. Hughes and Rijkenberg (1985) studied the initiation and formation of the infection peg, the development of the SSV and the primary and secondary hyphae of *Puccinia sorghi* Schw. on maize. All observed substomatal vesicles were orientated with their long axes parallel to the stomatal slit and therefore to the leaf. In the present paper we report on the formation and orientation of the SSV of *Uromyces transversalis* (Thüm.) Winter, an important gladiolus pathogen (Viennott-Bourgin 1978), in the leaves of *Gladiolus* L. and a non-host, *Zea mays* L. In this article the terminology of Hughes and Rijkenberg (1985) is followed.

MATERIALS AND METHODS

Rust propagation and inoculation. Freshly harvested urediospores of *U. transversalis* (PREM 47693, National Collection of Fungi, Plant Protection Research Institute, Pretoria) produced on two-month-old susceptible gladiolus cv. Goldfield plants in a glasshouse (18°C - 35°C) were used to inoculate plants. For inoculation (Appendix I), spores were brushed over both surfaces of the distal third of mature gladiolus and maize leaves. Morphology and position of the gladiolus leaf preclude distinction between an ab- and adaxial surface. Maize leaves were inoculated abaxially. Inoculated plants were placed in a dew chamber (Appendix II) at 20°C for 24 h in the dark, and then moved to the glasshouse. The experiment was repeated twice with two gladiolus and two maize plants.

Specimen preparation. Four pieces per leaf from two leaves of each plant were taken at 12, 24, 48 and 96 h post-inoculation (HPI). The pieces were cut into 3 mm by 3 mm squares and fixed in 3% glutaraldehyde in a 0.05 M sodium cacodylate buffer, pH 6.8 - 7.2, for 12 h or overnight, washed twice in the buffer, post-fixed for 3 h in 2% osmium tetroxide in the buffer, washed twice in the buffer and dehydrated in a graded ethanol series. The leaf specimens were then critical point dried with carbon dioxide as a transition fluid and mounted on stubs. The epidermis of the gladiolus leaf specimens was removed manually with a pair of No. 5 Dumont forceps under a stereomicroscope and that of maize with the stub method. Two stubs, both coated with double-sided cellotape, one with a mounted specimen and the other without, were pressed together and then separated (Hughes 1983). The stripped epidermis and that of the tissue remaining on the stubs were gold/palladium coated in a Polaron® sputter coater. Both stripped epidermis and stripped leaf material were examined. Electron micrographs were taken with a Hitachi® S-570 or S-450 scanning electron microscope operating at either 5.0, 8.0 or 10.0 kV.

Data analysis. Chi-square tests (Siegel 1956) were used to test the hypothesis of equal frequency of the orientation of developing primary hyphae on the SSV in relation to the stomatal slit and to check for trends in the observations which would suggest an intrinsic tendency toward orientation on the non-host. Fischer's exact probability test (Siegel 1956) was necessary for non-host data, because low frequency of penetration of the stomata limited the availability of data (20 observations). Two data sets for orientation in the host were collected. The orientation (at right angles plus half turned or parallel) to the stomatal slit of developing primary hyphae on 62 SSVs in the host was observed and analyzed. Categoric observations on the orientation (at right angles or half turned or parallel) to the stomatal slit of 100 SSVs were made and the categories paired for further analysis.

RESULTS

In the results that follow, for a specific time HPI, the most advanced developmental stages are described.

Development of the substomatal vesicle. At 12 HPI, the SSVs were seen in an incipient development stage (Stage 1) where the tip of the infection peg was swollen to form a globose SSV initial (Fig. 1). The SSV position on the stomatal slit was often off-centre (Figs. 1 - 4). At 24 HPI, primary hyphae were initiated (Stage 2); these were formed either singly or two were formed (Fig. 2) on opposite sides of the SSV. Usually the development of the two lateral protrusions was asynchronous (Stage 3, Fig. 3). From 24 - 48 HPI the primary hypha (Fig. 4) delimited terminally a haustorial mother cell (HMC) (Stage 4) by septum formation. A septum was only seen in the primary hypha that elongated and not in the other primary hypha (Fig. 4). In Figure 4 the inset depicts a collapsed primary hypha which clearly shows the septum of the HMC. No detachment scar was observed on any of the HMCs which were not in contact with a host cell. The most

Scanning electron micrographs of substomatal *Uromyces transversalis* infection structures on the interior surface of the removed epidermis (Figs. 1 - 5) and in the mesophyll tissue after epidermis removal (Fig. 6).
Abbreviations: HMC, haustorial mother cell; I, interconnective tube; PH, primary hypha; SH, secondary hypha; S, septum; X, long axis of the stomatal slit; Y, long axis of the substomatal vesicle. Scale bar = 5 µm.

Fig. 1. Stomatal slit with substomatal vesicle initial and interconnective tube (I) - 12 HPI (hours post-inoculation).

Fig. 2. Young substomatal vesicle with primary hypha initials (arrows) - 12 HPI.

Fig. 3. Interconnective tube (I) and one developed primary hypha (PH) opposite to protrusion on substomatal vesicle - 24 HPI.

Fig. 4. Primary hypha with septum (S) having delimited haustorial mother cell (HMC). Inset depicting collapsed haustorial mother cell (HMC) with septum (S) - 48 HPI.

Fig. 5. Primary hypha (PH) terminating in haustorium mother cell (HMC) and secondary hypha (SH) branching off and extending beyond primary hypha - 48 HPI.

Fig. 6. Final stage substomatal vesicle with interconnective tube (I); primary hypha (PH) delimited into haustorial mother cell and septum (S); secondary hypha (SH) forms by branching off from primary hyphae (PH) - 96 HPI.


i
1
2
ph
i
3
hmc
s
hmc
s
4
sh
hmc
ph
5
X
sh
i
s
Y
ph
ph
sh
6

advanced stage (Stage 5) on the stripped epidermis was found at 48 HPI. The primary hypha that developed from the SSV had terminated in a haustorial mother cell and a secondary hypha had formed by branching off the primary hypha (Fig. 5).

After the SSV has differentiated, the tube between the appressorium and the SSV is referred to as an interconnective tube. Figure 6 shows a SSV in its final stage at 96 HPI with part of the interconnective tube visible and with developed primary and secondary hyphae. One primary hypha has formed a hemispherical HMC with a secondary hypha branching off between the HMC and SSV. A septum delimiting an HMC has formed in the opposite primary hypha, and a secondary hypha had arisen on the SSV-side of it. During the stripping of the tissue the guard cell leaves a scar adjacent to the interconnective tube (Fig. 8). Where stripping has been incomplete, as in Figure 9, a guard cell wall remnant has remained attached to the SSV, and, above this, the pleat-like interconnective tube is visible. In Figure 7, stripping has revealed both the interconnective tube and, apparently, an appressorium remnant. Occasionally two appressoria were formed over the same stoma, resulting in two SSVs (Fig. 10) in the substomatal chamber.

Orientation of the substomatal vesicle in the host. The stomata of gladiolus leaves have distinct and prominent guard cells; the slit is markedly recessed and is orientated along an axis parallel to the leaf veins. Primary hyphae (Figs. 2 - 4) were initiated at each apex of the long axis of the SSV, which usually was orientated at right angles to the stomatal opening. At 96 HPI, the interconnective tube orientation was indicative of the position of the stomatal slit and the orientation of the long axis of the SSV to the stomatal slit could be determined (Figs. 6 and 10 - 12).

Chi-square tests indicated that, on gladiolus, significantly more SSVs developed with their long axes at angles (either half-turned or at right angles) than developed with their long axes parallel to the stomatal slit (Table 1). A comparison of primary hyphae developed at

Table 1. Orientation of the long axes of the substomatal vesicles of *Uromyces transversalis* at right angles, half turned and parallel to the stomatal slits of the host (gladiolus) and a non-host (maize)

HOST			NON-HOST		
Orientation	Observed	Expected	Orientation	Observed	Expected
Right angles & Half turned	55	31	Right angles & Half turned	17	10
Parallel	7	31	Parallel	3	10
$X^2_{(1)} = 37.16;\ P > 0.001$			Fisher P = 0.020371		

HOST

Orientation	Observed	Expected
Right angles	65	33
Half turned	25	33
Parallel	10	33

$X^2_{(2)}$ (Right angles vs. Half turned vs. Parallel) = 49.00; P > 0.001

$X^2_{(1)}$ (Right angles vs. Half turned) = 32.97; P > 0.001

$X^2_{(1)}$ (Right angles vs. Parallel) = 47.06; P > 0.001

$X^2_{(1)}$ (Half turned vs. Parallel) = 17.97; P = 0.001

$\alpha = 0.05/3 = 0.01667$

Scanning electron micrographs (Figs. 7 - 12 at 96 HPI, Fig. 15 at 24 HPI) of substomatal vesicles of *Uromyces transversalis* in the substomatal chambers of gladiolus (Figs. 7 - 14) and maize leaves (Fig. 15) after removal of the epidermis, and a light micrograph of the uredium on the gladiolus leaf surface (Fig. 13 at 312 HPI).
Abbreviations: SSV, substomatal vesicle; I, interconnective tube; AP, appressorium remnant; G, guard cell wall; M, mesophyll cell; PH, primary hypha; P, uredium; SC, substomatal chamber; V, vein; X, long axis of the stomatal slit; Y, long axis of the substomatal vesicle.

Fig. 7. Substomatal vesicle (SSV) with interconnective tube (I) and appressorium (AP) remnant. Scale bar = 10 µm.

Fig. 8. Substomatal vesicle with interconnective tube (I) adjacent to scar where guard cell (G) was attached prior to removal of epidermis. Scale bar = 5 µm.

Fig. 9. Substomatal vesicle with attached guard cell (G) wall and interconnective tube (I). Scale bar = 5 µm.

Fig. 10. Double penetration of same stomatal slit showing interconnective tubes (I) and two substomatal vesicles. Scale bar = 5 µm.

Fig. 11. Interconnective tube developed parallel to long axis of stomatal slit as determined by the long axes X and Y. Scale bar = 10 µm.

Fig. 12. Interconnective tube on substomatal vesicle developed at acute angle as shown by angle between long axes X and Y. Scale bar = 5 µm.

Fig. 13. Mature uredium (P) of gladiolus rust fungus on exterior leaf surface at right angles (long axes X and Y) to vein (V), 312 HPI. For clear colour micrographs, See Chapter 3, p. 42. Scale bar = 1 mm.

Fig. 14. View of mesophyll tissue after epidermis removal showing tightly packed mesophyll cells (M) in rows with elongated substomatal chamber (SC) in between. The orientation of this micrograph is in accordance with that of Fig. 13. Scale bar = 20 µm.

Fig. 15. Right angled orientation of substomatal vesicle (SSV) and primary hypha (PH) to long axis of stomatal slit in substomatal chamber of maize. Scale bar - 10 µm.

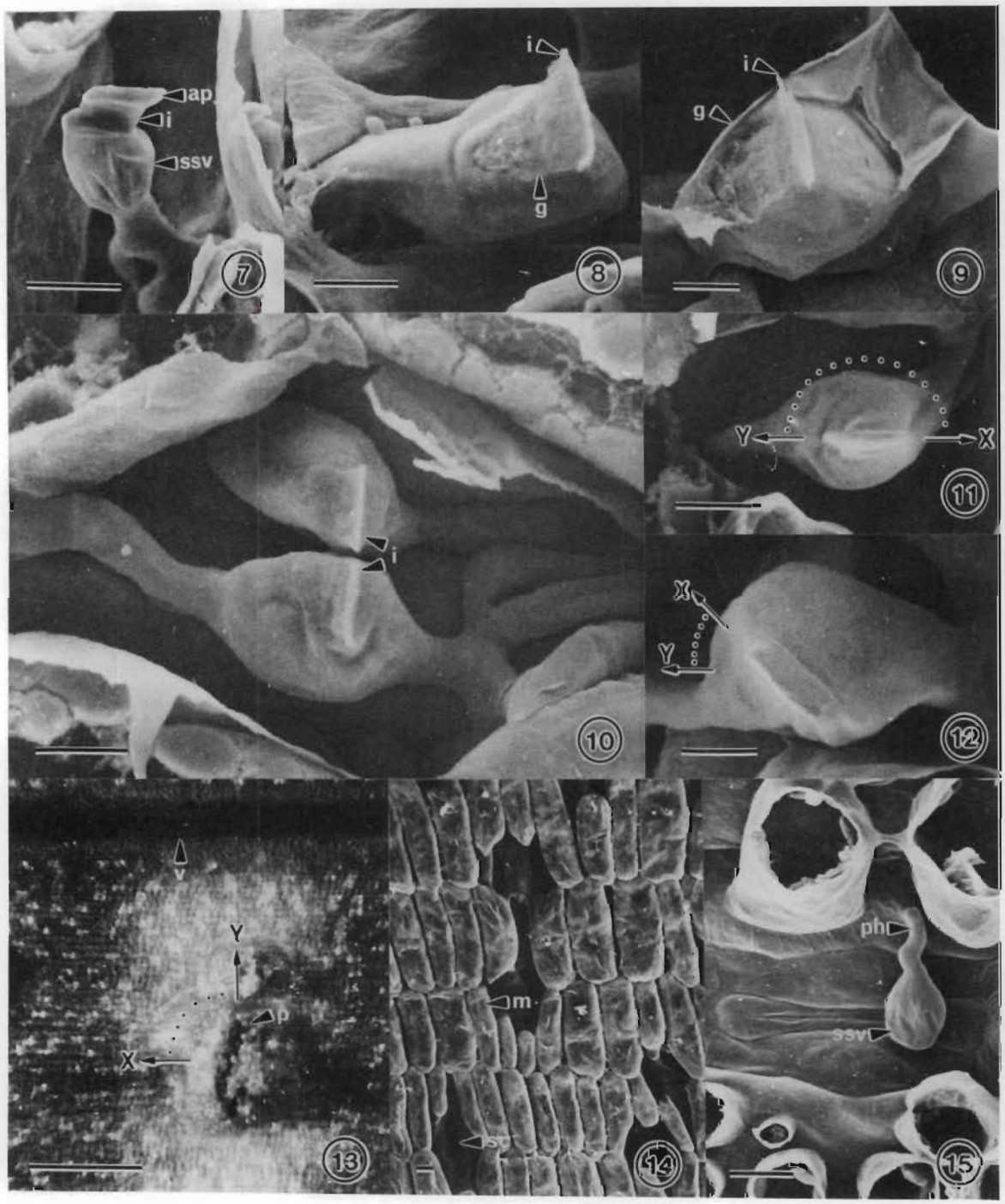
ap
i
ssv
7
i
g
8
i
g
9
i
10
Y
X
11
X
Y
12
v
Y
p
X
13
m
st
14
phc
ssvl
15

right angles to half turned to parallel primary hyphae, indicated a very strong tendency for all SSVs to position their long axes at right angles to the stomatal slit and therefore the veins (Table 1). The uredium of gladiolus rust (Fig. 13) elongates at right angles to the parallel veins and the stomatal slits. The mesophyll cells of gladiolus leaves are arranged in dense rows at right angles to the veins, thus causing the long axes of the substomatal chambers to be at right angles also to the long axis of the leaf (Fig. 14).

Orientation of the substomatal vesicle in a non-host. Twenty instances of primary hypha development by *U. transversalis* were recorded in maize. Counts were very low because many germ tubes aborted when unable to locate a stoma. Of the appressoria that were formed, many appeared unable to penetrate the stomatal slit. Those that penetrated the stomatal slit aborted and very few developed to Stage 4 or 5. However, a similar preference of the developing primary hyphae (Fig. 15) of *U. transversalis* to orientate at right angles to the stomatal slit of the host was observed in the non-host tissue (Table 1). No sign of attachment of the HMC to a non-host cell was found on the SSVs which had aborted.

DISCUSSION

Unlike the infection peg of *P. sorghi* described by Hughes and Rijkenberg (1985), which appears to be bifurcate in early development stages, the infection peg of *U. transversalis* is single. The differences in infection peg morphology can be related to the morphological differences in the stomatal openings of the respective hosts, those of maize being slim and long, those of gladiolus being ellipsoid, apparently providing a more easy access to the infection peg of the penetrating rust fungus. Infection pegs of both fungi ultimately form a pleat-like interconnective tube. The relative inability of the *U. transversalis* infection apparatus to penetrate the stomatal slits of the maize leaf might partially be explained by abortion of the infection apparatus on maize leaves after the formation of an

appressorium, a lack of peg bifurcation rendering maize leaf penetration by *U. transversalis* difficult. On the other hand, successful penetration may have been the result of open maize stomata at the time that the infection peg was formed.

Hughes and Rijkenberg (1985) have shown that the long axis of the SSV of *P. sorghi* is arranged parallel to the long axis of the stomatal slit, the substomatal chamber and the leaf. The present study showed that uredium development across the gladiolus leaf, which is responsible for the specific epithet of this rust, i.e. *transversalis*, is associated with transverse orientation of mesophyll cells and substomatal chambers. The fungus has apparently adapted itself to the host cell arrangement by orienting the long axis of its SSV at a right angle to the long axis of the leaf. Although the orientation of the substomatal chamber in maize is parallel to the long axis of the leaf, the long axis of the SSV of *U. transversalis* in maize leaves is at a right angle to that of the substomatal chamber, indicating that the orientation of the SSV is genetically programmed by the fungus and not induced by host configuration. It appears, therefore, that SSV orientation has co-evolved with, or adapted to, substomatal chamber orientation. The reason for such co-evolution or adaptation is not yet understood.

LITERATURE CITED

DAVIES, M. E., and G. M. BUTLER. 1986. Development of infection structures of the rust, *Puccinia porri*, on leek leaves. Trans. Br. Mycol. Soc. 86:475-515.

HUGHES, FIONA, and F.H.J. RIJKENBERG. 1983. An epidermis removal technique for studying infection processes of *Puccinia sorghi* in maize leaves. Proc. Electron Microsc. Soc. S. Afr. 13:17-18.

HUGHES, F. L., and F. H. J. RIJKENBERG. 1985. Scanning electron microscopy of early infection in the uredial stage of *Puccinia sorghi* in Zea mays. Plant Pathol. 34:61-68.

PALIWAL, Y. C., and W. K. KIM. 1974. Scanning electron microscopy of differentiating and non-differentiating uredosporelings of wheat stem rust fungus (*Puccinia graminis* f.sp. *tritici*) on an artificial substrate. Tissue and Cell 6:391-397.

SIEGEL, S. S. 1956. Non-parametric statistics for the behavioural sciences. McGraw-Hill. London.

STAPLES, R. C., H -J., GRAMBOW, H. C. HOCH, and W. K. WYNN. 1983. Contact with membrane grooves induces wheat stem rust uredospore germlings to differentiate appressoria but not vesicles. Phytopathology 73:1436-1439.

STAPLES, R. C., H. C. HOCH, L. EPSTEIN, L. LACETTI, and S. HASSOUNA. 1985. Recognition of host morphology by rust fungi: responses and mechanisms. Can. J. of Plant Pathol. 7:314-322.

VIENNOTT-BOURGIN, M. G. 1978. *Uromyces transversalis* (Thüm.) Winter, parasite dangereux des cultures de glaieuls. Academie d'Agriculture de France, Paris 64:880-885.

WYNN, W. K. 1976. Appressorium formation over stomates by the bean rust fungus: Response to a surface contact stimulus. Phytopathology 66: 136-146.

CHAPTER 2

Ultrastructural Morphology of the Uredium and Collar Formation During Urediosporogenesis of *Uromyces transversalis* on Gladiolus

ABSTRACT

The transverse uredia of *Uromyces transversalis* on gladiolus leaves were investigated by scanning and transmission electron microscopy. The basal cell distally forms one or more protruberances, each being delimited by a septum to become a urediospore initial. The initial elongates and lays down a septum to form a urediospore and pedicel. The first protruberance on the basal cell forms holoblastically and evidence for the subsequent enteroblastic formation of up to three successive urediospore initials may be found at the same locus. The pedicel of a spore thus formed remains on the basal cell and becomes a collar around the next protruberance. The basal layer, of the two-layered septum that delimited the pedicel from the basal cell, grows out to form the wall of the subsequent protruberance, in the process rupturing, and laterally displacing, the terminal septal layer. A new basipetal septum forms to delimit the subsequent urediospore initial. In this manner, several collars form retrogressively and concentrically at one locus. The urediospore spines apparently play an active role in schizolytic secession, possibly by exerting pressure on the pedicel apex, causing the terminal layer of the septum to tear from the basal layer along the middle layer.

INTRODUCTION

Initially, electron microscopic studies of the Uredinales mainly dealt with the development of the urediospores and their structure at maturity (Ehrlich and Ehrlich 1969, Littlefield and Bracker 1971). Later, interest focused on specific aspects of urediosporogenesis (Harder 1976, Hassan and Littlefield 1979, Hennen and Figueiredo 1979, Littlefield and Heath 1979, Müller *et al.* 1974, Rajendren 1970, Rey and Garnett 1983, Spiers and Hopcroft 1985).

Terminology regarding urediosporogenesis shows considerable variation. It is therefore necessary to state which terms are used in this article, together with their respective synonyms.

Basal cell (Hassan and Littlefield 1979, Rajendren 1970, Spiers and Hopcroft 1985). Synonym: sporogenous cell (Hassan and Littlefield 1979, Hennen and Figueiredo 1979, Hughes 1970, Rajendren 1970, Rey and Garnett 1983, Spiers and Hopcroft 1985). This cell is defined as producing, having, or supporting spores (Hawksworth *et al.* 1983). Since it is strictly speaking the urediospore initial that gives rise to the urediospore the author prefers to use the term basal cell.

Collar (Blackman 1904, Heath and Bonde 1983, Hennen and Figueiredo 1979, Olive 1944, Rajendren 1970, Rey and Garnett 1983). The collar is the wall of a pedicel, which upon urediospore secession remains attached to the basal cell and through which the subsequent urediospore initial develops.

Pedicel (Harder 1976, Hassan and Littlefield 1979, Hawksworth *et al.* 1983, Hennen and Figueiredo 1979, Spiers and Hopcroft 1985). Synonyms: " a small stalk " (Hawksworth *et al.* 1983) or sporophore (Müller *et al.* 1974, Rey and Garnett 1983).

Anomalies in urediosporogenesis have been reported for three genera of the Uredinales. In *Kernkampella breyniae-patentis* (Munk. and Thirum.) the urediospores are seceded by rhexolysis. Successive generations of urediospores are produced by rejuvenation of the basal cell through the persistent pedicel. The persistent pedicels of successive urediospores form a distinct collar around the base of the developing urediospore at the apex of its pedicel (Rajendren 1970). Observations by Hennen and Figueiredo (1979) revealed that, in the then newly described genus *Intrapes*, collars formed on the distal end of the basal cell after successive generations of urediospores. Transmission electron microscopy by

Rey and Garnett (1983) showed that, during urediosporogenesis of *Puccinia digitariae*, collars are formed from pedicels that were split at the apex or laterally. The remnants of pedicels remain on the basal cell and contribute to the collar at the base of the pedicel. Of particular interest in their study is the fact that it is not only the pedicel that contributes to the collar; the old septum, which has been pushed laterally by the new basal septum, contributes to the collar as well.

In their monumental publication on the ultrastructure of rust fungi, Littlefield and Heath (1979) commented that the formation of collars would: " . . . provide exceptionally interesting objects for ultrastructural study."

Gladiolus rust, first described as *Uredo transversalis* by F. von Thümen in 1876 and later renamed *Uromyces transversalis* (Winter 1884), is a serious disease affecting *Gladiolus* L. in South Africa. Restricted to Southern and Western Africa for many years, it has since spread to production areas in North Africa, South America, Italy and Malta (Viennott-Bourgin 1978). In the present study the author describes the uredium morphology, urediosporogenesis and subsequent collar formation of the uredial stage of *U. transversalis* (Thüm.) Winter.

MATERIALS AND METHODS

Plants and Inoculation. Two-month-old gladiolus cv. Goldfield plants, susceptible to *Uromyces transversalis* were used in this experiment. The plants were inoculated (Appendix I) by brushing viable urediospores (PREM 47693, National Collection of Fungi, Plant Protection Research Institute, Pretoria) onto the distal third of the fully expanded fifth leaf. Morphology and position of the gladiolus leaf preclude distinction between an ab- and adaxial surface. The inoculated plants were then incubated in a dew chamber in

the dark (Appendix II) for 24 h at 20°C and transferred to a glasshouse in which the temperatures varied between 20°C and 35°C. Samples were taken at 20 days post-inoculation.

Scanning electron microscopy. Pieces, 3 mm by 3 mm, cut through the uredium, were taken from the leaf and fixed overnight in 3% glutaraldehyde in sodium cacodylate buffer (pH 6.8 - 7.2), washed twice in the buffer, post-fixed for 3 h in 2% buffered osmium tetroxide, washed twice in buffer and dehydrated in an ethanol series. The dehydrated material was then critical point dried with carbon dioxide as a transition fluid before being mounted upright in grooves, or flat, on copper stubs. Specimens were coated with gold/palladium in a Polaron® sputter coater and examined at 5, 8 and 10 kV with a Hitachi® S-570 scanning electron microscope. After freeze-fractioning in a Biorad® E7400 cryo unit, fresh material was viewed with a Jeol® JSM-840 scanning electron microscope at 10 kV.

Transmission electron microscopy. From leaves, 2 mm by 4 mm pieces, containing the uredium in the middle, were removed and fixed overnight under 200 mm Hg vacuum in 3% glutaraldehyde in a 0.05M sodium cacodylate buffer (pH 6.8 - 7.2), washed twice in buffer and post-fixed for 3 h in 2% buffered osmium tetroxide. Material was dehydrated either in an ethanol series and embedded in Spurr's resin (Spurr 1969), or in an acetone series including two changes in propylene oxide followed by embedding in Epon/Araldite (Anderson and André 1969) resin. The specimen blocks were sectioned parallel and perpendicular to the long axes of the uredia. Sections were stained with 2% uranyl acetate in boiled, double-distilled water for 15 min, washed in double-distilled water and post-stained in lead citrate (Reynolds 1963) for 15 - 20 min, washed in double-distilled water and viewed with a Jeol® 100 C or CX transmission electron microscope.

RESULTS AND DISCUSSION

The scanning and transmission electron microscope studies conducted showed that the uredium morphology (Fig. 1), and urediospore ontogeny, of *Uromyces transversalis* is similar to that of other rusts that have pedicellate urediospores (Fig. 2). Typical of the genus *Uromyces* (Cummins and Hiratsuka 1983), uredia of gladiolus rust lack a periderm and paraphyses. On gladiolus leaves, elongate uredia are oriented at right angles to the veins between and along densely packed rows of the mesophyll cells similarly oriented at right angles to the long axis of the leaf (See Chapter 1).

One (Fig. 4) or two (Fig. 3) sporogenous loci were observed on a basal cell. This does not preclude the possibility of more such loci per basal cell being present in another plane. Basal cells varied considerably in size and shape. The sporogenous locus develops holoblastically as a protruberance on the distal surface of the basal cell (Fig. 3), which, after receiving two nuclei from the basal cell and septum formation, becomes a urediospore initial (Fig. 4). Subsequently a septum delimits the initial into a urediospore and pedicel. Various stages of post-septation development and concomitant swelling of the urediospore and pedicel elongation are shown in Figures 5 to 7 and 19. Figures show that basal cells (Fig. 3), mycelium cells (Fig. 4), urediospore initials (Fig. 4) and urediospores (Fig. 6) are dikaryotic. Collars are identified (Figs. 8 - 10) in uredia after the development of the second urediospore initial, since it is confined within the pedicel left behind by the secession of the first urediospore. The older collars degrade, so that the most recent collar or pedicel or urediospore is easily discernable under the scanning electron microscope. The basal cell of *U. transversalis* produces successive urediospore initials at a particular locus. In Figure 11 are depicted three sporogenous loci: the left basal cell protruberance inside the collar of the first urediospore, the middle basal cell protruberance inside the collars of two previous urediospores and the right basal cell locus

Scanning (Figs. 1 and 2) and transmission (Figs. 3 - 7) electron micrographs of the uredium and spore-producing apparatus of *Uromyces transversalis* on gladiolus leaves.

Abbreviations: BC, basal cell; C, collar; E, epidermis; M, mesophyll layer; MC, mycelium cell; N, nucleus; NU, nucleolus; P, pedicel; PR, protruberance; U, urediospore; UI, urediospore initial

Fig. 1. Cross section through long axis of uredium showing epidermis (E) bulging to accommodate underlying urediospores (U) and underlying layer of mesophyll cells (M). Scale bar = 50 µm.

Fig. 2. Lateral view of pedicellate urediospores (U), left one partially detached (arrow) from apex of pedicel (P). Scale bar = 5 µm.

Fig. 3. Section of dikaryotic (N), basal cell (BC) with protruberance (PR) and pedicel. Scale bar = 2 µm.

Fig. 4. Section of spore apparatus sectioned through basal cell (BC) and urediospore initial (UI) extended through collar (C). In lefthand mycelium cell (MC), two nuclei (N) are evident and in urediospore initial also two, one of which has been sectioned through nucleolus. Scale bar = 5 µm.

Fig. 5. Composite transmission electron micrograph of urediospore initial (UI) on basal cell (BC) developing inside collar (C) left behind by first urediospore. Scale bar = 2 µm.

Fig. 6. Longitudinal section of urediospore (U), pedicel (P), and urediospore initial (UI) from same basal cell (BC). Scale bar = 5 µm.

Fig. 7. Longitudinal section of pedicel (P) and attached urediospore (U) with dense cytoplasm. Large vacuole in pedicel (P) is evident. Scale bar = 5 µm.

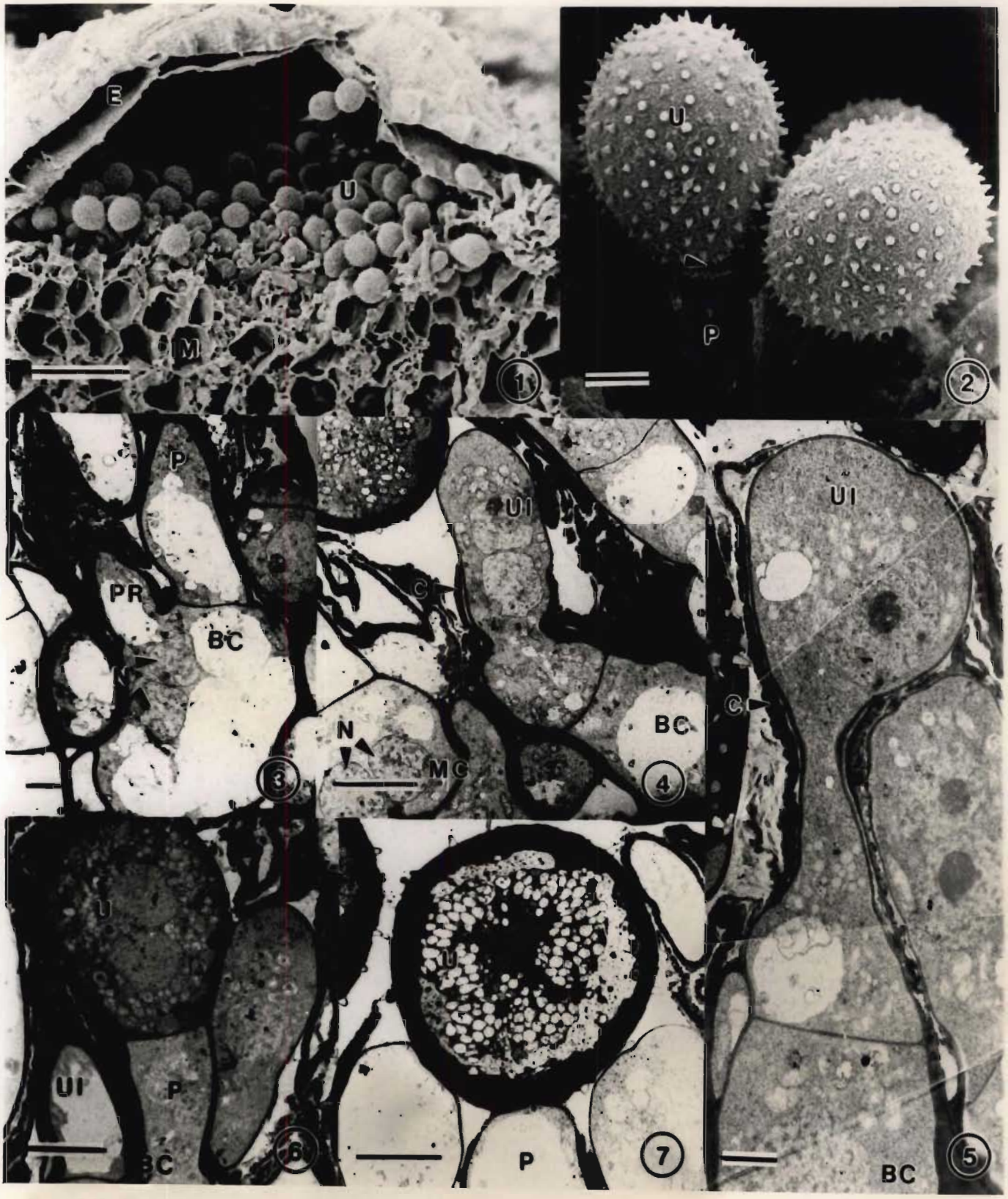
E
U
M
1
U
P
2
P
PR
BC
3
UI
C
N
MC
BC
4
UI
C
BC
5
U
UI
P
BC
6
U
P
7

(highlighted in Fig. 12 - 3°) inside the collars of two previous urediospores (Fig. 12 - 1° and 2°). The apical and lateral growth of the protruberance or new urediospore initial inside the pedicel, which is now dead and not maintained by its cytoplasm, causes the pedicel to tear apically (Figs. 8 and 9). The number of collars present, one within the other, reflects the number of spores formed at that locus. The first urediospore lacks a collar, the second has one collar (Figs. 4 and 10), and the third has two collars (Fig. 12). Urediosporogenesis of *U. transversalis* however, differs from descriptions provided by Hughes (1970) and by Spiers and Hopcroft (1985), in that successive urediospores of *Melampsora medusae* develop on new growing points (loci) on the basal cell. In the micrograph presented by Spiers and Hopcroft (1985) as evidence for the development of a new growing point, the basal cell is, in fact, developing a protruberance within the pedicel of a previous urediospore. The micrograph suggests, as stated correctly in the legend accompanying it, that successive urediospores are produced at the same locus, or at new growing points/loci, but in the text only the new growing points are mentioned.

Figure 12 is a higher magnification of the rightmost basal cell depicted in Figure 11. Clearly shown on either side of the site where the protruberance for the third (3°) urediospore initial, will form are collars of two previous pedicels (1° and 2°). The septum that previously separated the basal cell from the pedicel forms the periclinal wall of the new protruberance (Fig. 11). During the formation of the protruberance the outer layer of the septal wall ruptures (although evidence was found, the micrographs are not presented) and the inner septal wall constitutes the wall of the urediospore initial. The degenerate cytoplasm (Fig. 12) in contact with the outer layer cannot maintain the latter's development, and may be the reason for the rupture of the layer. Between the pedicel of the previous urediospore (1°) and the wall of the urediospore initial (2°), the remnants of the outer layer of the septum close to the juncture can be observed (arrow) in Figure 14. The protruberance grows little at the juncture with the collar compared to its apex, leaving the outer layer of the former septum intact at the juncture. These outer septal wall

Scanning (Figs. 8 and 9) and transmission (Figs. 10 - 14) electron micrographs of the uredium and spore-producing apparatus of *Uromyces transversalis* in gladiolus leaves.

Abbreviations: BC, basal cell; C, collar; D, relative distance between the pedicel attachment of one urediospore to the pedicel or protruberance attachment of the next urediospore; P, pedicel; PR, protruberance; UI, urediospore initial; 1°, first; 2°, second; 3°, third; 4°, fourth successive urediospore, urediospore initial or protruberance

Fig. 8. Lateral view of intact collar (C) closely associated with urediospore initial (UI). Collar (C) bears scars of spines that possibly developed on neighbouring urediospore. Scale bar = 10 µm.

Fig. 9. Oblique view of pedicel (P) after secession of urediospore bearing torn collar (C) around its base. Scale bar = 10 µm.

Fig. 10. Longitudinal section of urediospore initial (UI) with torn first urediospore collar (C) evident around base of urediospore initial. Scale bar = 2 µm.

Fig. 11. Section of three basal cells (BC) in different stages of development. Cells are forming second and third urediospore protruberances (PR) with protruberance loci at base of pedicels. Peripheral walls of two collars (C) are evident; pedicel is filled with cellular debris. Basal cell (BC, middle) is developing third urediospore protruberance (PR), collars of first and second generation pedicels are evident. Basal cell (BC, left) has developed further than other two. Scale bar = 3 µm.

Fig. 12. Close-up of section of basal cell (BC, right) in Figure 13 with septum (3°). Evident are walls and basipetal junctures (D) of first (1°) and second (2°) collars of urediospores and moribund contents at apex of third urediospore protruberance (3°). Scale bar = 2 µm.

Fig. 13. Section of elongated third urediospore initial (UI) contained within virtually intact collars (1° and 2°) of previous urediospores. Septum (4°) separates urediospore initial (UI) and basal cell (BC). Scale bar = 3 µm.

Fig. 14. Close-up of longitudinal section of part of basal cell (BC) and urediospore initial (UI). Collar of first urediospore's pedicel (1°) shows continuity with urediospore initial wall (2°), which is continuous with septum (3°). Between wall of urediospore initial (2°) and pedicel (1°), remnants of outer layer (arrow) of old septum and of protruberance can be observed. Scale bar = 0.5 µm.

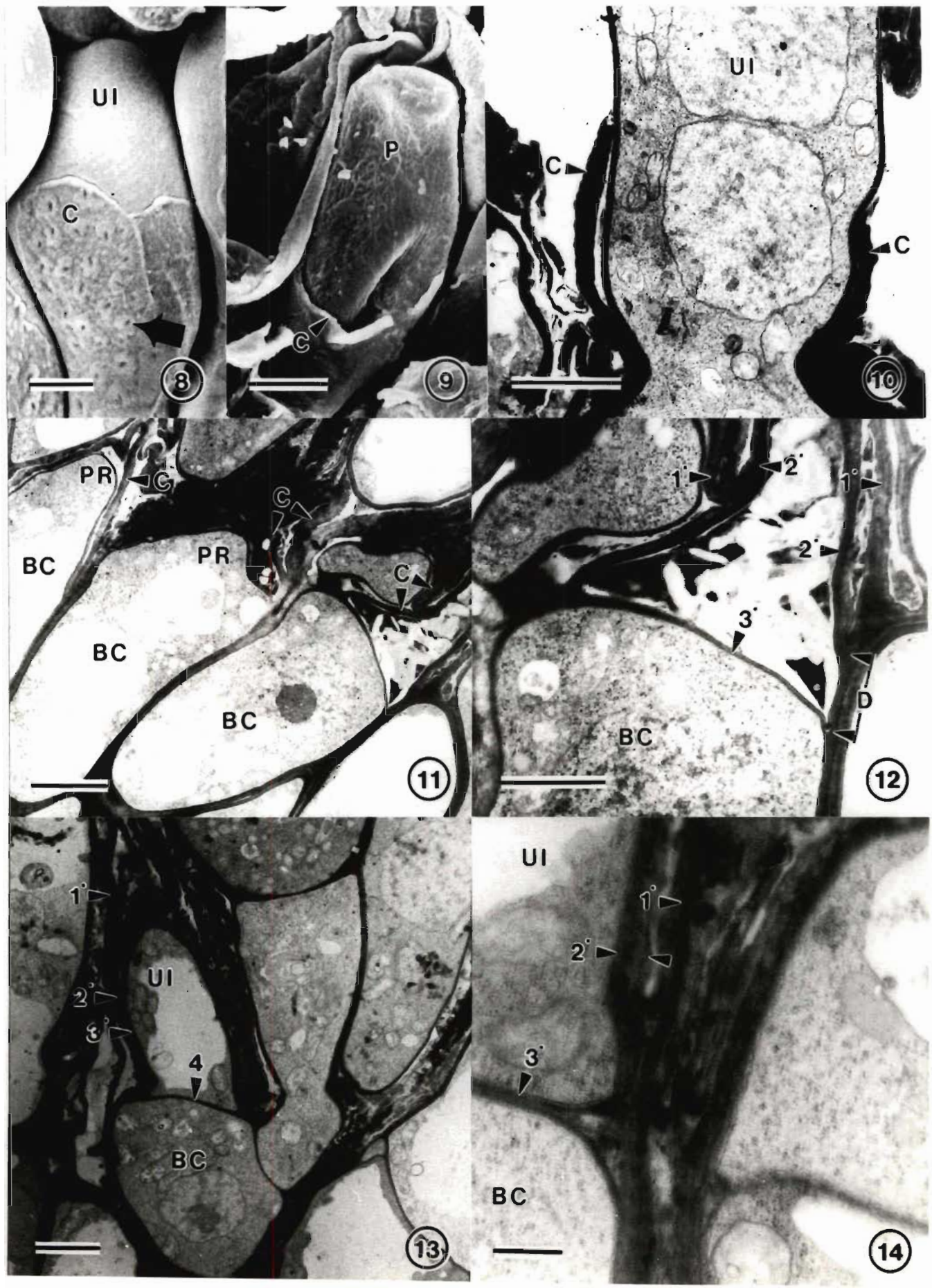
UI
C
8
P
C
9
UI
C
C
10
PR
C
C
BC
PR
C
BC
BC
11
1°
2°
1°
2°
3°
D
BC
12
1°
UI
2°
3°
4
BC
13
UI
1°
2°
3°
BC
14

fragments, however, contribute very little to the structure of the collar. The inner layer of the protruberance remains in contact with the cytoplasm and wall apposition can, therefore, continue. Although the first urediospore develops holoblastically, successive urediospores at a particular locus develop enteroblastically. The wall of the urediospore initial remains continuous with that of the collar of the previous urediospore (Figs. 13 and 14). The protruberances on the basal cells of *Physopella zeae* on leaves of *Zea mays* (Heath and Bonde 1983) develop in a manner similar to that of *U. transversalis* as described here. Successive collars of *U. transversalis* form retrogressively, since the new septum that delimits the protruberance to form a new urediospore initial is initiated below the point (the line D in Fig. 12) where the previous septum, which had delimited the basal cell from the pedicel, arose.

This is the first report of collar formation in the genus *Uromyces*. There are distinct differences, as illustrated in Figures 15 to 18 between the types of collar development and urediosporogenesis in the four different genera of the Uredinales for which this process has been described. Light microscope studies of Rajendren (1970) (Fig. 15) and Hennen and Figueiredo (1979) (Fig. 16) showed that the same locus of a basal cell forms successive urediospores through the same pedicel, thus giving rise to collars. In *K. breyniae-patentis* the collars are formed at the apex of the pedicel and in *Intrapes* the collars are flared above the basal cell. The major contribution of these authors was defining and describing collar formation in the Uredinales. The structure of collar formation was further investigated ultrastructurally by Rey and Garnett (1983). They determined that collars of *P. digitariae* (Fig. 17) are not only formed by the persisting pedicels, as is the case with *U. transversalis* (Fig. 18), but also by the two halves of the septum which separate the pedicel from the basal cell. The formation of "annellidic remnants" during sporogenesis has been shown by Rijkenberg and Truter (1974a, b) to occur in aeciosporogenesis and pycniosporogenesis of *Puccinia sorghi*. During aeciosporogenesis the periclinal wall is ruptured when the continuous inner wall expands to form an aeciospore initial. The

Diagrammatic representations of collar formation during urediosporogenesis in the four species of Uredinales in which collar formation has been described (Figs. 15 - 18).

Abbreviations: BC, basal cell; C, collar; P, pedicel; PR, protruberance; UI, urediospore initial; 1°, first, and 2°, second collar; S, septum or septal remnants

Fig. 15. *Kernkampella breyniae-patentis*. Above: protruberance (PR) extended within pedicel (P). Below: urediospore initial (UI) extended beyond pedicel and flaring pedicel apex to constitute collar (C).

Fig. 16. *Intrapes*. Above: one flared collar (C) with extending protruberance (PR) within pedicel (P). Below: extended protruberance (PR) caused pedicel to flare open to form second urediospore collar (C) on basal cell (BC).

Fig. 17. *Puccinia digitariae*. Above: pedicel (P) on basal cell (BC) with three-layered septum (S) delimiting pedicel from basal cell and below it initials of new septum of developing protruberance (PR). Below: urediospore initial (UI) extended within pedicel pushing old septum (S) laterally which together with pedicel make up collar (C).

Fig. 18. *Uromyces transversalis*. Left: Collar (C) and septum (S) which delimited it from basal cell (BC) extending as protruberance (PR) within collars of previous urediospore. Middle: new septum (S) formed basipetally from old septum (S) to delimit second urediospore initial (UI) within first urediospore pedicel or collar. Right: third urediospore initial (UI) delimited from basal cell (BC) by septum (S) extended within two pedicels or collars (1^{o} and 2^{o}).

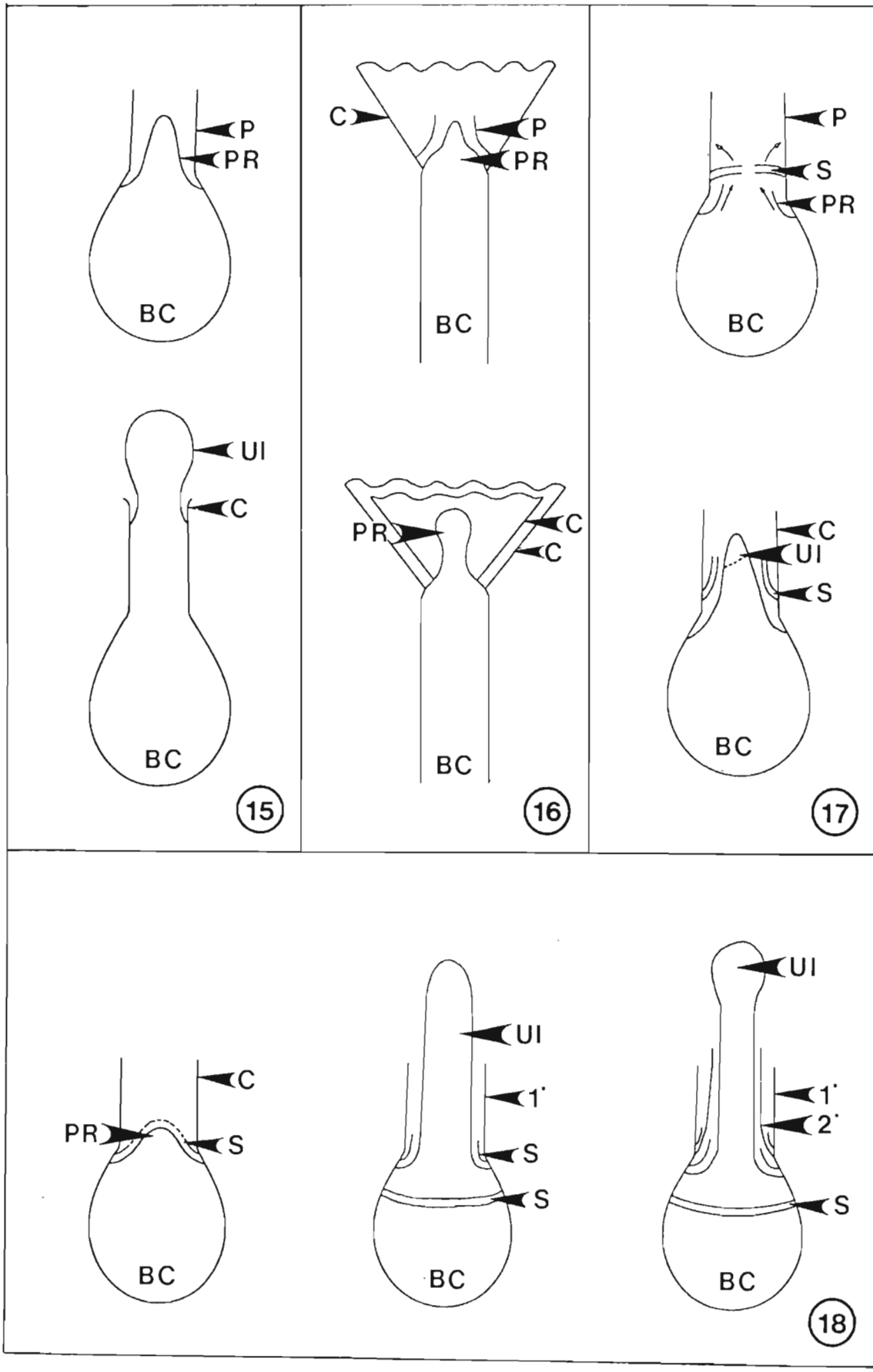
P
PR
BC
UI
C
BC
15
C
P
PR
BC
PR
C
C
BC
16
P
S
PR
BC
C
UI
S
BC
17
C
PR
S
BC
UI
1'
S
S
BC
UI
1'
2'
S
BC
18

ruptured periclinal wall persists and gives rise to annellations or collarettes formed by successive aeciospore initials in a basipetal chain. Harder (1976) observed a rupturing of the periclinal wall of the basal cell during the urediosporogenesis of *Puccinia coronata avenae*. The pedicels, having fulfilled their function, form collars which apparently have no function. It is possible that the collars protect the urediospore initials against the spines of the adjacent urediospores and against desiccation of the fragile septum during the incipient stages of protruberance development.

The length of a urediospore initial is determined by the number of urediospore initials and/or pedicels and urediospores in its close proximity (Fig. 19). In older uredia the abundance of structures in and above the fertile layer leads to very long pedicels so as to accommodate the increase in urediospore size that occurs on maturation.

Within the cytoplasm of the urediospore, a short distance from the spine, a thin layer of endoplasmic reticulum (Fig. 21) was discernible similar to that described in reports by Amerson and Van Dyke (1978), Ehrlich and Ehrlich (1969), Littlefield and Bracker (1971) and Müller *et al.* (1974). Except for the earliest observed stage (Fig. 21) where the periphery of the urediospore wall appeared electron-lucent, different layers of the wall, as reported by Ehrlich and Ehrlich (1969) and others, were not observed. In fact, the wall, except for a thin layer in the immediate vicinity of the spine, appeared equally electron-dense in the subsequent developmental stages (Figs. 22 - 24). When the tip of a spine emerges from the spore wall, a small crater forms in the wall (Figs. 20 and 23). The process of wall formation embeds the spines, forming characteristic wall undulations into the cytoplasm (Figs. 21 - 23) until the wall is uniformly thickened (Fig. 7) and the spines fully extended (Fig. 24). The degree of undulation corresponds with the length that the spines eventually extend to beyond the urediospore wall (Figs. 21 - 24). The straightening out of the wall may be due to the stretching of the wall as spore volume increases during maturation. Internal pressure of the cytoplasm may contribute to forcing the spines

Scanning (Figs. 19 and 20) and transmission (Figs. 21 - 27) electron micrographs of the spore producing apparatus of *Uromyces transversalis* on gladiolus leaves.

Abbreviations: P, pedicel; U, urediospore; UI, urediospore initial; S, spine; W, urediospore wall

Fig. 19. View of urediospores (U) at different stages of maturity. Bumps (lower arrow) appeared on surface of urediospore (U) as first exterior sign of incipient spine extrusion; later fully extended (top arrow) to create urediospore (U) ornamentation. Very long pedicel (P) to accommodate the expansion of adjacent urediospores during maturation. Scale bar = 5 µm.

Fig. 20. Lateral view of urediospore initial (UI), pedicellate (P) urediospore (U) and pedicel (P). Right urediospore initial (UI) devoid of spines and left urediospore (U) with slightly protruding spines surrounded by dark cavities (arrow). Long pedicel (P) released urediospore above developing urediospores. Scale bar = 5 µm.

Fig. 21. Section of two immature spines (S) with wall (W) invaginated into cytoplasm. Urediospore wall has two layers, outer layer more electron-lucent than the electron-dense inner layer. Scale bar = 0.5 µm.

Fig. 22. Section of spine (S) in single layer wall (W). Spine (S) is invaginated into cytoplasm, however to lesser extent than before. Scale bar = 0.5 µm.

Fig. 23. Section of spine (S) in single layer wall (W) of urediospore. Invagination into cytoplasm less than before with secondary wall deposition evident on spine base. Shallow indentations caused by wall (W) fragmentation adjoins spine (S). Scale bar = 0.5 µm.

Fig. 24. Section of fully developed spine (S) extended beyond perimeter of thickened urediospore wall (W). Scale bar = 0.5 µm.

Fig. 25. Close-up of section of plane of secession showing fragmented urediospore wall (W) partially separated at electron-lucent middle layer from electron-dense inner layer invaginated by spine (S) extending during schizolytic secession of urediospore (U) from pedicel (P) apex. Scale bar = 2 µm.

Fig. 26. Close-up of longitudinal section of urediospore attachment to apex of pedicel (P). Wall of urediospore (U) has funnel-shaped indentation which is partially occluded by spherical Woronin body (arrow) in pedicel apex. Scale bar = 0.5 µm.

Fig. 27. Section exhibiting possible role of spines (S) in mechanical detachment of urediospore (U). Spines exerted pressure on pedicel (P) apex so that it becomes invaginated at point of contact. Apex of spine (S) is separating from wall (W) at point of contact. Scale bar = 0.5 µm.

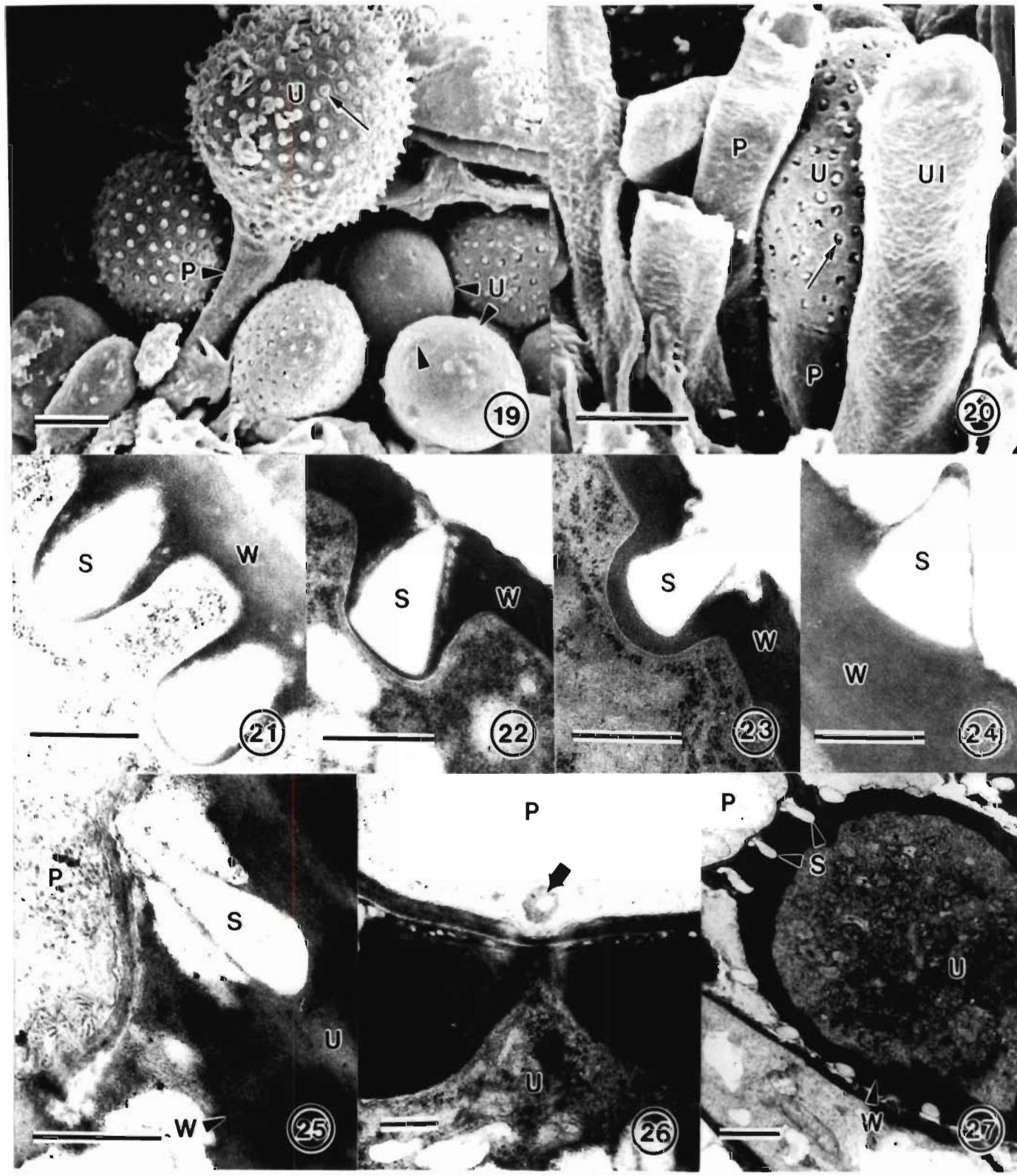
U
P
U
19
P
U
UI
P
20
S
W
21
S
W
22
S
W
23
S
W
24
P
S
U
W
25
P
U
26
P
S
U
W
27

outwards. The extrusion of the spines is co-ordinated with the deposition of wall material on the inside of the spine (compare Fig. 22 with Fig. 23). Amerson and Van Dyke (1978) came to the conclusion that lytic action was involved in echinulation. In the case of gladiolus rust, however, the rigidity of the spine during extension probably causes the urediospore wall to be laterally torn away from the spine during its passage to full extension (Figs. 22 and 23). This is in contrast with the observations of Spiers and Hopcroft (1985) on urediospores of *Melampsora epitea*. The spine of *M. epitea* remains laterally attached to the urediospore wall while being extruded beyond the wall and no evidence of craters was shown. It is therefore possible that the emergence of spines of *M. epitea* urediospores is different from that described in the present study. Examination with the light microscope revealed the presence of six to eight small scattered germ pores.

The terminal layer of the septum at the pedicel apex is continuous with the wall of the urediospore, while the basal layer remains an integral part of the pedicel. The terminal layer separates from the basal layer during secession by schizolysis at the electron-lucent layer between them. Figures 25 and 27 provide evidence for an active role of the spines in the schizolytic secession of a urediospore. The detachment force appears to be at least partly mechanical, because, as shown in Figure 25, the septal wall of the pedicel apex is invaginated where it is in contact with the spines. The degree of fragmentation of the outer urediospore wall in Figure 27 possibly reflects the extent of the force exerted by the spines. After liberation (Fig. 2) of the urediospore, the contents of the pedicel degenerate and become moribund (Fig. 12).

At the point of urediospore attachment to the pedicel, transmission electron microscopy elucidated a funnel-shaped indentation (Fig. 26) in the spore wall, which terminated in a pore linking the pedicel to the urediospore. In the pedicel near the pore, a Woronin body (Fig. 26), similar in structure to that described by Müller *et al.* (1974), was found. The

function of this structure is not known. The tightly packed layer of sub-epidermal urediospores (Fig. 1) and further urediospore development exert sufficient pressure on the epidermis to rupture it, resulting in the release of urediospores to the atmosphere.

LITERATURE CITED

AMERSON, H. V., and C. G. VAN DYKE. 1978. The ontogeny of echinulation (spines) in uredospores of *Puccinia sparganioides*. Exp. Mycol. 2:41-50.

ANDERSON, W. A., and J. ANDRé. 1969. The extraction of some cell components with pronase and pepsin fron thin sections of tissue imbedded in an Epon-Araldite mixture. Journal de Microscopie 7:343.

BLACKMAN, V. H. 1904. On the fertilization, alternation of generations, and general cytology of the Uredineae. Ann. Bot. (London) 18:323-373.

CUMMINS, G. B., and Y. HIRATSUKA. 1983. Illustrated genera of rust fungi. Revised Edition. The American Phytopathological Society. St Paul.

EHRLICH, M. A., and H. G. EHRLICH. 1969. Uredospore development in *Puccinia graminis*. Can. J. Bot. 47:2061-2064.

HARDER, D. E. 1976. Electron microscopy of urediospore formation in *Puccinia coronata avenae* and *P. graminis avenae*. Can. J. Bot. 54:1010-1019.

HASSAN, Z. M., and L. J. LITTLEFIELD. 1979. Ontogeny of the uredium of *Melampsora lini*. Can. J. Bot. 57:639-649.

HAWKSWORTH, D. L., B. C. SUTTON, and G. C. AINSWORTH. 1983. Ainsworth and Bisby's Dictionary of the Fungi. 7th ed. Commonwealth Agricultural Bureaux, Slough.

HEATH, M. C., and M. R. BONDE. 1983. Ultrastructural observations of the rust fungus *Physopella zeae* in *Zea mays*. Can. J. Bot. 61:2231-2242.

HENNEN, J. F., and M. B. FIGUEIREDO. 1979. *Intrapes*, a new genus of fungi imperfecti (Uredinales) from Brazilian cerrado. Mycologia, 71:836-840.

HUGHES, S. J. 1970. Ontogeny of spore forms in Uredinales. Can. J. Bot. 48:2147-2157.

LITTLEFIELD, L. J., and C. E. BRACKER. 1971. Ultrastructure and development of urediospore ornamentation in *Melampsora lini*. Can. J. Bot. 49:2067-2073.

LITTLEFIELD, L. J., and M. C. HEATH. 1979. Ultrastructure of rust fungi. Academic Press. New York.

MüLLER, L. Y., F. H. J. RIJKENBERG, and S. J. TRUTER. 1974. Ultrastructure of the uredial stage of *Uromyces appendiculatus*. Phytophylactica, 6:73-104.

OLIVE, L. S. 1944. Spermatial formation in *Gymnosporangium clavipes*. Mycologia 36:211-214.

RAJENDREN, R. B. 1970. Cytology and developmental morphology of *Kernkampella breyniae-patentis* and *Ravenelia hobsoni*. Mycologia, 62:1112-1121.

REY, M. E. C., and H. M. GARNETT. 1983. Sporogenesis in the uredial stage of *Puccinia digitariae*. Trans. Br. Mycol. Soc. 80:521-526.

REYNOLDS, E. S. 1963. The use of lead citrate at high pH as an electron-opaque stain in electron microscopy. J. Cell Biol. 17:208-212.

RIJKENBERG, F. H. J., and S. J. TRUTER. 1974a. The ultrastructure of the *Puccinia sorghi* aecial stage. Protoplasma 81:231-245.

———————————————— 1974b. The ultrastructure of sporogenesis in the pycnial stage of *Puccinia sorghi*. Mycologia 66:319-326.

SPIERS, A. G., and D. H. HOPCROFT. 1985. Ultrastructural studies of pathogenesis and uredinial development of *Melampsora larici-populina* and *M. medusae* on poplar and *M. coleosporoides* and *M. epitea* on willow. N. Z. J. Bot. 23:117-133.

SPURR, A. R. 1969. A low-viscosity epoxy resin embedding medium for electron microscopy. J. Ultrastr. Res. 26:31-43.

VIENNOTT-BOURGIN, M. G. 1978. *Uromyces transversalis* (Thüm.) Winter parasite dangereux des cultures de glaieuls. Academie d'Agriculture de France, Paris 64:880-885.

WINTER, G. 1884. Exotische Pilze. Flora 67:259-274.

CHAPTER 3

The Phenotypical Responses of Gladiolus Germplasm with Different Degrees of Resistance to *Uromyces transversalis*

ABSTRACT

The evaluation of populations of breeding lines, cultivars and species of the genus *Gladiolus* resulted in the development of an evaluation schedule and a standardized artificial inoculation technique. The population of cultivars that was evaluated is susceptible to *Uromyces transversalis*. However, some breeding lines did show an almost immune reaction as did some of the species. The parent species: *G. tristis* var. *tristis* and *G. daleni* show particular promise as parents in a breeding programme for resistance provided that they are used as the male parent. The results also indicate that a single rather than a complex resistance inheritance mechanism is involved. The spectrum of resistant and susceptible infection types of the evaluated breeding lines and species are similar. Thus, it has been possible, during the breeding for flower qualities, scent and resistance to thrips, to maintain a resistance and susceptiblity spectrum similar to that of the species base population.

INTRODUCTION

The genus *Gladiolus* L. is found in many places on the African continent, on the island of Madagascar and in countries bordering the Mediterranean from where several species found their way to other countries in Europe and Asia. The presence of two endemic species unique to Madagascar indicates the antiquity of the genus, for their ancestors must have inhabited the island before it was separated from the African mainland. According to Lewis *et al.* (1972), water-colour paintings of gladiolus species were made by Heinrich Claudius as early as 1685/6. These were preserved as part of the diary of Simon van der Stel on his trek to Bushmanland. By 1727, African gladioli (*G. angustus*) were seen flowering in Leiden gardens by Linnaeus, who published, in 1738, a description of this African species (Lewis *et al.* 1972).

The total number of species is about 180, of which 103 occur in Southern Africa (Lewis *et al.* 1972, Ohri and Khoshoo 1983). Southern Africa appears to be the primary centre of genetic diversity (Leppik 1970, Vavilov 1949 - 1950). According to Ohri and Khoshoo (1983), Eurasian species were initially cultured, but the real impetus to cultivated gladioli was provided by the introduction of South African species. Out of the known 180 species only eight species are credited for the origin of the cultivated gladioli. These eight elemental species, namely, *G. tristis* var. *concolor*, *G. cardinalis*, *G. papilio*, *G. primulinus*, *G. carneus* (described as a yellow-flowered form of *G. natalensis* from Victoria Falls, Zimbabwe, by Lewis *et al.* 1972) *G. oppositiflorus*, *G. natalensis* (syn. *G. daleni*, Hilliard and Burtt 1979) and *G. saundersii* (Ohri and Khoshoo 1983) are all native to South Africa. The South African species, *G. cruentus*, was only later introduced and used in crosses (Wilfret 1980).

The garden gladiolus cultivars were mainly bred by crossing of elemental African species, first in Europe and later in the United States of America. The attractive flower of gladiolus ensured that it came to be produced in a variety of cultivars in several countries. The breeding was primarily directed towards the improvement of flower quality. The current cultivars have long flower spikes adorned with large flowers compared with the short spikes and small flowers of the natural species, subspecies and varieties. Since gladiolus rust, *Uromyces transversalis* (Thüm.) Winter was absent from the main breeding areas, such as The Netherlands, no selection was made against the rust. Instead, resistance to diseases such as fusarium rot (*Fusarium oxysporum* f.sp. *gladioli)*, dry rot *(Stromatinia gladioli*), etc. was sought.

Currently, however, the rust has established itself in Southern and Western Africa and Morocco (Viennott-Bourgin 1979), Italy (Garibaldi and Aloj 1980), Malta (Collingwood 1970), Southern France and Spain (Cuzier *et al.* 1987), Argentine (Lindquist *et al.* 1979)

and Brazil (Goris, pers. comm.). The wide South African selection of readily available gladiolus germplasm that has been exposed to gladiolus rust for many years, provides an ideal base for a gladiolus rust resistance breeding programme.

This chapter is a progress report of the gladiolus rust resistance programme since its inception in 1984. The programme was carried out in collaboration with a geneticist, who was responsible for the other important qualities needed in a gladiolus cultivar, such as resistance to thrips (*Taeniothrips simplex*), good flower quality and length, scent, plant size and number of inflorescences. The author was responsible for the screening of the accessions for rust resistance.

MATERIALS AND METHODS

Since the inception of the rust evaluation programme in 1984, the inoculation technique has been improved considerably. Throughout this study the inoculations were done with a multi-spore isolate obtained from Cedara (Appendix I). The plants were evaluated either by the initial or finally developed techniques as follows:

Initial inoculation technique. Different nine-week-old gladiolus accessions were inoculated with a suspension of urediospores in a 0,1% aqueous suspension of Triton® B1956 by means of a De Vilbiss atomizer (Appendix I). The atomizer traversed in a horizontal plane at a distance of 30 cm from the upright gladiolus leaves. The plants were then kept overnight at free water conditions (Appendix II) by placing a plastic bag over the potted plant.

Final inoculation technique. Urediospores were applied to the leaf surface with an inoculating device (Appendix I) which ensured a uniform deposition of urediospores. The device was used in its horizontal mode to correspond as closely as possible with the

previously used hand-held method. Differences in the viability of urediospores used for inoculation between different trials, required the standardization of urediospore age. Consequently, urediospores were collected (Appendix I) from plants 2 d after the rupture of the uredium, and immediately used for inoculation. This method ensured maximum infection and uniform development of uredia. Inoculated plants were kept overnight (16 h) at free water conditions in a dew chamber in the dark (Appendix II).

Evaluation schedule. After inoculation the plants were transferred to a glasshouse in which the temperature varied between 15°C to 35°C. The plants were evaluated according to a schedule of infection types (Table 1). The evaluation scheme used was that drawn up by Roelfs (1984) for cereal rusts, but adapted by the present author for the requirements of gladiolus rust rating (Figs. 1 - 6). The plants were initially evaluated 15, 25 and 41 d post-inoculation and finally at 30 d post-inoculation only.

RESULTS

A large number of accessions were screened, but no statistically significant data are presented because the number of corms per accession was too small for an ANOVA. The results are divided into those obtained with commercially available cultivars, those with species naturally occurring in South Africa and those with breeding lines bred at the Vegetable and Ornamental Plant Research Institute.

The results of the evaluation of gladiolus cultivars for rust resistance are presented in Table 2. Twenty-three commercially available cultivars were evaluated and all fell in the class "susceptible" (for definition See Table 1). The distribution of the host responses defined in Table 1 within the cultivar population was 13% very susceptible, 30% susceptible and 57% moderately susceptible (Fig. 7).

Table 1. Types of responses[a] of gladiolus to infection by *Uromyces transversalis*

		Disease
Host response (class)[b]	Infection type	Symptoms
Immune (Res)	0	No uredia or other macroscopic sign of infection
Almost immune (Res)	;	No uredia, but a hypersensitive reaction expressed as necrotic or chlorotic flecks
Very resistant (Res)	1	Small uredia with necrosis
Moderately resistant (Res)	2	Small to medium-sized uredia often with chlorosis, necrosis or purple border
Heterogeneous (Mes)	X	Random distribution of different sizes of uredia or borders (chlorotic, necrotic or purple)
Moderately susceptible (Sus)	3	Small uredia without a border
Susceptible (Sus)	4	Medium-sized uredia without a border
Very susceptible (Sus)	5	Large uredia without a border initially developing first transversely and then parallel to the leaf veins

[a] After Roelfs (1984), adapted to gladiolus rust.

[b] Res, resistant; Mes, Mesothetic; Sus, susceptible.

Stereo micrographs (Figs. 1 - 6) of the infection types on cultivars or breeding lines or species after artificial inoculation of the leaves.

Fig. 1. Fleck (;), or almost immune host response in class resistant.

Fig. 2. Very resistant (1) host response in class resistant.

Fig. 3. Moderately resistant (2) host response in class resistant.

Fig. 4. Moderately susceptible (3) host response in class susceptible.

Fig. 5. Susceptible host response (4) in class susceptible.

Fig. 6. Very susceptible (5) host response in class susceptible.


1
2
3
4
5
6

Table 2. The responses of gladiolus cultivars to infection with *Uromyces transversalis*

Cultivar ([a])	Mean infection type[b]	Class
Alibaba (1)	5	Sus
Breakdown (6)	3	Sus
Breaklaw (1)	3	Sus
Campanella (8)	4	Sus
Comet (7)	3	Sus
Dancing Doll (7)	3	Sus
Fortuna (1)	5	Sus
Impromptu (1)	5	Sus
Lucette (2)	4	Sus
Madrilene (2)	4	Sus
Miss America (3)	3	Sus
Peter Pears (3)	3	Sus
Picollo (7)	3	Sus
Poseidon (2)	3	Sus
Prins Claus (2)	3	Sus
Red Bantam (4)	3	Sus
Schipper (8)	4	Sus
Shamrock (8)	4	Sus
Sunset (8)	3	Sus
Tieplo (2)	4	Sus
Tinkerbell (5)	3	Sus
Velvet Ruby (4)	3	Sus
Venus (1)	4	Sus

[a] the number of pots (three plants per pot) of the cultivar that were evaluated.

[b] infection type as described in Table 1.

Table 3. The response of Gladiolus species and varieties to infection with *Uromyces transversalis*

Species ([a]) and subspecies	Mean infection type[b]	Class
G. alatus v. *alatus* (4)	3	Sus
G. alatus v. *meliusculus* (2)	3	Sus
G. alatus v. *speciosus* (1)	5	Sus
G. angustus (2)	4	Sus
G. bellus/papilio (4)	3	Sus
G. carinatus s. *carinatus* (4)	3	Sus
G. carneus (4)	3	Sus
G. crassifolius (1)	2	Res
G. daleni (19)[c]	1	Res
G. elliotii (7)	3	Sus
G. embroys (2)	2	Res
G. equitans (3)	4	Sus
G. floribundus s. *floribundus* (2)	2	Res
G. floribundus s. *miniatus* (2)	2	Res
G. invenustus (1)	2	Res
G. microcarpus (1)	4	Sus
G. ochroleucus (2)	1	Res
G. orchidiflorus (2)	3	Sus
G. papilio (7)	1	Res
G. quandrangulus (6)	5	Sus
G. rogersii v. *graminifolius* (2)	4	Sus
G. scullyi (5)	4	Sus
G. tristis (4)	2	Res
G. tristis v. *concolor* (5)	1	Res
G. tristis v. *tristis* (6)[d]	1	Res
G. undulatus (2)	2	Res
G. uysiae (1)	5	Sus

[a] the number of pots (three plants per pot) per species that were evaluated; v. = variety and s. = subspecies.
[b] infection type as described in Table 1.
[c] this species consisted of seven ecotypes with different host responses (infection type - number of pots (three plants per pot) evaluated); ;-4, 1-1, 1-2, 1-2, 2-9, 2-1 and 2-1.
[d] this variety consisted of three ecotypes which differed in their host response (infection type - number of pots three plants per pot) evaluated; ;-2, 2-2 and 2-2.

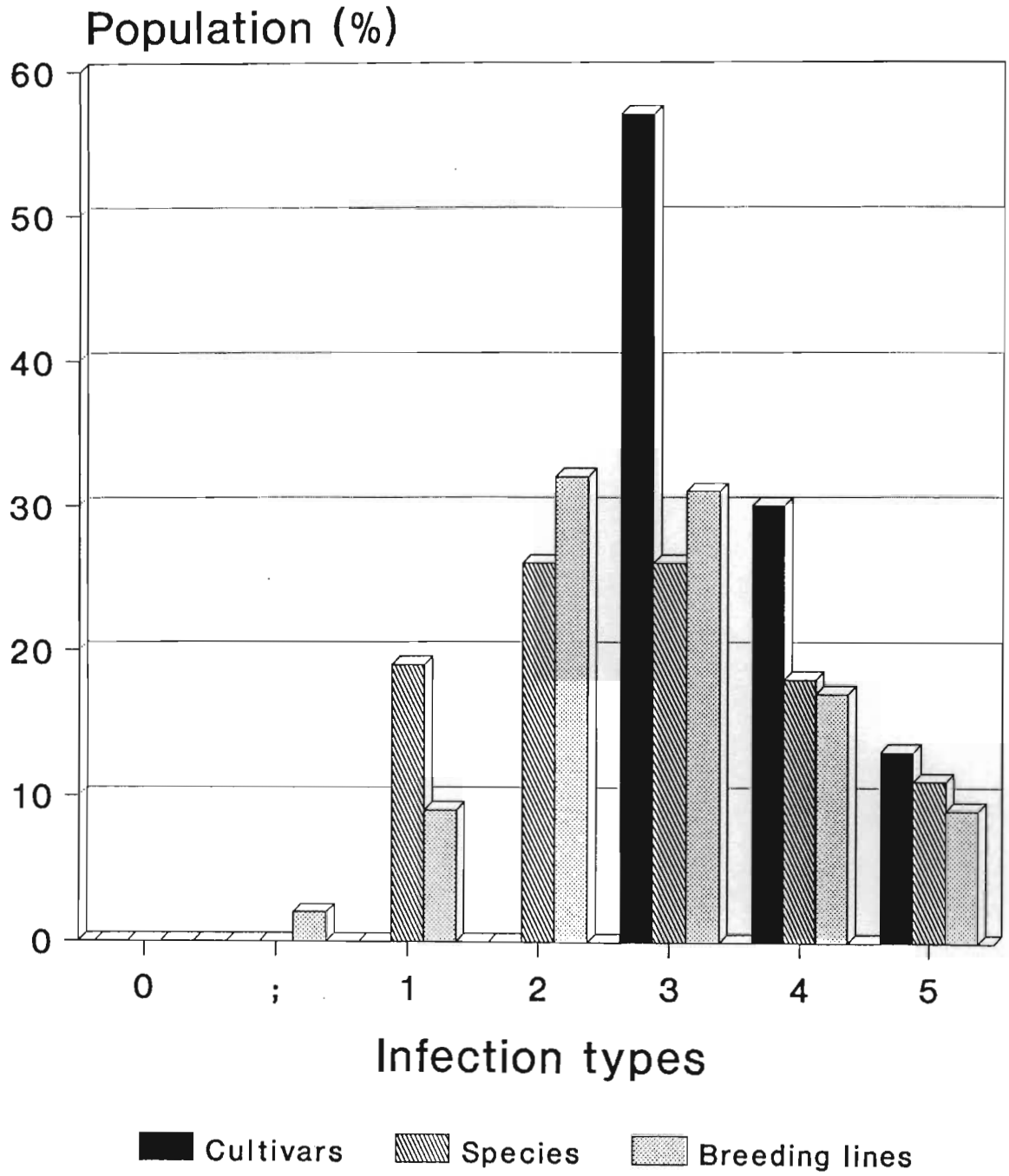

Fig. 7. A histogram of the profile of the responses (Table 1) of cultivars, species and varieties and breeding lines to infection by *Uromyces transversalis* under controlled conditions.

The different responses to infection by *U. transversalis* in a population of species and varieties are presented in Table 3. The results differed from those recorded for the gladiolus cultivars. The species exhibited a wider variety in host response, ranging from very resistant to very susceptible. The distribution of host responses was 11% very susceptible, 18% susceptible, 26% moderately susceptible, 26% moderately resistant and 19% very resistant. The responses appear to be almost normally distributed as would be expected of a natural population (Fig. 7). Species such as *G. tristis* var *tristis* and *G. daleni* were represented by three and seven ecotypes respectively. These ecotypes showed different responses to infection, for example the response of *G. daleni* ecotypes varied from infection type 2 to a type ; (fleck) reaction.

The response of the selected siblings of crosses between species, cultivars and other breeding lines to infection are presented in Table 4. As expected, in the selected crosses there was a much wider range of responses than that obtained with the species. The responses were distributed as follows: 2% almost immune, 9% very resistant, 32% moderately resistant, 31% moderately susceptible, 17% susceptible and 9% very susceptible.

Where information on both parents is available, it is evident that the resistance of certain parent species is inherited by the siblings. The inheritance of resistance from *G. daleni* and the more extensively used *G. tristis* var *tristis* is presented in Table 5. The table shows that the resistant parent does not necessarily convey its resistance to the siblings; different levels of resistance can be encountered in the progeny of the same cross. The cross *G. tristis* var *tristis* X Vuurland resulted in selections which ranged from a type 5 to a fleck reaction. The lack of intermediate reactions in this cross, where the progeny exhibits either susceptibility or resistance, implies that resistance is dominant. Although the genes involved in the inheritance of the resistance could not be identified in this study, it appears from the data that a simple inheritance system is present.

Table 4. The response of gladiolus crosses to infection by *Uromyces transversalis*

Crosses[a]	Selection[b]	Infection type[c]	Class[c]
76/204	32 (2)	2	Res
	95 (2)	2	Res
76/207	24 (2)	2	Res
76/210	109 (2)	2	Res
	169 (2)	3	Sus
	19 (1)	3	Sus
	70 (2)	3	Sus
	83 (2)	4	Sus
76/211	106 (2)	2	Res
	123 (2)	2	Res
	129 (2)	1	Res
	138 (2)	2	Res
76/212	1 (2)	3	Sus
	2 (2)	3	Sus
	3 (2)	3	Sus
	6 (2)	3	Sus
76/213	43 (2)	3	Sus
	92 (2)	2	Res
78/220	8 (2)	4	Sus
79/201	32 (2)	2	Res
79/209	(2)	3	Sus
79/214	(1)	3	Sus
79/215	(2)	3	Sus
79/236	(3)	3	Sus
79/249	(3)	3	Sus
79/252	(3)	2	Res
80/201	(1)	2	Res
80/202	34 (4)	3	Sus
80/207	(2)	3	Sus
80/216	(1)	2	Res
80/216	12 (2)	2	Res
80/223	8A (1)	4	Sus
80/225	(1)	4	Sus
	1 (1)	4	Sus
	6 (2)	3	Sus
80/226	1 (3)	5	Sus
	9 (6)	4	Sus
80/233	(2)	3	Sus
80/240	(2)	5	Sus
	16 (1)	2	Res
	2 (1)	1	Res
	24 (2)	2	Res
	26 (3)	;	Res
	7 (1)	2	Res
80/245	(1)	2	Res
80/247	(1)	2	Res
80/248	(2)	5	Sus
80/272	(2)	3	Sus
80/277	(1)	1	Res
80/279	(2)	3	Sus
80/280	(1)	4	Sus
80/284	(1)	1	Res
80/285	(1)	4	Sus
80/289	(3)	3	Sus
80/293	(1)	4	Sus
80/294	(2)	4	Sus
80/295	(1)	2	Res
81/210	(1)	2	Res
81/222	(2)	2	Res
84/202	(2)	5	Sus
87/43	(1)	5	Sus
87/44	(1)	5	Sus
87/72	(1)	4	Sus
87/90	(1)	1	Res

[a] the cross is designated by year and number eg. 76/213, the 213 th cross made in 1976.
[b] the number pots (three plants per pot) of that selection that were evaluated.
[c] infection type as described in Table 1.

Table 5. Comparison of the responses of Gladiolus parents and siblings to infection by *Uromyces transversalis*

Female parent ([a])	Male parent ([a])	Sibling selection(s) ([a])
G. carneus (3-4)	*G. tristis* v. *tristis* (1-6)	76/204 (2-4)
G. liliaceus (0-0)	*G. tristis* v. *tristis* (1-6)	76/207/24 (2-2)
G. lewisiae (0-0)	*G. tristis* v. *tristis* (1-6)	79/252 (2-3)
Vuurland (0-0)	*G. tristis* v. *tristis* (1-6)	80/240 (5-2)
		80/240[b] (2-4)
		80/240/2 (1-1)
		80/240/26 (;-3)
Magic eye (0-0)	*G. tristis* v. *tristis* (1-6)	80/245 (2-1)
Picollo (3-7)	*G. tristis* v. *tristis* (1-6)	80/247 (2-1)
Campanella (4-8)	*G. tristis* v. *tristis* (1-6)	80/248 (5-2)
G. tristis v. *tristis* (1-6)	*G. orchidiflorus* (3-2)	80/233 (3-2)
White Friendship (0-0)	*G. daleni* (1-19)	80/216/12 (2-2)

[a] the infection type (Table 1) followed by the number of pots (three plants per pot) that were evaluated.

[b] this is the bulked result of 80/240/3, 80/240/7 and 80/240/24.

The results of an evaluation of the progeny of two different reciprocal crosses are presented in Table 6. *G. tristis v. tristis* was used as either male or female parent in a cross with *G. alatus v. alatus*. *G. daleni* was similarly crossed with *G. bellus/papillio* F1. In both cases the resistant donor gave rise to a more resistant sibling when used as a male parent. Thus, the sex of the parent appears to play a role in the inheritance of resistance in gladiolus breeding.

DISCUSSION

In these trials none of the cultivars showed resistance to gladiolus rust, and therefore their cultivation in areas in South Africa known for *U. transversalis* epidemics is not feasible. Since none of these cultivars was locally bred, the reason for their susceptibility is most probably the absence of naturally occurring rust during the breeding programme, even though the elemental species were of Southern African origin. This illustrates the danger of breeding cultivated plants outside their primary centre of genetic diversity. The loss of natural resistance to diseases specific to gladiolus in commercially available gladiolus cultivars could prove disastrous if, for instance, *U. transversalis* were introduced into Florida (USA) where conditions would be conducive to the development of this disease.

The species and varieties collected from various areas in South Africa showed a large variation in their response to infection by *U. transversalis*. The distribution of infection types in the population of breeding lines was very similar to that found in the population of species and varieties, indicating that basically the same germplasm was maintained in the breeding lines. Since some breeding lines have improved flower and market qualities over the wild parent species and have retained resistance to rust, breeding for resistance has been met with some success.

Table 6. Two examples of the inheritance of a gladiolus species and a variety subjected to reciprocal interspecific crossing

Female parent [a]		Male parent [a]
	Sibling selection [a]	
G. tristis v. *tristis* (1-6)	X	*G. alatus* v. *alatus* (3-4)
	↓	
	76/212/1,2,3,6 (3-8)	
G. alatus v. *alatus* (3-4)	X	*G. tristis* v. *tristis* (1-6)
	↓	
	76/211/106,123,138 (2-6) and 129 (1-2)	
G. bellus/papillio F1 (3-4)	X	*G. daleni* (1-19)
	↓	
	79/201/32 (1-2)	
G. daleni (1-19)	X	*G. bellus/papillio* F1 (3-4)
	↓	
	80/201 (2-1)	

[a] the infection type followed by the number of pots (three plants per pot) that were evaluated. The sibling selections gave consistent readings unless otherwise stated.

Differential ecotypical responses to the rust pathogen probably relate to the exposure of ecotypes to the periodic presence, absence or varying levels of disease. The development of rust on a gladiolus plant is largely dependent on the length of the free water period (Appendix II). Therefore, the frequency with which disease occurs will depend on the environmental conditions in a particular habitat. Resistant ecotypes have thus evolved in an environment prone to gladiolus rust epidemics, whereas lesser resistance has evolved in areas with less severe and possibly more infrequent epidemics. If resistance has evolved *de novo* in different ecosystems, or if different levels have evolved in different plant communities, it is probable that several different types of resistance exist. It is important that these should be identified to be harnessed in various ways. For example: the fleck infection type can be utilized in cultivars for export, since no urediospores would develop and phytosanitary measures would not restrict exports from countries in which *U. transversalis* is known to occur. An infection type 1 resistant response would be suitable for the breeding of a gladiolus cultivar for the local market, should such a cultivar be excellent in other respects, because limited sporulation would result in sufficient suppression of the epidemic.

The reciprocal crosses show that, to gain maximum resistance, it is important, at least in some cases, that the resistant parent should be used as a male rather than the female parent. The reason for this is not clear. The results also indicate that resistance is dominant, simplifying their deployment in the breeding of rust resistant gladiolus cultivars.

The gladiolus breeding lines appear to have a tremendous future, and by widening the germplasm base, desirable changes are possible in blooming period, constitution of spike shape, colour of flowers, scent, and disease resistance, in particular gladiolus rust resistance.

LITERATURE CITED

COLLINGWOOD, E. F. 1970. New records, - Malta. Rust disease of gladiolus. Plant Protection Bulletin F.A.O. 18:69.

CUZIER, J -P., J -M. GAILIETON, R. CUESTA, and S. REGIS. 1987. The gladiolus rust in Southern Europe (Translated from French). Gladiograms 67:2-3.

GARIBALDI, A., and ALOJ, B. 1980. Observations on biology and control of *Uromyces transversalis* (Thüm) Winter on gladiolus in Southern Italy. Acta Hortic. 109:409-411.

GORIS, MARIJKE. Klaas Schoenmaker & Filhos, Fazenda Holambra, Caixa Postal 61, CEP 13.820, Jaguarina, Sao Paolo, Brazil.

HILLIARD, O. M., and B. L. BURTT. 1979. Notes on some plants of Southern Africa chiefly from Natal. No. VIII. Notes of the Royal Botanic Garden, Edinburgh 37:297-299.

LEPPIK, E. E. 1970. Gene centers of plants as sources of disease resistance. Ann. Rev. Phytopathol. 8:323-344.

LEWIS, JOYCE G., A. AMELIA, OBERMEYER, and T. T. BARNARD. 1972. Gladiolus : A revision of South African species. Edited by H. B. Rycroft. J. South Afr. Bot. 10 (Supplement), Purnell, Cape Town. p. 316.

LINDQUIST, J. C., H. E. ALIPPI, and C. M. MEDERA. 1979. Una grave epidemia de roya del gladiolo (*Uromyces gladioli* P. Henn.), en la provincia de Santa Fe (Republica Argentina). Jorn. Fitosan. Argent. 2:719-724.

OHRI, D., and T. N. KHOSHOO. 1983. Cytogenetics of garden gladiolus. IV. Origin and evolution of ornamental taxa. Proc. Indian Natn. Sci. Acad. B49:279-294.

ROELFS, A. P. 1984. Race specificity and methods of study. *In* The cereal rusts. Vol 1. Edited by W. R. Bushnell and A. P. Roelfs. Academic Press, Orlando. pp. 131-164.

VAVILOV, N. I. 1949 - 1950. The origin, variation, immunity, and breeding of cultivated plants (Translated from Russian by K. S. Chester). Chron. Bot. 13:1-364.

VIENNOTT-BOURGIN, M. G. 1978. *Uromyces transversalis* (Thüm.) Winter, parasite dangereux des cultures de glaieuls. Academie d'Agriculture de France, Paris 64:880-885.

WILFRET, G. 1980. Gladiolus. *In* Introduction to floriculture. Edited by R. A. Larson. Academic Press, New York. pp. 165-181.

CHAPTER 4

The Ultrastructural Morphology of *Uromyces transversalis* Infection of a Resistant Gladiolus Species and a Susceptible Cultivar

ABSTRACT

The infection structures of gladiolus rust, *Uromyces transversalis*, on and in the leaves of the susceptible gladiolus cv. Goldfield and the resistant species, *Gladiolus daleni*, were examined by scanning electron microscopy. The haustorial apparatus in mesophyll cells of the susceptible and resistant hosts, and intercellular hyphae, were viewed by transmission and scanning electron microscopy. The major determinant of resistance was manifested in the abortion of substomatal vesicles with primary hyphae with a swollen tip prior to the formation of a haustorial mother cell septum. This was attributed to the incomplete putatively adhesion of haustorial mother cells. Despite their incomplete putatively adhesion, a few haustorial mother cells formed and successfully penetrated mesophyll cells. After penetration, such haustoria aborted in the mesophyll cells in various ways: apparently immature haustoria aborted, the periphery of developed haustoria became undulated, or both severely undulated and electron-dense, and some developed into apparently normal haustoria except for the close association of mitochondria with the extra-haustorial membrane. Although the mesophyll cells in the resistant reaction showed degrees of disorganization, haustorium death appeared to occur prior to cell death. No urediospores were formed in the incompatible reaction.

INTRODUCTION

The host range of *Uromyces transversalis* includes the following genera: *Gladiolus*, *Tritonia*, *Watsonia*, (Doidge 1950), *Crocosmia* (Bisby and Wiehe 1953, Kuiper and Boerema 1972) and *Freesia* (Jørstad 1956). These five genera are divided into four sub-tribes which according to Goldblatt (1971) belong to the tribe Ixieae. Later this tribe was elevated to sub-family level, Ixiodeae, by Dahlgen *et al.* (1985). Unfortunately no

research has been conducted on the interaction of *U. transversalis* with its hosts. Therefore, there is no information on the existence of formae speciales and/or races of the pathogen.

In the past, quantitative studies on the morphology of rust infection structures in susceptible and resistant hosts and non-hosts have been done successfully with the aid of light (Heath 1971, Heath 1972, Heath 1974, Hilu 1965, Leath and Rowell 1966, Littlefield 1973) and fluorescence (Niks 1983a, Niks 1983b, Niks and Kuiper 1983) microscopy. Preliminary trials by the author to conduct this study quantitatively with either light or fluorescence microscopy, using the methods of Kuck *et al.* (1981) and Rohringer *et al.* (1977), failed due to the extraordinary thickness of the leaves of gladiolus plants. Electron microscopy has also previously been employed to highlight certain aspects of infection structures in resistant or susceptible tissue (Littlefield and Heath 1979). The author reports on the development of infection structures of *U. transversalis* as studied with the aid of scanning and transmission electron microscopy on and in the leaves of a susceptible cultivar and a resistant species of the genus *Gladiolus*, and a non-host, *Zea mays*. The terminology used by Littlefield and Heath (1979) is followed throughout unless otherwise indicated.

MATERIALS AND METHODS

Rust propagation and inoculation. Freshly harvested urediospores of *U. transversalis* (PREM 47693, National Collection of Fungi, Plant Protection Research Institute, Pretoria) produced on two-month-old susceptible gladiolus plants (cv. Goldfield) in a glasshouse (18°C - 35°C) were used to inoculate plants. For inoculation, spores were brushed over one surface of the distal third of mature gladiolus leaves of "Goldfield" and a resistant species, *G. daleni* (See Chapter 3), hereafter called " the cultivar" and "the species" respectively, as well as a non-host, maize. Morphology and position of the

gladiolus leaf preclude distinction between an ab- and adaxial surface; on maize the adaxial surface was inoculated. Inoculated plants were placed in a dew chamber at 20°C for 16 h in the dark, and then moved to the glasshouse. The experiment was conducted twice with two cultivar, two species and two maize plants.

Scanning electron microscopy.

Standard technique. Four pieces per leaf from two leaves of two plants of both the cultivar, species and non-host were excised at 96 h post-inoculation (HPI). The pieces were cut into 2 mm by 4 mm specimens and fixed in 3% glutaraldehyde in a 0.05 M sodium cacodylate buffer, pH 6.8 - 7.2, for 12 h or overnight, washed twice in the buffer, post-fixed for 3 h in 2% osmium tetroxide in the buffer, washed twice in buffer and dehydrated in a graded ethanol series. The leaf specimens were then critical point dried with carbon dioxide as a transition fluid and mounted on copper stubs. The epidermis of the gladiolus and maize leaf specimens were removed as described earlier (See Chapter 1). The epidermis and the tissue remaining on the stubs were gold coated in a Balzers® sputter coater. Both stripped epidermis and stripped leaf material were examined with a Jeol® JSM-35 scanning electron microscope operated at 15 kV.

Polyethylene glycol embedding. Specimens of gladiolus (cultivar and species) leaf tissue 10 d post-inoculation (DPI) were prepared as described above except that during dehydration the specimens were embedded in polyethylene glycol (M.W. 4000 - 6000) according to the method described by Hamilton-Attwell *et al.* (1986). The specimen blocks were trimmed perpendicularly and parallel to the leaf veins with an American Optical® Spencer "820" rotary microtome. Subsequently the material was critical point dried and examined according to the standard technique.

Freeze-fractioning. Fresh gladiolus cv. Goldfield leaf tissue 11 DPI was prepared for freeze-fractioning according to conventional techniques in a Polaron Biorad® E7400 cryo-unit and viewed with a Jeol® JSM-840 scanning electron microscope operated at 10 kV.

Data presentation. During processing of the leaf specimens for scanning electron microscopy many ungerminated urediospores were removed during preparation. These urediospores can therefore not be counted, nor used for the calculation of percentages. The total number of infection structures on and in leaf pieces of the species and the cultivar was determined by scanning electron microscopy. The data obtained from the leaf exterior were processed separately from data originating from the leaf interior, since the stripping method precludes the stripping of the entire specimen, and the fate of not all appressoria could therefore be determined. On the leaf exterior the total number of germinated urediospores with appressoria was expressed as a percentage of the germinated urediospores. In the leaf interior four stages in infection structure development were categorized, viz. substomatal vesicles (SSV), SSVs with primary hyphae and SSVs with secondary hyphae on the stripped epidermis, and SSVs that had developed haustorial mother cells (HMC) and intercellular hyphae in the leaf tissue after stripping (final stage). Since the attainment of eg. the final stage implies that the other three stages have been successfully completed, totals presented under each category are cumulative. These cumulative values were then expressed as a percentage of the total infection structures in the leaf interior.

Transmission electron microscopy. Leaves of the cultivar and the species, inoculated and uninoculated, were cut into 2 mm by 4 mm pieces and fixed overnight under 200 mm Hg vacuum in 3% glutaraldehyde in a 0.05M sodium cacodylate buffer (pH 6.8 - 7.2), washed twice in buffer and post-fixed in 2% osmium tetroxide in the same buffer. Dehydration was performed either in an ethanol series for embedding in Spurr's resin (Spurr 1969) or in an acetone series followed by two changes in propylene oxide leading to embedding in Epon/Araldite (Anderson and André 1969) resin. The specimen blocks were sectioned with glass knives (50 nm to 70 nm) parallel and perpendicular to the long axes of the uredia. Sections were stained for 15 min with 2% uranyl acetate in boiled, double-distilled water,

washed in double-distilled water and post-stained for 15 - 20 min in lead citrate (Reynolds 1963), washed in double-distilled water and viewed with a Jeol® 100 C or CX transmission electron microscope operated at 60 and 80 kV respectively.

OBSERVATIONS

Presented in Figure 1 are the percentages of observed infection structures on and in the leaf pieces of the species and cultivar. A total area of 35.42 mm^2 and 25.53 mm^2 with a total number of 1886 and 649 infection structures (including germtubes) were observed for the resistant species and the susceptible cultivar respectively. The development of the fungus was arrested at 96 HPI, and since the fate of not all appressoria could be determined the results for pre-penetration and post-penetration should be evaluated separately.

Pre-penetration events. On the leaf surface of the species, the percentage of germtubes that successfully located stomata and formed appressoria (Figs. 2 and 3) was much lower than on the leaf surface of the cultivar (Fig. 1). Germtubes that failed to locate stomata (Fig. 5) often reached a considerable length, and were frequently aerial (Fig. 7) on both the cultivar and the species. No evidence of directional growth of the germtubes towards stomata was found on either of the leaf surfaces, and germtubes often grew over stomata without forming appressoria. The latter phenomenon was observed more often on resistant than on susceptible leaf surfaces. The infection peg formed by an appressorium over a stoma of the species was occasionally (5%) bifurcate (Fig. 4). The trichomes on the resistant leaf surface were twice the height of those on the susceptible leaf surface (Figs. 6 and 7). In other respects the leaf surface morphology appeared similar.

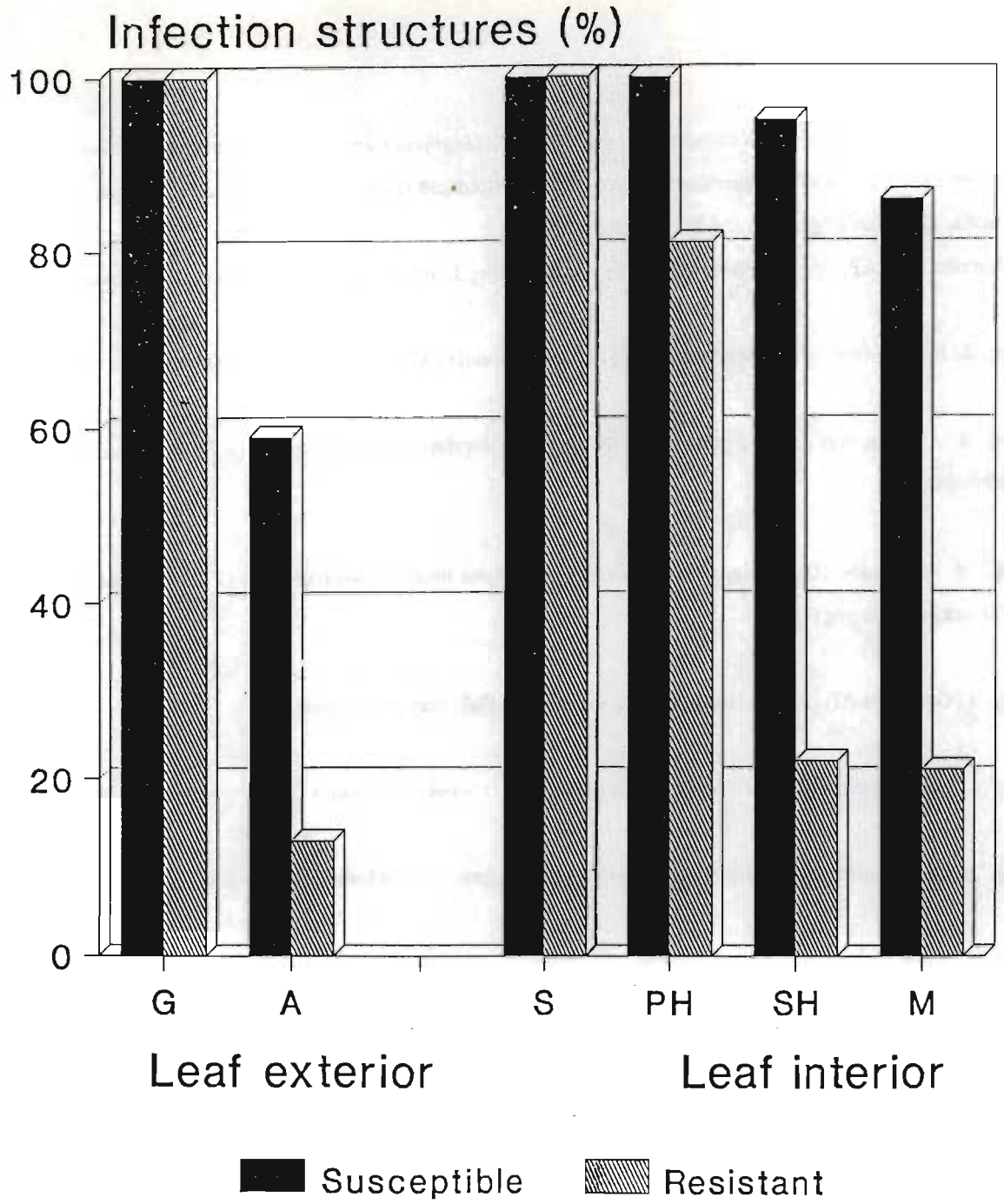

Fig. 1. A histogram of the developmental stages of infection structures of *Uromyces transversalis* interrupted at 96 h post-inoculation on and in leaves of a susceptible gladiolus cultivar and a resistant gladiolus species examined by scanning electron microscopy. The results are divided into infection structures on the exterior of the leaf and the intercellular infection structures in the leaf interior. On the leaf exterior the germinated urediospores that did form appressoria (A) on the resistant or susceptible host are expressed as a percentage of all the germinated urediospores (G) on the resistant or susceptible host respectively. The developmental stages of infection structures in the leaf interior of the resistant or susceptible host are expressed as a percentage of all infection structures within

Scanning electron micrographs of the infection structures of *Uromyces transversalis*, 96 h post-inoculation, on the exterior of the leaves of a susceptible gladiolus cultivar, Goldfield (Figs. 2, 3 and 6), and a resistant gladiolus species, *G. daleni* (Figs. 4, 5 and 7). Scale bar = 10 µm.

Abbreviations: AP, appressorium; C, cuticle; G, germtube; I, infection peg; T, trichome; U, urediospore

Fig. 2. Normal development of germtube (G) into appressorium (AP) located in pre-stomatal chamber of leaf.

Fig. 3. Urediospores (U) and germtubes (G) that have developed into appressoria (AP) on leaf surface with trichomes (T).

Fig. 4. Germtube (G) with appressorium (AP) over stoma between two trichomes (T). Appressorium has bifurcate infection peg (I).

Fig. 5. Germtube (G) that has failed to locate stoma. Note flaky texture of cuticle (C).

Fig. 6. Urediospore (U) with surface-adherent germtube (G) between trichomes (T).

Fig. 7. Urediospores (U) and aerial and surface-adherent germtubes (G) between trichomes (T).

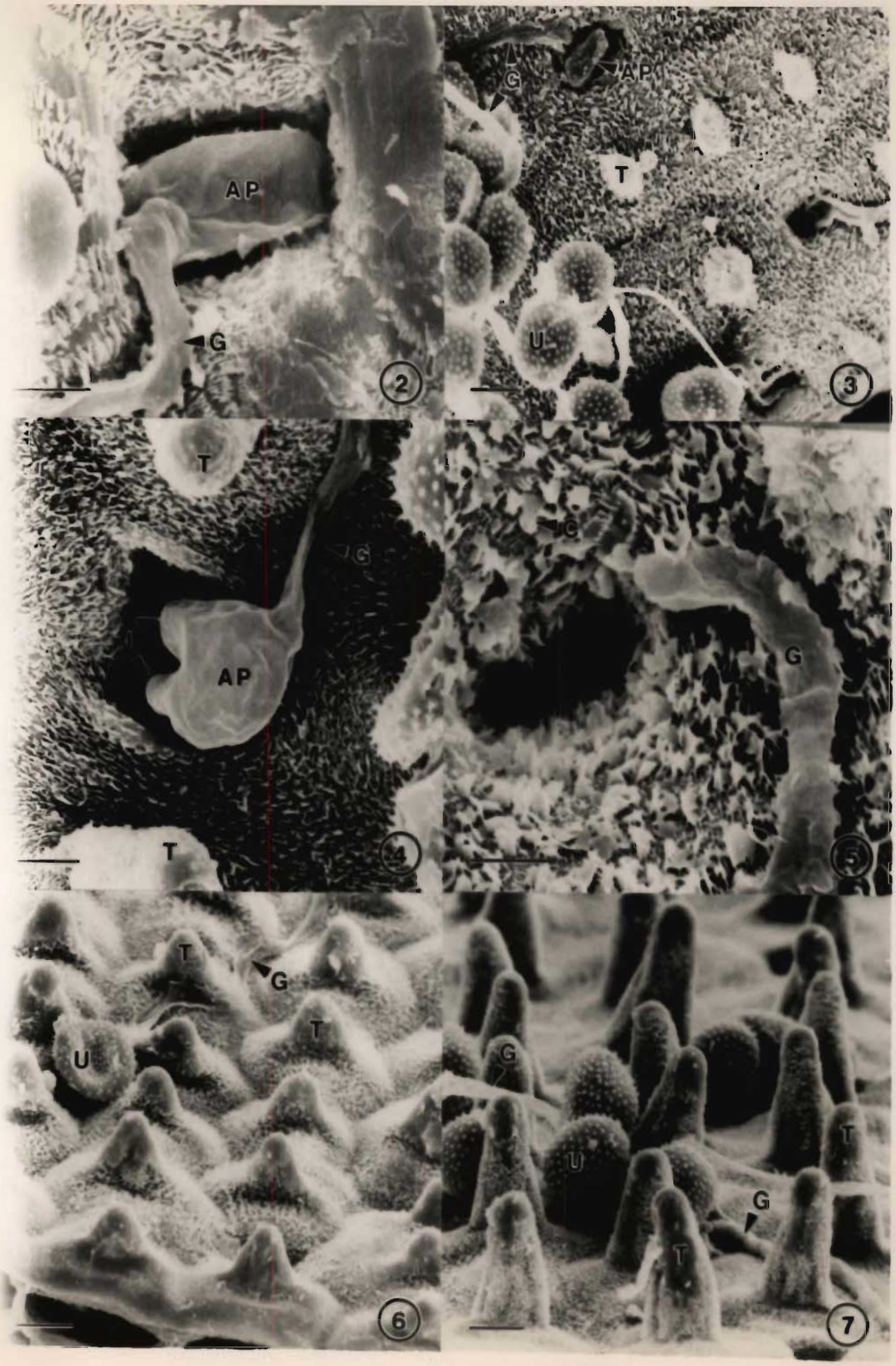
AP
G
2
G
AP
T
U
3
T
G
AP
T
4
G
G
5
T
G
T
U
6
G
T
U
G
T
7

Pre-haustorial events. The percentages of SSVs (Stage 1 or 2), SSVs with primary hypha(e) (Stage 3 or 4), SSVs with secondary hypha(e) (Stage 5) on the stripped epidermis, and SSVs together with HMCs and intercellular hyphae observed in the stripped tissue (See Chapter 1 for definitions of SSV stages) of infected susceptible or resistant gladiolus leaf tissue studied are presented in Figure 1. Ninety-six HPI, 86% of the infection structures inside the susceptible leaf tissue had developed into the final stage (Fig. 10) and very few Stage 1 to 4 SSVs were observed (Fig. 1). In the resistant tissue 21% of the infection structures had developed into the final stage (Fig. 1). Concomitantly, a higher percentage of pre-haustorial mother cell SSV stages (1, 2 and 3) was observed in the species tissue (Fig. 1). The Stage 1 and 2 SSVs in the resistant host appear normal, but their development had been arrested. Besides the normal infection structures, which are swollen and show no signs of structural disorganization, there are aborted infection structures which are structurally disorganized and show signs of collapse. An unusually high number of Stage 3 SSVs in the species aborted. A small percentage of infection structures in the resistant host aborted only at the final stage SSV (Fig. 11). The primary hyphae of gladiolus rust infection structures in the cultivar, after delimiting an HMC, would adhere to mesophyll cells and sever at or close to the SSV, during epidermis stripping. Primary hyphae of Stage 3 SSVs in the resistant host aborted (Fig. 15) after establishing loose contact (Fig. 12) with the mesophyll cell. Loose contact with mesophyll cells apparently also affects adherence of tip of the primary hypha to the mesophyll cell wall in the resistant host. The tips of such primary hyphae separated from the cell wall (Figs. 9, 12 and 13) during stripping of the epidermis and failed to delimit an HMC as shown by the absence of a haustorial mother cell septum. The tips of these primary hyphae often retained their shape at 96 HPI, whereas their SSVs normally collapsed (Fig. 9). In the susceptible reaction the primary hyphae developed asynchronously (Fig. 8, See Chapter 1), while in the resistance reaction the primary hypha opposite the first-developed primary hypha failed to develop on the often collapsed SSV (Figs. 9 and 12). The tip of the aborted primary hypha appeared electron-dense in section in the resistant leaf tissue


PH
SSV
8
PH
SSV
9
IH
S
I
SH
PH
10
PH
I
SSV
11
PH
CE
SSV
12
PH
13
HMC
S
PH
SSV
14

(Fig. 15). The few (1%) Stage 4 infection structures of *U. transversalis* that did develop on the stripped epidermis of the non-host, maize, aborted soon after the formation of the haustorial mother cell septum (Fig. 14).

The intercellular hyphae in the cultivar were more abundant and had a larger diameter (in section) than those observed in the species. Hyphae in the intercellular spaces of the susceptible leaf tissue were almost always in close contact with the host cells or one another (Fig. 19). A highly osmiophilic material, which the author interprets to be of an adhesive nature, was found between hyphae and between hyphae and the mesophyll cells (Fig. 19). In the resistance reaction, the hyphae were normally not in close contact with either the mesophyll cells or one another. Where adhesion to a mesophyll cell or to other hyphae did occur the adhesive material at the interface was less osmiophilic than in the susceptible reaction (Figs. 17 and 18). Less osmiophilic adhesive was also demonstrated where an HMC did form and penetrate the mesophyll cell wall (Fig. 21). Adherence at the HMC / mesophyll cell interface after haustorial neck formation in the resistant host was apparently partial and less of the adhesive material was evident. In those instances the connection between the HMC and the mesophyll cell occasionally can be severed (Fig. 16). This interface in the susceptible interaction was never observed to sever (Fig. 20). Two types of septa were observed in the intercellular hyphae: pseudosepta (Fig. 19) (Ehrlich *et al.* 1968) or infolded walls (Rijkenberg and Truter 1975) and typical septa (See Chapter 2).

Post-haustorial events. The development of intracellular infection structures that form after the penetration of the mesophyll cell wall of gladiolus by *U. transversalis* is reported in the following section.

In the susceptible cultivar, the penetration of the host cell wall appears to be enzymatic since the cell wall did not appear invaginated and signs of mechanical entry during penetration (Fig. 20) are absent. The haustorial mother cell wall consisted of six layers

Transmission electron micrographs of intercellular hyphae and haustorial mother cells of *Uromyces transversalis* in leaves of a susceptible cultivar (Figs. 19 and 20) and a resistant species, (Figs. 15 - 18 and 21).

Abbreviations: A, annulus part of the intrawall penetration torus; C, collar; CE, mesophyll cell; CW, mesophyll cell wall; HMC, haustorial mother cell; HN, haustorial neck; H1 - H6, haustorial mother cell wall layers close to the penetration site; IH, intercellular hypha; IW, infolded wall; ST, stem part of the intrawall penetration torus.

Fig. 15. Section of aborted primary hypha (PH) in contact with mesophyll cell (CE), 24 h post-inoculation. No haustorial mother cell septum has formed. Scale bar = 1 µm.

Fig. 16. Section of haustorial mother cell (HMC) severed from mesophyll cell (CE) at penetration site. Remnants (arrow) are visible close to haustorial neck (HN). Scale bar = 2 µm.

Fig. 17. Section through intercellular hypha (IH) attached to mesophyll cell wall (CW) with less osmiophilic material (arrows) at hypha/mesophyll cell interface. Scale bar = 1 µm.

Fig. 18. Section through intercellular hypha (IH) closely associated with mesophyll cell (CE) with less osmiophilic material (arrow) evident in the resistance reaction. Scale bar = 0.5 µm.

Fig. 19. Section through intercellular hyphae (IH) between mesophyll cells (CE) showing their close contact and osmiophilic material (small arrows) at their interfaces. Intercellular hypha (IH) with infolded wall (IW), opening partially occluded by vesicle (large arrow) in the susceptible reaction. Scale bar = 2 µm.

Fig. 20. Oblique section through haustorial mother cell (HMC) close to penetration site showing intrawall penetration site which consists of annulus (A) and stem (ST), and haustorial neck (HN) with collar (C) on either side. Evident in micrograph are the six layers in haustorial mother cell wall (H1 - H6) and osmiophilic material (arrow) at haustorial mother cell and host cell interface in susceptible reaction. Scale bar = 0.2 µm.

Fig. 21. Section through haustorial mother cell (HMC) and haustorial neck (HN) at penetration site showing less osmiophilic material (arrow) at interface with mesophyll cell. Careful observation of insert shows presence of six possible (H1 - H6) layers in haustorial mother cell wall in resistance reaction. Scale bar = 0.5 µm.

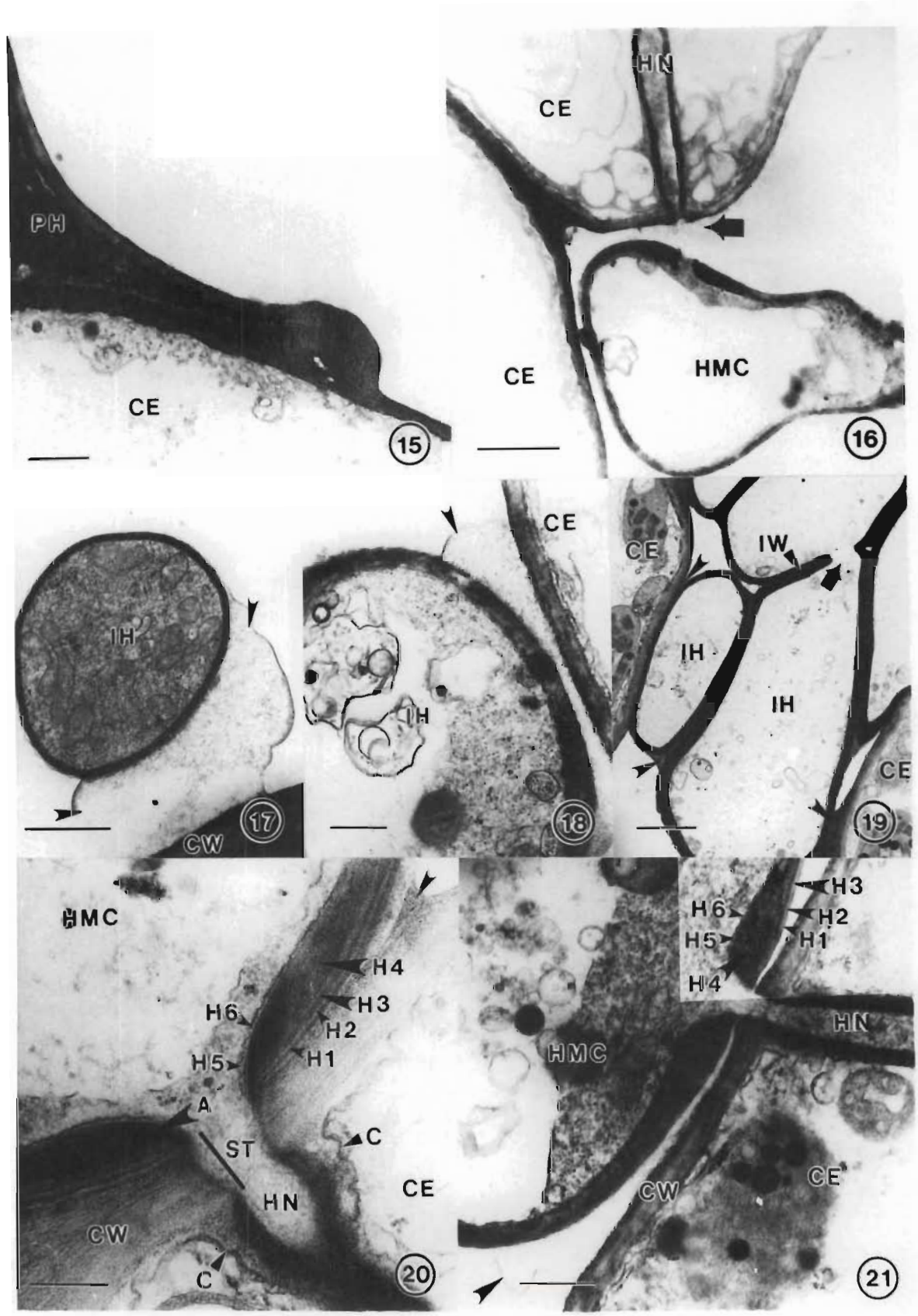
PH
CE
15
HN
CE
CE
HMC
16
IH
CW
17
CE
IH
18
CE
IW
IH
IH
CE
19
HMC
H6
H5
A
ST
HN
CW
C
H4
H3
H2
H1
C
CE
20
H3
H6
H2
H5
H1
H4
HN
HMC
CW
CE
21

(Figs. 20 and 21 - H1 to H6) in both the susceptible and resistance interactions. The breaching of the host cell wall results in an intrawall penetration torus (Chong *et al.* 1985b), which as shown in Figure 20, consists of an annulus (A) and a stem (ST). A HMC wall layer (Fig. 20 - H4) makes up the osmiophilic annulus which appears to be the only HMC wall layer involved in the stem. The annulus (A or H4 - Fig. 20) is also the thickest layer of the HMC wall at the penetration site. At the stem of the intrawall penetration torus, the wall layer (H4) remains continuous but very thin and merely lines the stem. This layer (H4) remains continuous in the haustorial neck, but is, however, considerably thicker in the haustorial neck than in the stem (Fig. 20). The other layers have no apparent role in the intrawall penetration torus. The proximal part of the neck is surrounded by a Type I collar (Fig. 23) (Littlefield and Heath 1979). A collar is deposited, presumably by the mesophyll cell, around the proximal part of the haustorial neck (Fig. 23). The haustorial neck (0.8 μm wide) was characterised by an electron-dense neck band except in one case where a possible break in the neck band area appeared electron-lucent (Fig. 23) bordered by electron-dense areas. The haustorial body varied in size and shape (Figs. 24, 26 and 27). Scanning electron microscopy showed that the haustorial body is a globose (Figs. 27 - 29), or an elongated oval (Fig. 24), or a lobed structure (Fig. 26), or a structure resembling an intracellular hypha (Fig. 34). The polyethylene glycol prepared scanning electron microscopy made possible the observation of the interior and exterior structure of the haustorial body in two different planes (Figs. 25 and 29). The haustorial body was associated with what appear to be host cytoplasmic vesicles (Fig. 26) which could also be seen in section. The haustorial body was separated from the mesophyll cell content by an electron-dense haustorial wall, extra-haustorial matrix and an extra-haustorial membrane (Fig. 22).

The haustorial apparatus in the resistant species was arrested or showed various degrees of degeneration in the mesophyll tissue. Probably the most dramatic manifestation of an intracellular resistance mechanism was the cytoplasmic disorganization of immature

Scanning electron micrographs after conventional (Fig. 28), freeze fracturing (Figs. 24 and 26) and polyethylene glycol (Figs. 25, 27 and 29) preparation, and transmission electron micrographs (Figs. 22 and 23) of the intracellular infection structures of *Uromyces transversalis*, 10 to 13 d post-inoculation in leaves of a susceptible cultivar.

Abbreviations: CL, chloroplast; CW, cell wall; EHM, extra-haustorial matrix; H, haustorium; HB, haustorial body; HL, haustorial lobe; HMC, haustorial mother cell; HN, haustorial neck; HW, haustorial wall; IH, intercellular hypha; M, mitochondrion; N, nucleus; V, vesicle.

Fig. 22. Section through host cell with cell wall (CW), chloroplasts (CL) and nucleus (N) of which shape had been affected by haustorial body (HB). Haustorial body (HB) contained within cell was sectioned through nucleus (N) and wall layers: haustorial wall (HW), extra-haustorial matrix (arrow) and extra-haustorial membrane (EHM). Scale bar = 2 µm.

Fig. 23. Section through haustorial mother cell (HMC) outside host cell (CE), and haustorial neck (HN) and haustorial body (HB) inside host cell. Proximal part of haustorial neck (HN) surrounded by Type I collar (C) and beyond second half of neck there is an electron-lucent neck band (arrow), bordered by smaller electron-dense bands on either side. Haustorial mother cell shows presence of mitochondria (M) at penetration site. Scale bar = 2 µm.

Fig. 24. Elongated oval shape of haustorial body (HB) with haustorial neck (HN) which became detached from host cell wall during freeze-fractioning of host tissue. Scale bar = 10 µm.

Fig. 25. View of haustorial body (HB) in host cell, after partial sectioning, revealing three-dimensional structure of haustorial body (HB). Scale bar = 10 µm.

Fig. 26. Haustorial lobe (HL) of haustorial body (HB) associated with vesicles (V) inside host mesophyll cell. Scale bar = 10 µm.

Fig. 27. Two globose haustorial bodies (HB) in mesophyll cell with intercellular hypha (IH) in intercellular space adjacent to cell. Scale bar = 10 µm.

Fig. 28. Globose haustorial body (HB) and haustorial neck (HN) exhibiting neck ring (arrow) inside host cell. Scale bar = 5 µm.

Fig. 29. Haustorial body (HB) content. Scale bar = 10 µm.

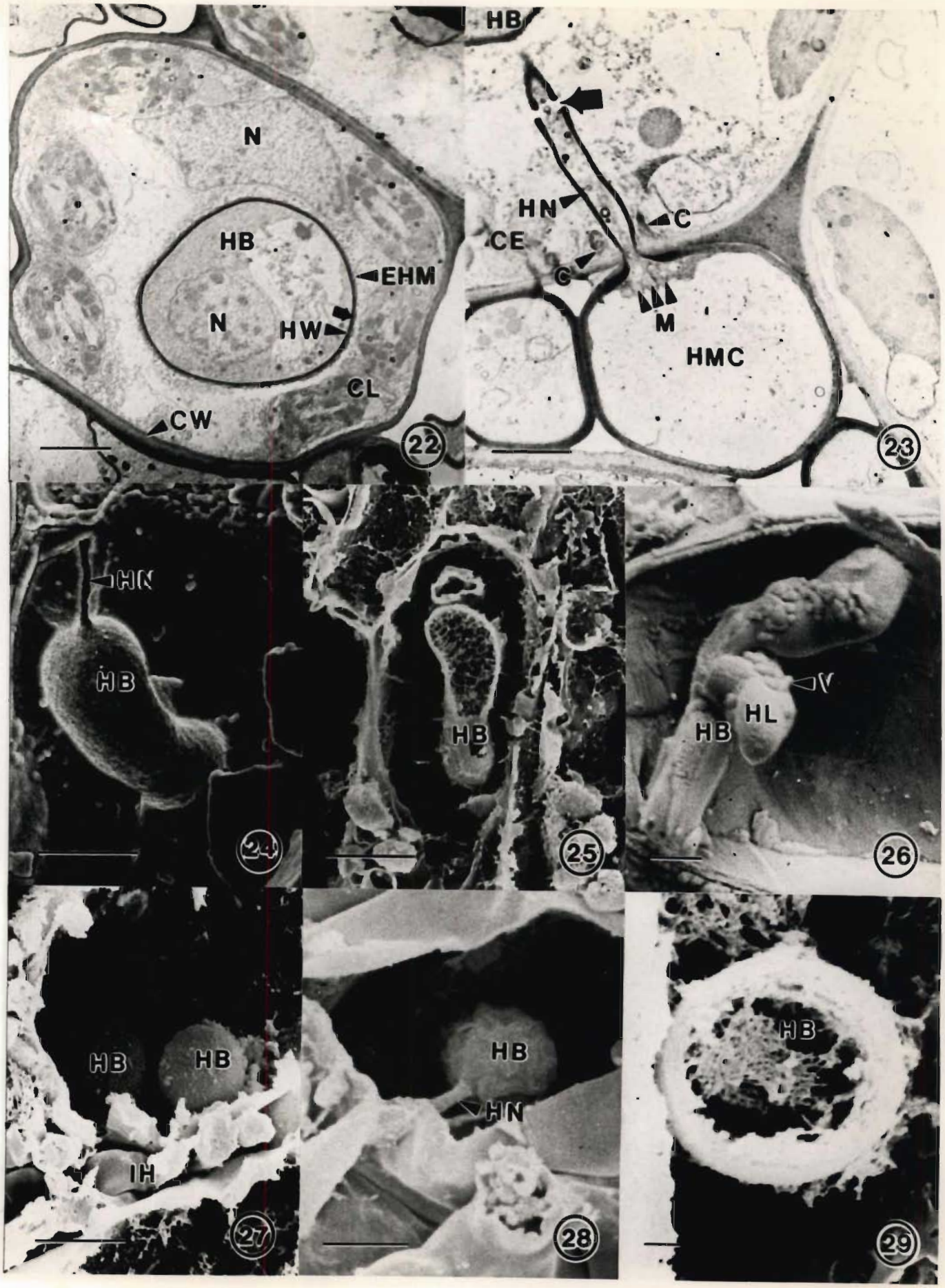
N
HB
EHM
N
HW
CL
CW
22
HB
HN
C
CE
C
M
HMC
23
HN
HB
24
HB
25
HB
HL
26
HB
HB
IH
27
HB
HN
28
HB
29

haustoria, whilst the extra-haustorial membrane of the host cell remained intact and the mesophyll cell showed signs of disorganization (Fig. 30). The contents of the immature haustorium and neck were electron-dense and a Type II electron-dense collar (one case) could be discerned at the proximal end of the neck (Fig. 30). Where the haustoria developed further, before resistance reactions set in, the periphery of haustoria with disorganized contents became slightly (Fig. 31) or severely (Fig. 32) undulated. Slight (Fig. 33) and severe (Fig. 36) undulations were also evident in the haustorial wall as viewed by the scanning electron microscope. Rarely, apparently normal haustoria (Fig. 37) were formed in the resistance reaction, and most showed signs of degeneration (Figs. 31, 32, 33 and 36). The extra-haustorial membrane at the periphery of the haustoria in the resistance reaction was always accompanied by an increase of host mitochondria (Fig. 37).

A close association of host cell nuclei with haustoria in invaded cells of the susceptible cultivar (Fig. 22) was observed. Such host nuclei were found to follow the contours of the haustoria (Fig. 22).

DISCUSSION

Although the gladiolus is a monocotyledonous plant, and rust germtubes on the leaves of several monocotyledonous plants are directional (Littlefield and Heath 1979) no directional growth was observed in this study and could, therefore, not be responsible for the higher percentage of appressoria formed on the susceptible cultivar. In particular, for *U. appendiculatus* on *Phaseolus vulgaris* (Hoch *et al.* 1987), the formation of appressoria was dependent on directional growth. On the surfaces of both the cultivar and the species, germtubes often grew over the stomata failing to recognize them, but the failure frequency on the leaf surface of the resistant host was higher. The aborted appressoria over the stomata of the resistant host had an infection peg morphology different to that described in

Scanning electron micrographs, after polyethylene glycol (Figs. 35, 37 - 40) preparation, and transmission electron micrographs (Figs. 30 - 34 and 36) of the haustorial bodies of *Uromyces transversalis*, 10 to 13 d post-inoculation in mesophyll cells of a resistant species.

Abbreviations: C, collar; CL, chloroplast; CW, mesophyll cell wall; EHM, extra-haustorial membrane; HB, haustorial body; HN, haustorial neck; HW, haustorial wall, M, mitochondrion; N, nucleus.

Fig. 30. Aborted electron-dense immature haustorial body (HB) and neck (HN), proximal part of which is encased in collar (C). Haustorial wall (HW), extra-haustorial membrane (EHM) and extra-haustorial matrix (arrow) are intact. Scale bar = 1 µm.

Fig. 31. Section through degenerate electron-dense haustorial body (HB) indicating disorganization of haustorial cytoplasm with slight undulations in haustorial wall (HW) elucidating fibrillar layer in extra-haustorial matrix (arrow) inside extra-haustorial membrane (EHM). Scale bar = 1 µm.

Fig. 32. Section through aborted haustorial body (HB) with severely undulated haustorial wall (HW) with intact extra-haustorial matrix (arrow) and extra-haustorial membrane (EHM). Scale bar = 1 µm.

Fig. 33. Haustorial body (HB) with undulations (arrow) in haustorial wall inside mesophyll cell. Scale bar = 10 µm.

Fig. 34. Haustorial body (HB) inside mesophyll cell resembling intracellular hypha. Scale bar = 10 µm.

Fig. 35. Globose haustorial body (HB) inside mesophyll cell partially covered by cell wall (CW). Scale bar = 10 µm.

Fig. 36. Sectioned haustorial body (HB) with extensive undulations (arrow) inside mesophyll cell. Scale bar = 10 µm.

Fig. 37. Section through apparently normal haustorial body (HB) with mitochondria (M) at periphery of haustorial wall (HW). Scale bar = 1 µm.

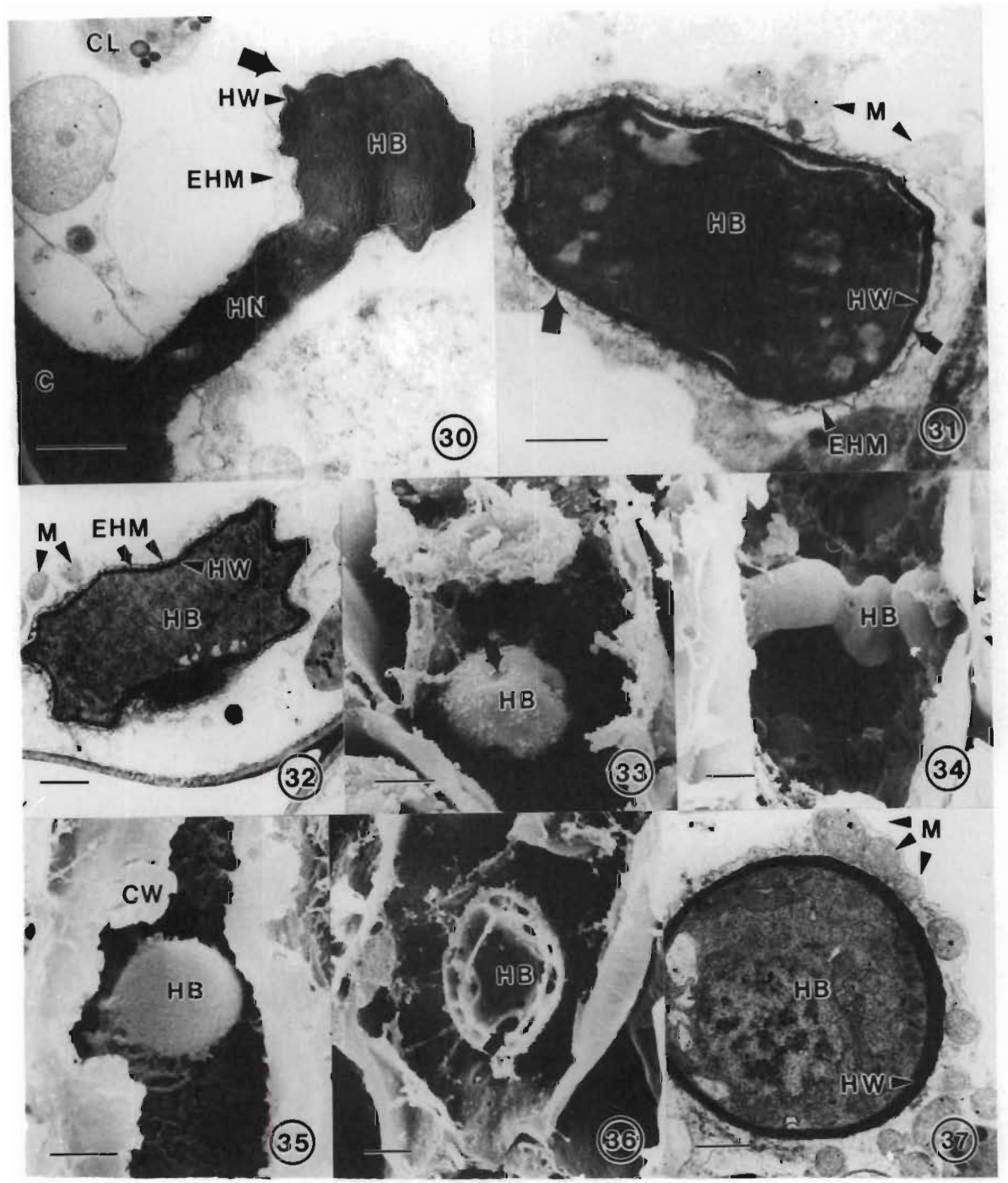
CL
HW
HB
EHM
HN
C
30
M
HB
HW
EHM
31
M
EHM
HW
HB
32
HB
33
HB
34
CW
HB
35
HB
36
M
HB
HW
37

Chapter 1 for *U. transversalis*. The bifurcate peg of the appressorium morphologically resembled that described by Hughes and Rijkenberg (1985) for *Puccinia sorghi* on maize. No abortion of appressoria was observed by scanning electron microscopy on the susceptible leaf surface.

Resistance to gladiolus rust appeared to be manifested in the loose adhesion of *U. transversalis* primary hyphae, haustorial mother cells and intercellular hyphae to the mesophyll cells of the species. Separation of the epidermis from the underlying mesophyll tissue during specimen preparation resulted in the tip of the primary hypha separating from the mesophyll cell of the species, whereas, in the susceptible reaction, this separation resulted in the severance of the primary hypha at or close to the SSV, since the tip of the primary hypha had developed into an HMC and adhered tightly to the mesophyll cell of the cultivar. Another aspect of resistance in the species was that no haustorial mother cell septum was observed in the primary hyphae of the aborted Stage 3 SSVs of *U. transversalis* on the stripped epidermis of the species. If such septa had been present the collapsed infection structure would have shown them clearly, as was demonstrated in Chapter 1. The primary hyphae of *U. transversalis* became swollen but failed to delimit an HMC and collapsed, eventually becoming completely disorganised. This indicated structural disorganization initiated in the SSV itself, an observation augmented by transmission electron microscopy; the second primary hypha opposite the collapsed one often also failed to develop. Also, all primary hyphae of *U. transversalis* collapsed after the formation of the haustorial mother cell septum during infection of a non-host (*Zea mays*). In the non-host the formation of haustorial mother cell septa appeared to be stimulated after which the infection structure aborted, whereas, in the resistant species, haustorial mother cell septa were not formed in the aborted infection structure. In a comparative study on non-host interactions of other rust fungi, it was shown that the non-hosts also induced the formation of haustorial mother cell septa (Heath 1977). Leath

and Rowell (1966) demonstrated that infection structures of *P. graminis* in a non-host, maize, were halted after the formation of appressoria and, with one exception, prior to the formation of HMCs.

The haustorial mother cells that had developed at 10 to 13 d post-inoculation in cells of the species and cultivar were morphologically similar, but the HMCs in the leaf tissue of the species loosely adhered to the mesophyll cells and were not associated with the osmiophilic adhesive material observed in the susceptible reaction. This confirms that adhesion to the gladiolus host cell wall is one of the prerequisites for the formation of haustoria during infection with *U. transversalis*. Loose adhesion, similar to that at the HMC / mesophyll cell interface, was also exhibited in the resistance reaction amongst intercellular hyphae. The fact that a haustorial apparatus occasionally formed, although the adhesion was loose, suggests that tight adhesion between fungus and cell is not always a prerequisite for penetration. It was shown by Chong *et al.* (1985a) that the outermost layer of the HMC of *P. graminis* f. sp. *tritici* is composed of glycoprotein containing α-linked glucose and/or mannose, glycoprotein-containing sugars with vicinal hydroxyl groups and unsaturated lipid (lipoprotein). It is possible that these molecules play a role in fungus/host cell contact and in the process of recognition or non-recognition between host cells and fungal infection hyphae.

The three-dimensional structure of some haustorial bodies was reminiscent of intracellular hyphae as described by Heath and Bonde (1983) for the tropical rust fungus, *Physopella zeae*, on maize. The wider intrawall penetration torus of intracellular hyphae in section as shown for the tropical rust was not demonstrated in this study. Hilu demonstrated as early as 1965 that the resistance mechanism of resistant lines of seedling maize (host) arrests the growth of *Puccinia sorghi* only at a post-haustorial mother cell level after normal development of earlier infection structures. Subsequently, this reaction has been shown to be typical of cultivar resistance compared to non-host resistance; formation of haustoria in

the latter situation being rare (Littlefield and Heath 1979, Heath 1977). However, infection of a resistant species of gladiolus by *U. transversalis* was followed by the abortion of Stage 3 SSVs and the arresting of haustorium development. The resistance mechanism has, therefore, the qualities of both cultivar resistance and a non-host reaction.

Ultrastructural changes as a result of resistance such as a decrease in mitochondrial size have been shown by Skipp *et al.* (1974). In the present study these subtle changes did not receive particular attention, but it was noted that host mitochondria were closely associated with apparently normal haustoria in incompatible reactions, whereas membrane-bound vesicles were associated with haustoria in compatible reactions. An association was found in the compatible *Avena sativa / P. coronata avenae* interaction by Chong and Harder (1982), between the cell organelles, golgi apparatus and endoplasmic reticulum, and developing haustoria. In susceptible mesophyll cells in which haustoria had formed - and given a fortuitous plane of section - it was found that the nucleus of the host was closely associated with the haustorium. Death of a haustorium in an infected mesophyll cell of the gladiolus species was followed by the disruption of mesophyll cell content. Host cell death in the present study, therefore, appears to occur after disorganization of haustorial contents and appears to be caused by haustorium death rather than as a result of the reverse. Other studies have shown similar disorganization of haustoria, which was also always accompanied by host cell disruption or death (Heath 1972, Mendgen 1977).

LITERATURE CITED

ANDERSON, W. A., and J. ANDRé. 1969. The extraction of some cell components with pronase and pepsin fron thin sections of tissue embedded in an Epon-Araldite mixture. Journal de Microscopie 7:343.

BISBY, G. R., and P. O. WIEHE. 1953. The rusts of Nyassaland. The Commonwealth Mycological Institute, Kew. Mycological Papers 54:12.

CHONG, J., and D. E. HARDER. 1982. Ultrastructure of haustorium development in *Puccinia coronata avenae*: Some host responses. Phytopathology 72:1527-1533.

CHONG, J., D. E. HARDER, and R. ROHRINGER. 1985a. Cytochemical studies on *Puccinia graminis* f. sp. *tritici* in a compatible wheat host. I. Walls of intercellular hyphal cells and haustorium mother cells. Can. J. Bot. 63:1713-1724.

——————————————————— 1985b. Cytochemical studies on *Puccinia graminis* f. sp. *tritici* in a compatible wheat host. II. Haustorium mother cell walls at the host cell penetration site, and the extra haustorial matrix. Can. J. Bot. 64:2561-2575.

DAHLGEN, R. M. T., H. T. CLIFFORD, and P. S. YEO. 1985. The families of the monocotyledons. Structure, evolution, and taxonomy. Springer-Verlag. Berlin. pp. 238-249.

DOIDGE, ETHEL M. 1950. The South African fungi and lichens to the end 1945. Bothalia 5:450.

EHRLICH, M. A., H. G. EHRLICH, and J. F. SCHAFER. 1968. Septal pores in Heterobasidiomycetidae, *Puccinia graminis* and *P. recondita*. Am. J. Bot. 55:1020-1027.

GOLDBLATT, P. 1971. Cytological and morphological studies in the Southern African Iridaceae. J. S. Afr. Bot. 37:317-460.

HAMILTON-ATTWELL, V. L., Tamar ORION, D. ORION, and G. C. LOOTS. 1986. Polyethylene Glycol (PEG) embedding vs freeze-fracture in SEM studies of nematode-infested roots. Proc. Electron Microsc. Soc. S. Afr. 16:105-106.

HEATH, M. C. 1971. Haustorial sheath formation in cowpea leaves immune to rust infection. Phytopathology 61:383-388.

HEATH, M. C. 1972. Ultrastructure of host and nonhost reactions to cowpea rust. Phytopathology 62:27-38.

HEATH, M. C. 1974. Light and electron microscope studies of the interactions of host and non-host plants with cowpea rust - *Uromyces phaseoli* var. *vignae*. Physiol. Plant Pathol. 4:403-414.

HEATH, M. C. 1977. A comparative study of non-host interactions with rust fungi. Physiol. Plant Pathol. 10:73-88.

HEATH, M. C., and M. R. BONDE. 1983. Ultrastructural observations of the rust fungus, *Physopella zeae* in *Zea mays*. Can. J. Bot. 61:2231-2242.

HILU, H. M. 1965. Host-pathogen relationships of *Puccinia sorghi* in nearly isogenic resistant and susceptible seedling corn. Phytopathology 55:563-569.

HOCH, H. C., R. C. STAPLES, B. WHITEHEAD, J. COMEAU, and E. D. WOLF. 1987. Signaling for growth orientation and cell differentiation by surface topography in *Uromyces*. Nature (London) 235:1659-1662.

HUGHES, F. L., and F. H. J. RIJKENBERG. 1985. Scanning electron microscopy of early infection in the uredial stage of *Puccinia sorghi* in Zea mays. Plant Pathol. 34:61-68.

JϕRSTAD, I. 1956. Re liquiae Lagerheimianae. African uredinales. Archiv for Botanik. 2:563-598.

KUCK, K. H., R. TIBURZY, G. HäNSSLER, and H. -J. REISENER. 1981. Visualization of rust haustoria in wheat leaves by using fluorochromes. Physiol. Plant Pathol. 19:439-441.

KUIPER, K., and G. H. BOEREMA. 1972. Quarantine aspects of the epidemiology of soil-borne pathogens. EPPO Bulletin. 7:61-68.

LEATH, K. T., and J. B. ROWELL. 1966. Histological study of the resistance of *Zea mays* to *Puccinia graminis*. Phytopathology 56:1305-1309.

LITTLEFIELD, L. J. 1973. Histological evidence for diverse mechanisms of resistance to flax rust, *Melampsora lini* (Ehrenb.) Lev. Physiol. Plant Pathol. 3:241-247.

LITTLEFIELD, L. J., and M. C. HEATH. 1979. Ultrastructure of rust fungi. Academic Press. New York.

MENDGEN, K. 1977. Reduced lysine uptake by bean rust haustoria in a resistant reaction. Naturwissenschaften 64:438.

NIKS, R. E. 1983a. Comparative histology of partial resistance and nonhost reaction to leaf rust pathogens in barley and wheat seedlings. Phytopathogy 73:60-64.

———— 1983b. Haustorium formation by *Puccinia hordei* in leaves of hypersensitive, partially resistant, and nonhost plant genotypes. Phytopatholgy 73:64-66.

NIKS, R. E., and H. J. KUIPER. 1983. Histology of the relation between minor and major genes for resistance of barley to leaf rust. Phytopathology 73:55-59.

REYNOLDS, E. S. 1963. The use of lead citrate at high pH as an electron-opaque stain in electron microscopy. J. Cell Biol. 17:208-212.

RIJKENBERG, F. H. J., and S. J. TRUTER. 1975. Cell fusion in the aecium of *Puccinia sorghi.* Protoplasma 83:233-246.

ROHRINGER, R., W. K. KIM, D. J. SAMBORSKI, and N. K. HOWES. 1977. Calcofluor: An optical brightener for fluorescence microscopy of fungal plant parasites in leaves. Phytopathology 67:808-810.

SKIPP, R. A., D. E. HARDER, and D. J. SAMBORSKI. 1974. Electron microscopy studies on infection of resistant (Sr6 gene) and susceptible near-isogenic wheat lines by *Puccinia graminis* f. sp. *tritici.* Can. J. Bot. 52:2615-2620.

SPURR, A. R. 1969. A low-viscosity epoxy resin embedding medium for electron microscopy. J. Ultrastr. Res. 26:31-43.

CHAPTER 5

Evaluation of Bitertanol and Triadimefon for the Control of Gladiolus Rust Caused by *Uromyces transversalis*

ABSTRACT

Weekly applications of either bitertanol or triadimefon gave significantly better control of *Uromyces transversalis* than fenarimol and the control, and performed better than oxycarboxin, penconazole, EDTA, CuEDTA and DTPA. There was a direct relationship between the number of bitertanol and triadimefon applications and rust incidence. Corm yield was adversely affected by rust incidence, and weekly applications of one of the two triazoles were necessary to ensure a reasonable yield. Marketable gladiolus inflorescences were harvested only from plots treated weekly with either bitertanol or triadimefon. Internode length on the flower spike was closely related to the lengths of the intervals between bitertanol or triadimefon applications.

INTRODUCTION

Gladiolus (*Gladiolus* L.) rust is a serious disease caused by *Uromyces transversalis* (Thüm.) Winter. The causal organism was originally named *Uredo transversalis* by Thümen in 1876 and renamed by Winter (1884) on account of his investigation of diseased gladiolus samples from Somerset East, South Africa. The disease has since spread to Eastern and Northern Africa, Malta, Italy (Viennott-Bourgin 1978) and South America (Lindquist *et al.* 1979). Under conditions conducive to the disease, i.e. temperatures between 16°C and 23°C and one to two days of fog (personal observation), the disease can reach epidemic proportions inflicting heavy losses. In the province of Natal, South Africa, outbreaks of gladiolus rust can cause losses of up to 100% and make the production of cut flowers without chemical control impossible. In drier areas, rust is considered a problem during exceptionally wet seasons only. The disease is characterized by bright orange pustules that form transversely across the leaf blade. Spores from leaf pustules may infect the inflorescence and render the flower spike unmarketable. The presence of pustules on any part of the flower spike precludes export to other countries. The mere fact that gladiolus

rust occurs in the Republic of South Africa has resulted in an export ban on corms as well as flowers to the United States of America. Garibaldi & Aloj (1980) evaluated the fungicidal control of gladiolus rust in a plastic glasshouse. They concluded that dithiocarbamates gave poor control of the disease and that weekly sprays of benodanil (Calirus® 50WP) and oxycarboxin (Plantvax® 75WP) prevented the development of a rust epidemic. Magie (1984) conducted glasshouse trials on two artificially inoculated gladiolus cultivars and found that oxycarboxin and three chelates gave good control.

This paper compares bitertanol and triadimefon with other fungicides including chelates in field trials, with special reference to the timing of the applications.

MATERIALS AND METHODS

The field trials were conducted under mistbelt conditions at Cedara in Natal, a locality known to be conducive to outbreaks of gladiolus rust. The trials were laid out in a randomized block design with either four or five replicates and protected by a hail shelter. The 0.02 ha field (Hutton soil type with pH(KCl) of 4.4) was prepared with a rotavator and fertilised with 900 kg/ha 2-3-2(22). Weeds were controlled prior to planting with linuron (Afalon® 45SC). Corms were planted either in spring (September) or in midsummer (January) at a depth of 4 cm, spaced 15cm by 15cm and 36 (6 by 6) corms per plot of 0.81 m^2. A wire mesh that could be raised as plant height increased was put over the plots to provide plant support, preventing the breaking off of shoots and inflorescences during thunderstorms or very windy conditions. After planting, and before watering, the soil was treated with disulfoton (1 g Disyston® 5G per 15 cm by 15 cm area) for the preventative control of thrips.

Prior to spraying, after the first sign of rust, an assessment (according to the scale in use during that particular season) of rust incidence was made to establish the uniformity of rust infection. The fungicides and chelates were applied to run-off with a knapsack sprayer equipped with a flat fan nozzle. Portable plastic screens were used to limit fungicidal drift between plots. The control plots were left unsprayed.

1984 Trial. Four replicates of six plots of thirty-six corms of each of the gladiolus cultivars Day Dream, Fire Chief, Goldfield, Green Isle and Spectacular were planted in summer. From the first sign of rust, the disease incidence was assessed (as below) and plants were treated weekly with bitertanol (Baycor® 30EC), triadimefon (Bayleton® 25EC), oxycarboxin (Plantvax® 25EC), fenarimol (Rubigan® 12EC) or penconazole (Topaz® 10EC). The fungicides were applied at 50 ml per 100 L water (bitertanol, triadimefon and oxycarboxin) and 100 ml per 100 L water (fenarimol and penconazole). In view of the wax layer on the leaves, an adjuvant, Agral 90® at 25 ml per 100 L water was added throughout. Two rows of four plants in the centre of the plot were rated according to a 0 - 5 scale; 0 - no visible pustules, 1 - very slight infection (< 1%), 2 - slight infection (< 10%), 3 - moderate infection (< 40%), 4 - moderately severe infection (< 60%) and 5 - severe infection (> 80%). Two assessments - apart from the assessment prior to spraying - were made: the first assessment conducted nine weeks after planting and the second thirteen weeks after planting. Results were analyzed according to the methods outlined in Table 1.

1985 Trial. Four replicates of eight plots of thirty-six corms of "Goldfield", were planted. After the first sign of rust, the trial was sprayed weekly with triadimefon (50 ml per 100 L), bitertanol (50 ml per 100L) or commercially available chelates, viz. ethylenediaminetetraacetic acid (EDTA) which contained 14% copper (Librel Cu® 14WP) at 100 g per 100L, EDTA (Tetralon A® 40EC) at 65 ml per 100 L or diethylenetriaminepentaacetic acid (DTPA - Tetralon B® 40EC) at 65 ml per 100 L water.

The adjuvants were added as indicated in Table 2 at a rate of 25 ml per 100 L. An assessment of rust incidence was made after six weeks of spraying by employing the Horsfall & Barratt (1945) scale and converting the figures according to the tables of Redman, King and Brown (1967). Results were analyzed according to the methods outlined in Table 2.

1986 Trial. Four weeks prior to the planting of a bitertanol and triadimefon trial, rows of Goldfield corms were planted, 1.5 m apart, peripherally and between the plots of the laid out trial. These rows were not sprayed. In this way an even spread of the rust was ensured. Five replicates of ten plots each with twenty-four corms of "Goldfield" were planted. Bitertanol and triadimefon were applied at 50 ml per 100 L including 25 ml Agridex® and 25 ml Agral 90® per 100 L water respectively. Both fungicides were applied at the following intervals: once a week before the first sign of rust, once after the first sign of rust, every three weeks after the first sign of rust, every fortnight after the first sign of rust and weekly after the first sign of rust. An assessment similar to that done during the 1985 trial was conducted, but two assistants made their individual assessment, and the means of the three assessments were used for analysis. Results were analyzed according to the methods outlined in Figure 2. The corm yield for each plot was determined and the results analyzed according to the methods outlined in Figure 3. Polynomial analysis with BMDP® statistical software (Dixon 1985) and regression analysis were performed on the disease incidence and corm yield in relation to the application intervals of bitertanol and triadimefon.

RESULTS

During 1984 to 1986, rust appeared in the gladiolus trials six weeks after planting. The assessments shortly before spraying were not used in the final analysis, but were used as an indication of the uniformity of rust infection.

1984 Trial. As shown in Table 1, significant (P = 0.01) control was obtained with bitertanol and triadimefon. These fungicides were significantly (P = 0.05) more effective than fenarimol. Control of gladiolus rust in this trial was evident at the time of the first assessment and remained similar for the second assessment, except that the difference between the bitertanol and fenarimol treatments became less significant.

1985 Trial. There were no significant differences between treatments. The infection pressure was lower in this season compared with the previous or following seasons, apparently due to drought conditions in the Natal region. No rust was observed in the plots sprayed with bitertanol or triadimefon. These treatments were not included in the statistical analysis. This analysis (Friedman) showed significant (P = 0.05) differences between EDTA or CuEDTA and DTPA or control treatments (Table 2).

1986 Trial. Very high infection pressure prevailed under field conditions due to favourable weather conditions and the presence of rust-infected trap rows. Presented in Figure 1 are photographs of flower spikes harvested from plots after six weeks of triadimefon treatment at various intervals, indicating that treatment of gladioli with triadimefon results in a shortening of internodes of the flower spikes. The internodes of an inflorescence treated only once with triadimefon were considerably longer than those treated weekly with triadimefon; intermediate application intervals showed a marked progressive shortening. The fewer the number of applications of triadimefon (Fig. 2) the more disease developed, which in turn caused the flowers to abort so that in the control treatment no flower spikes developed or no flowers on the spike opened. One treatment in six weeks, resulted in the partial opening of the sixth acropetal flower. Two applications resulted in the abortion of the first five flowers after bud break while some of the later flowers opened partially. Three applications resulted in the first two flowers aborting after partial opening, while later flowers developed more normally. Weekly applications resulted in the flowers on the florescences developing normally (Fig. 1).

Table 1. Gladiolus rust incidence in a field spraying trial at Cedara in 1984

Fungicides[x]	Disease incidence[y]	
	assessment 1[z]	assessment 2[z]
Bitertanol	1.2[c]	1.8[c]
Oxycarboxin	2.9[abc]	3.5[abc]
Triadimefon	1.1[c]	1.5[c]
Fenarimol	3.8[ab]	4.3[ab]
Penconazole	2.2[abc]	3.2[abc]
Control	3.5[a]	4.6[a]

[x] Fungicides were applied weekly with 25 ml Agral 90 per 100 L on four replicates of 36 plants for six weeks after the first sign of the rust.

[y] Average disease incidence rated according to a 0 - 5 scale where 0 represents no infection and 5 severe infection.

[z] Mean in a column followed by the same letter did not differ after analysis with Kruskal-Wallis, all differences were significant at P=0.01 except the difference between bitertanol and fenarimol in the 2nd assessment which was significant at P=0.05.

Table 2. Disease assessments of gladiolus rust in a field trial at Cedara in 1985 after weekly treatments with bitertanol and triadimefon (with both adjuvants, Agridex and Agral 90) and chelates

Treatments[y]	Disease incidence (%)[z]
Bitertanol + Agridex	0
Bitertanol + Agral 90	0
Triadimefon + Agridex	0
Triadimefon + Agral 90	0
Control + Agral 90	37.3[b]
EDTA + Agral 90	2.7[a]
DTPA + Agral 90	29.7[b]
CuEDTA + Agral 90	5.3[a]

[y] The treatments were applied weekly for six weeks after the first sign of disease.

[z] Average disease incidence of each treatment (four replicates of blocks with 36 plants) rated according to the Horsfall and Baratt (1945) scale and converted with tables of Redman, King and Brown (1967). Analysis conducted disregarding the zero disease incidences. Mean in a column followed by the same letter did not differ significantly at P = 0.05 after analysis with Friedman test.

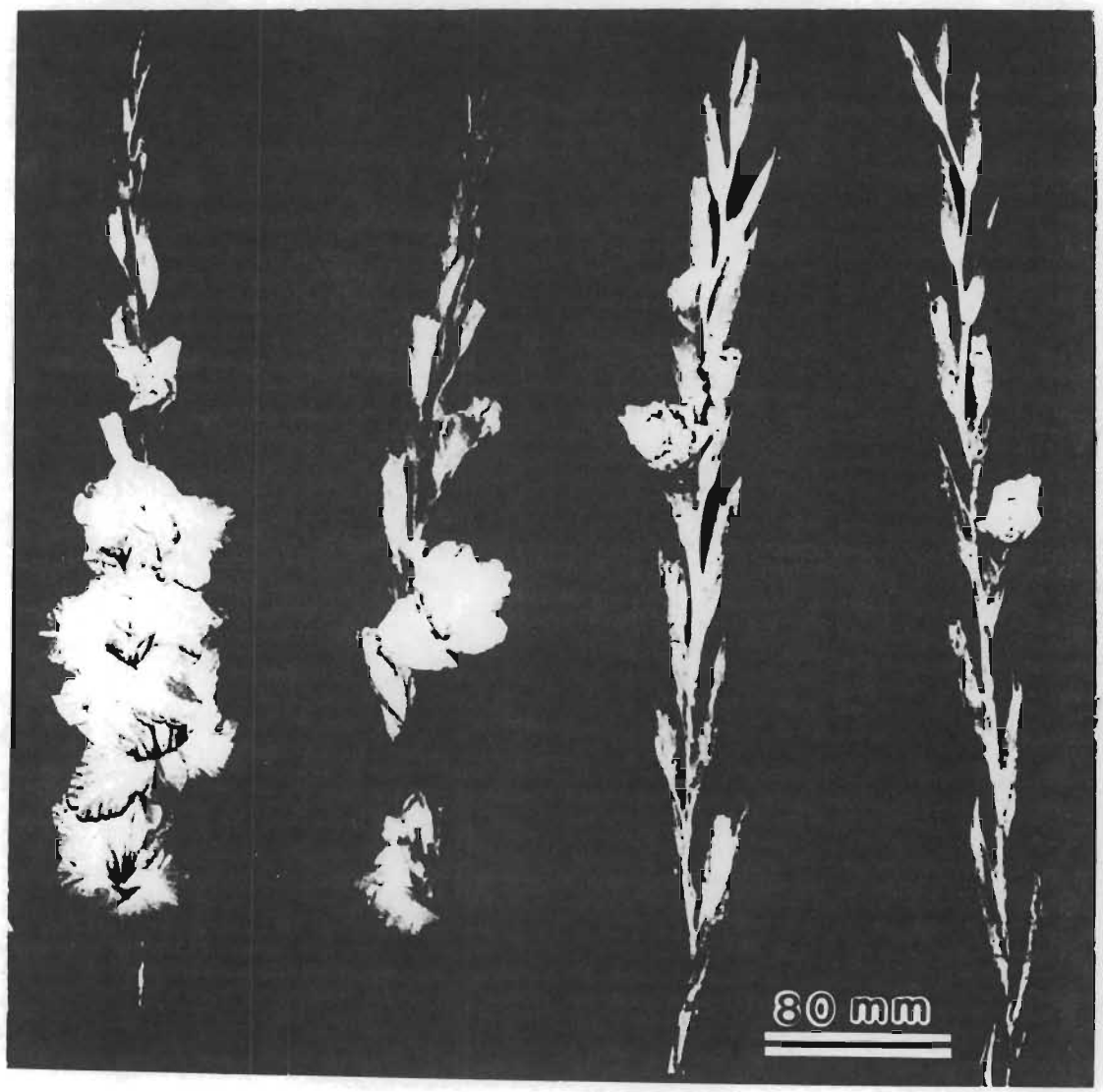
80 mm

Differences between weekly or fortnightly applications of triadimefon and the control were significant (P = 0.05). Weekly applications of triadimefon were significantly (P = 0.05) different from the control and one application before the onset of gladiolus rust.

Differences between weekly or fortnightly applications of bitertanol and the control were significant (P = 0.05). Weekly applications of bitertanol were significantly (P = 0.05) different from the control and an application after the first sign of rust. Disease incidence was, therefore, closely related to the intervals between bitertanol or triadimefon applications (Fig. 2).

Polynomial analysis of disease incidence in relation to application intervals for bitertanol and triadimefon (Presented in Fig. 2) resulted in polynomial equations of the first degree, indicating a linear relationship (Table 3). Therefore, the more regularly either triadimefon or bitertanol was applied, the better the control. Regression analysis of disease incidence versus the application intervals for triadimefon and bitertanol showed that one fungicide did not give significantly better control than the other over the range of application intervals.

The average corm yield from plots treated with weekly applications of triadimefon differed significantly (P = 0.05) from the control treatment or those that were sprayed before the first sign of gladiolus rust (Fig. 3). Weekly or fortnightly applications of bitertanol yielded significantly (P = 0.05) more corms than the control treatment, or a single treatment once before the first sign of rust, or once after the first sign of rust or once every three weeks (Fig. 3). Polynomial equations were calculated from the results for corm yield after different application intervals with triadimefon and bitertanol. Table 3 shows that second or third degree equations fit the data reliably. So there is no direct linear relationship

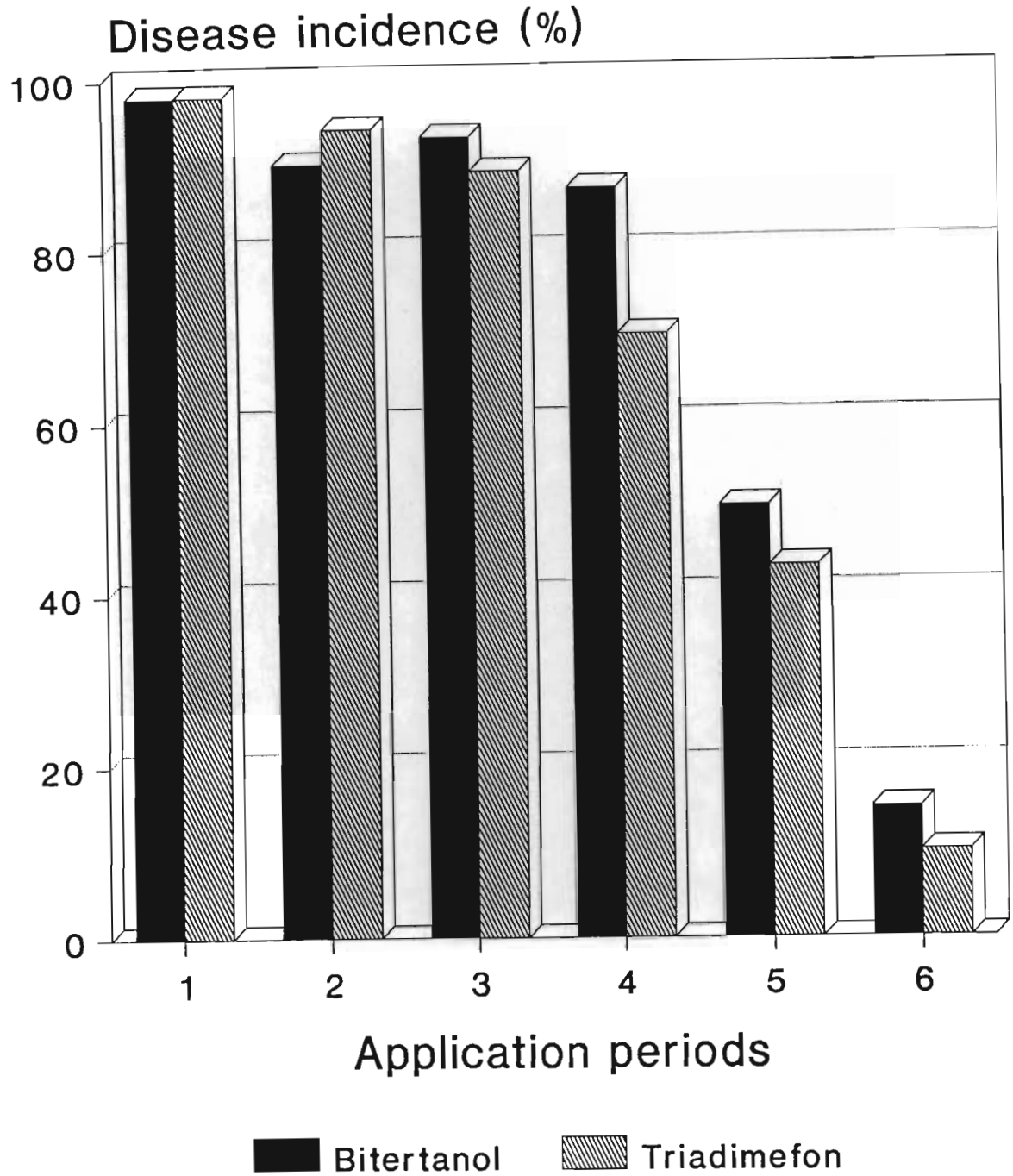

Fig. 2. A graphic representation of gladiolus rust incidence, six weeks after commencement of spraying, versus application intervals of triadimefon and bitertanol. The application intervals were: 1, no treatment; 2, once before first sign of rust; 3, once after first sign of rust; 4, two three-weekly applications; 5, three fortnightly applications and 6, weekly applications. According to a Friedman analysis of the triadimefon application, treatments 5 and 6 differed significantly from 1, and 6 differed significantly from 1 and 2 at P = 0.05. For bitertanol the applications 5 and 6 differed significantly from 1, and 6 differed significantly from 1 and 2 at P = 0.05.

Table 3. The percentage fit of polynomial equations to the disease index / application intervals and corm yield / application intervals for both bitertanol and triadimefon in the control of gladiolus rust at Cedara in 1986

Fungicide[a]	Disease incidence[b]	Corms harvested[d]	
	1 st degree[c]	2 nd degree[c]	3rd degree[c]
Bitertanol	85 %	91 %	93 %
Triadimefon	80 %	82 %	82 %

[a] The fungicides were applied once before the first sign of disease, once after, every three weeks, every two weeks and weekly for six weeks at 50 ml / 100 L including Agral 90 with triadimefon and Agridex with bitertanol both at 25 ml per 100 L.

[b] Incidence determined with Horsfall and Barratt (1945) scales and converted with tables by Redman, King and Brown (1967) for each treatment.

[c] The percentage fit of first, second and third degree polynomial equations calculated with BMDP® for disease incidence and corms harvested.

[d] Based on the average number of corms harvested from each treatment.

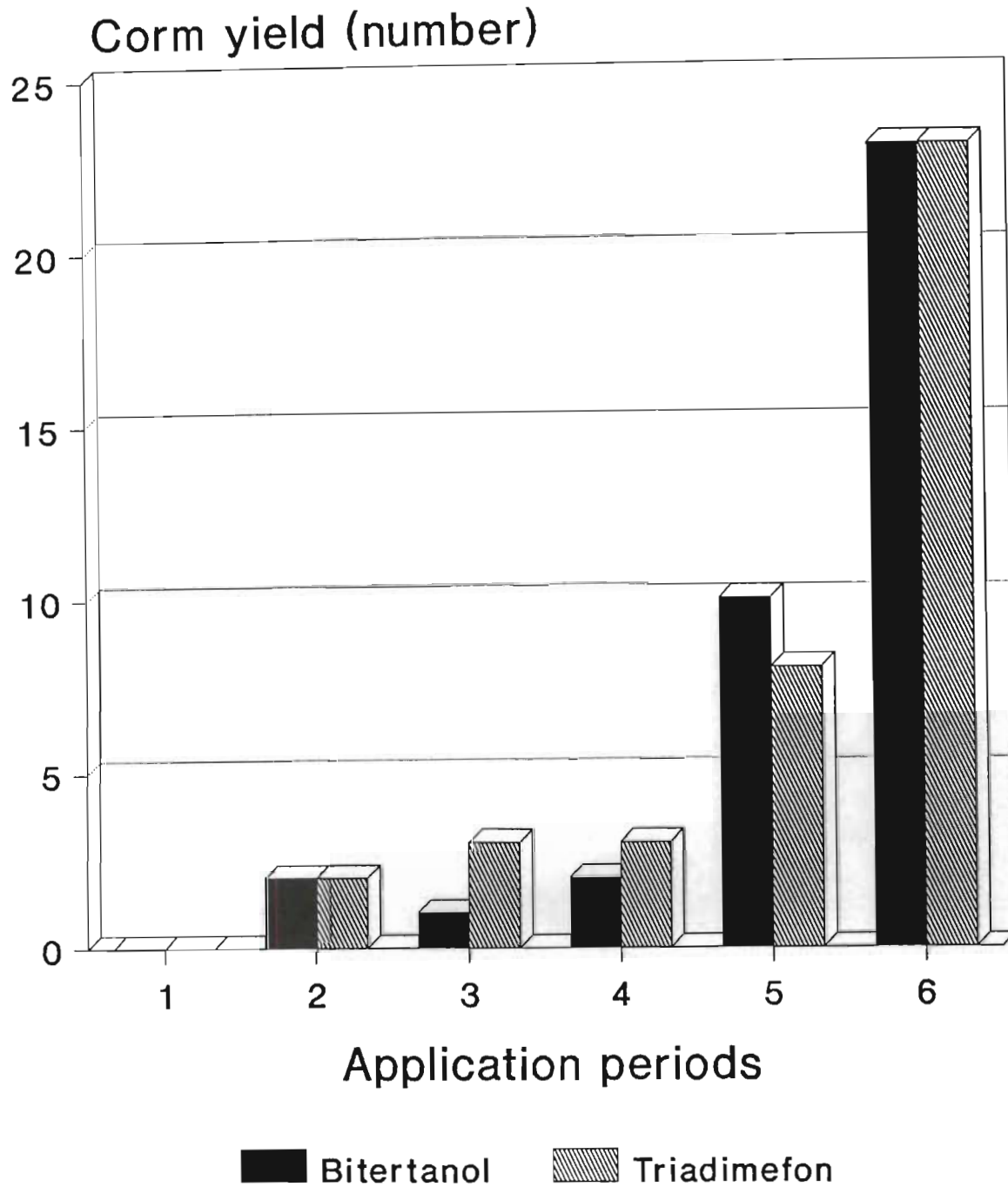

Fig. 3. A graphic representation of the corm yield per plot versus the application intervals of triadimefon and bitertanol. The application intervals were: 1, no treatment; 2, once before the first sign of rust; 3, once after first sign of rust; 4, two three-weekly applications; 5, three fortnightly applications and 6, weekly applications. According to a Friedman analysis on the triadimefon application, treatment 6 differed significantly from 1 and 2 at P = 0.05. According to the Student-Newman-Keuls test the bitertanol applications 5 and 6 differed significantly from 1, 2, 3 and 4 at P = 0.05.

between the application intervals and the corm yield per plot. Theoretically there is an exponential increase in corm yield with the shortening of application interval if the intervals are shorter than a fortnight.

DISCUSSION

The trials conducted during 1984 to 1986 clearly show the differences in disease incidence between seasons, such differences in turn depend on the weather and the presence of rust. In the spring of 1986 the infection pressure reached the highest level for the three seasons under review. In treatments other than weekly applications of triadimefon and bitertanol, no marketable flowers or corms were harvested. To be able to market gladiolus flowers when a high infection pressure is prevalent, weekly sprays of either bitertanol or triadimefon are, therefore, essential. A direct relationship between the application interval and disease incidence was found. Magie (1984) reported that three chelates gave significant control of gladiolus rust under glasshouse conditions. The present results substantiate his conclusion that EDTA controls the disease. However, in contrast with his findings, DTPA did not control rust caused by *U. transversalis* under field conditions. This is possibly due to a lower infection pressure in glasshouse trials. Normally, i.e. in the absence of rust infection and without triazole sprayings, a gladiolus plant in addition to the new corm produces approximately 10 cormels (personal observation). Weekly applications of bitertanol and triadimefon resulted in the development of the new corm only and no cormels were formed. It is likely that the lack of cormel production in the treated plots is due to the use of these fungicides. The triadimefon used in these field trials caused a shortening of the internodes on the flower spike compared to plants grown in the absence of rust in the glasshouse. A similar observation on the reduction in the length of flower spikes was made by Garibaldi and Aloj (1980) after spraying gladiolus plants with triadimefon. Such shortening may be rectified with gibberellic acid treatments as suggested by Siegel (1981). Another possibility is the marketing of short-internode gladiolus

inflorescences as an attractive alternative to the longer spikes. The presence of high levels of rust infection resulted in the incomplete bud break or abortion of flowers on inflorescences and the absence of corm production. This can possibly be attributed to the reserves that are in short supply as a result of the rust infection, consequently the plant is unable to produce either the blooms or the corms.

The control of gladiolus rust is of benefit not only to the producer of gladiolus flowers and corms but also to importers for quarantine treatment in countries which do not have *U. transversalis*, such as the United States of America.

LITERATURE CITED

GARIBALDI, A., and ALOJ, B. 1980. Observations on biology and control of *Uromyces transversalis* (Thüm) Winter on gladiolus in Southern Italy. Acta Hortic. 109:409-411.

HORSFALL, J. G., and BARRATT, R. W. 1945. An improved grading system for measuring plant diseases. Phytopathology 35:655.

LINDQUIST, J. C., ALIPPI, H. E., and MEDERA, C. M. 1979. Una grave epidemia de roya del gladiolo (*Uromyces gladioli* P. Henn.), en la provincia de Santa Fe (Republica Argentina). Jorn. Fitosan. Argent. 2:719-724.

MAGIE, R. O. 1984. Chelates may control gladiolus rust disease. Gladiograms 55:2-5.

REDMAN, C. E., KING, E. P., and BROWN, I. F. 1967. Tables for converting Barratt/Horsfall rating scores to estimated mean percentages. Eli Lilly & Co., Research Laboratories.

SIEGEL, M. R. 1981. Sterol-inhibiting fungicides: Effects on sterol biosynthesis and sites of action. Plant Disease 65:986-989.

VIENNOTT-BOURGIN, M. G. 1978. *Uromyces transversalis* (Thüm.) Winter parasite dangereux des cultures de glaieuls. Academie d'Agriculture de France, Paris 64:880-885.

WINTER, G. 1884. Exotische Pilze. Flora 67:259-274.

CHAPTER 6

Effect of Bitertanol on the Ultrastructure of *Uromyces transversalis* Infection Structures in Gladiolus Leaves

ABSTRACT

The effect of bitertanol on the infection structures of *Uromyces transversalis* in and on gladiolus leaves in field and glasshouse trials was examined by electron microscopy. The percentages of germinated urediospores that formed appressoria on leaves, treated weekly for six weeks and treated once before the onset of rust in field trials, and treated and not treated with bitertanol in glasshouse trials, were similar. In field trials the percentages of all infection structures inside leaves of plants treated weekly for six weeks were lower than those recorded in leaves of plants treated with bitertanol, once before the onset of the rust. In glasshouse trials the preventative effect of bitertanol applied 48 h prior to inoculation, on the development of infection structures in gladiolus leaves, 120 h after inoculation, resulted in a high percentage of infections aborting at the substomatal vesicle development stage. A higher percentage of substomatal vesicles developed to their final stage in the untreated than in the treated leaves. Some of these substomatal vesicles in the treated tissue either escaped the fungicidal action of bitertanol or showed signs of partial collapse of the intercellular hyphae and/or substomatal vesicle. If bitertanol is present in leaf tissue it can inhibit the development of substomatal vesicles. However, it appears that the fungicide is not translocated well within the lamina.

INTRODUCTION

Bitertanol (Baycor®) is a broad-spectrum fungicide which belongs to the triazole group. Chemically it is ß ([1,1-bimethyl]-4-yloxy) -α- (1,1-dimethylethyl)- 1 H - 1,2,4-triazole -1-ethanol. One of its main uses is the control of rusts and powdery mildews in vegetables and ornamentals (Brandes *et al.* 1979). It is primarily used as a protective fungicide having a translaminar action, and has therefore an eradicative as well as a prophylactic action, whereas triadimefon (Bayleton®) has a systemic action (Brandes *et al.* 1979). The fungicidal action is directed against the lipid metabolism of the fungus. According to Kraus

(1979) it causes the inhibition of the end product and an accumulation of the intermediates associated with sterol biosynthesis and bitertanol, therefore, has an action similar to that of the triazoles, triadimefon and triadimenol (Baytan®).

Until now the effects of systemic fungicides on the ultrastructure of rust fungi appear to have been studied more extensively than the effects of contact fungicides. Transmission electron microscopy and autoradiography of the curative effect of a member of this group, oxycarboxin (Plantvax®), on *Uromyces phaseoli* infecting beans (Pring and Richmond 1976) and the effect of oxycarboxin on haustoria of *Puccinia coronata* var. *avenae* infecting oats (Simons 1975) have been studied. The effect of benomyl (Benlate®) and benodanil (Calirus®) on the translocation of carbohydrates in *Puccinia hordei* infecting barley (Whipps *et al.* 1987), have been investigated by autoradiography. Other studies include scanning electron microscopy of *P. coronata* on the exterior of oats leaves treated preventatively and curatively with the triazole fenpropimorph (Corbel®), an ergosterol inhibitor belonging to the class morpholines (Zobrist *et al.* 1982).

In the scanning electron microscopic study described in this Chapter, the action of six weekly applications and one application before the onset of the rust of bitertanol on the development of *Uromyces transversalis* infection structures on and in gladiolus cv. Goldfield leaves under field conditions is reported. The preventative effect of bitertanol applied 48 h post-treatment, on the development of infection structures on/in gladiolus leaves cv. Goldfield, 120 h post-inoculation with *U. transversalis*, was investigated under glasshouse conditions.

MATERIALS AND METHODS

Field trials. Bitertanol (Chapter 5) was applied to gladiolus cv. Goldfield plants weekly for six weeks or once, a week before the onset of the disease. The plants were subjected to natural infection only and in 1986, the year in which the experiment was conducted, the rust incidence was high (Chapter 5). Five days after the last application, samples were taken from the distal third of the fifth leaf of randomly selected plants in the plots treated once before the onset of the rust and treated weekly for six weeks. The plants in the control plots were dead and could not be used for the study. These samples were subsequently prepared for scanning electron microscopy.

Glasshouse trials. Six weeks after planting, gladiolus plants, cv. Goldfield, were either sprayed with bitertanol (50 ml Baycor® 30EC per 100 L water containing 20 ml Agridex) or water containing 20 ml Agridex® per 100 L water as the control. The fungicide was applied with a knapsack sprayer equipped with a flat fan nozzle to run-off. The plants were placed in a glasshouse (temperatures ranging from 15°C to 35°C) for 48 h and then the distal third of the fifth fully expanded leaf was inoculated with a camel hair brush (for details on exposure to free water and incubation see Appendix I). Two leaf samples, 120 h post-inoculation, of each, of two treated and two control plants, were prepared for scanning electron microscopy.

Scanning electron microscopy. The leaf samples of the respective treatments were cut into 3 mm by 3 mm pieces. Leaf pieces were fixed in 6% glutaraldehyde in a 0.05 M Sodium cacodylate buffer, pH 6.8 - 7.2, washed twice in the buffer, post-fixed for 3 h in 2% osmium tetroxide in buffer, washed twice in the buffer and dehydrated in a graded ethanol series. The leaf pieces were then critical point dried with carbon dioxide as a transition fluid and mounted on copper stubs. The epidermis of the leaf pieces was removed manually with a pair of No. 5 Dumont® forceps under a stereomicroscope (See Chapter 1). The epidermis and the stripped tissue remaining on the stubs were coated with Gold or

Gold/Palladium in a Balzers® or Polaron® sputter coater respectively. Epidermis and stripped leaf pieces were examined with a Hitachi® S-570 or Jeol® JSM-35 scanning electron microscope operated at 10 kV and 15 kV respectively.

Data presentation. During processing of the leaf specimens for scanning electron microscopy many ungerminated urediospores are removed during preparation. These urediospores can therefore not be counted, nor used for the calculation of percentages. The total number of infection structures on and in leaf pieces of the leaves treated in field trials once before the onset of rust, weekly for six weeks, and in glasshouse trials treated and untreated was determined by scanning electron microscopy. The data obtained from the leaf exterior were processed separately to data obtained from the leaf interior, since the stripping method precluded the stripping of the entire specimen; the fate of not all appressoria could therefore be determined. On the leaf exterior the total number of germinated urediospores with appressoria was expressed as a percentage of the germinated urediospores. In the leaf interior four stages in infection structure development were categorized, viz. substomatal vesicles (SSV), SSVs with primary hyphae, SSVs with secondary hyphae on the stripped epidermis, and SSVs that had developed haustorial mother cells (HMC) and intercellular hyphae (final stage) in the stripped leaf tissue. Since the attainment of eg. the final stage implies that the other three stages have been successfully completed, totals presented under each category are cumulative. These cumulative values were then expressed as a percentage of the total infection structures in the leaf interior.

RESULTS

Field trials. A total of 258 mm^2 and 142 mm^2 leaf pieces and 519 and 1022 infection structures from plants treated weekly for six weeks (TWS) and plants treated once before the onset of the rust (TOD), respectively, were examined. The percentages of scanning electron microscopic observations of the infection structures on and in TWS and TOD

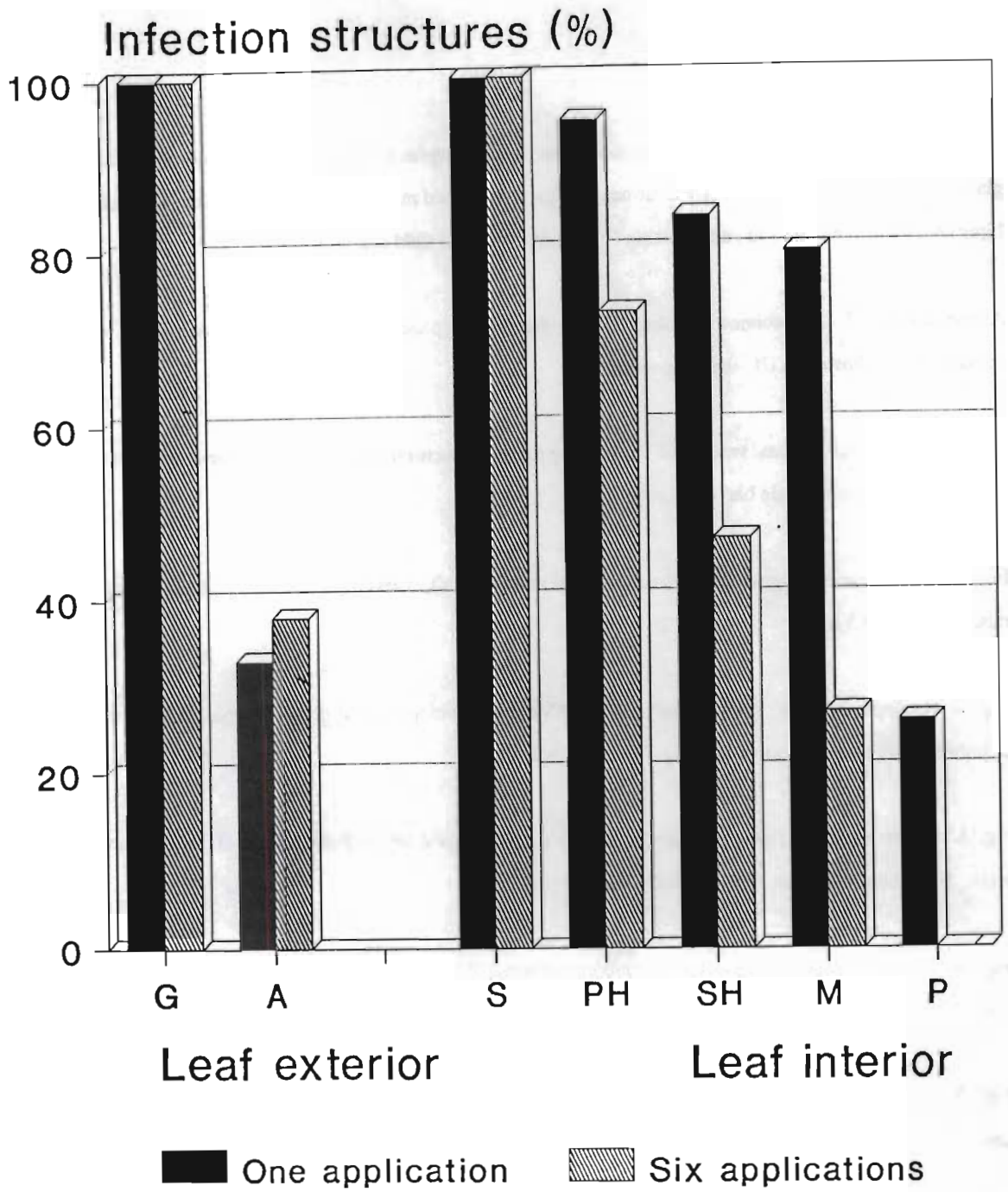

Fig. 1. A histogram of the development of infection structures of *Uromyces transversalis* one week after being treated weekly for six weeks (TWS) or once before the onset of the rust (TOD) with bitertanol under field conditions examined by scanning electron microscopy. The results are divided into infection structures on the exterior of the leaf and the intercellular infection structures in the leaf interior. On the leaf exterior the germinated urediospores that did form appressoria (A) are expressed as a percentage of all the germinated urediospores (G). The developmental stages of infection structures in the leaf interior of TOD and TWS leaves are expressed as a percentage of all infection sites within the TOD and TWS leaves respectively.

Scanning electron micrographs of infection structures of *Uromyces transversalis* formed inside the leaves of the gladiolus cv. Goldfield after weekly treatments (Figs. 2 to 5) and micrographs of uredia after one treatment with bitertanol before the onset of rust infection (Figs. 6 and 7) under field conditions.

Abbreviations: I, interconnective tube; IH, intercellular hyphae; PH, primary hypha; SSV, substomatal vesicle; U, urediospore; UI, urediospore initial.

Fig. 2. Aborted substomatal vesicle (SSV), showing signs of structural decline (arrow), viewed on interior surface of stripped epidermis. Scale bar = 2 µm.

Fig. 3. Aborted and collapsed (arrow) substomatal vesicle (SSV), viewed on interior surface of stripped epidermis. Scale bar = 5 µm.

Fig. 4. Collapsed (arrow) substomatal vesicle (SSV) after development of primary hypha (PH) in substomatal chamber. Note interconnective tube (I). Scale bar = 2 µm.

Fig. 5. Collapsed (arrow) substomatal vesicle (SSV) and collapsed intercellular hyphae (IH) after their development. Note interconnective tube (I). Scale bar = 5 µm.

Fig. 6. Mature urediospores (U) and a urediospore initial (UI) showing abnormal development. Scale bar = 2 µm.

Fig. 7. Closely packed urediospores (U) in uredium of which covering epidermis was removed. Scale bar = 5 µm.

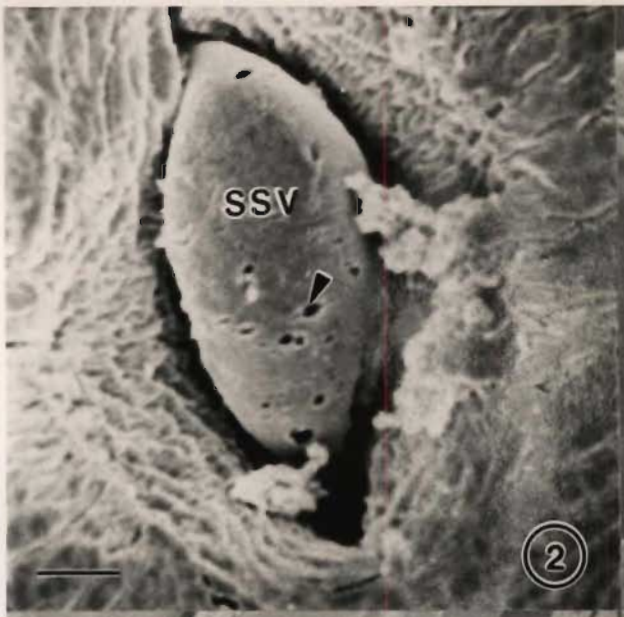
SSV
2

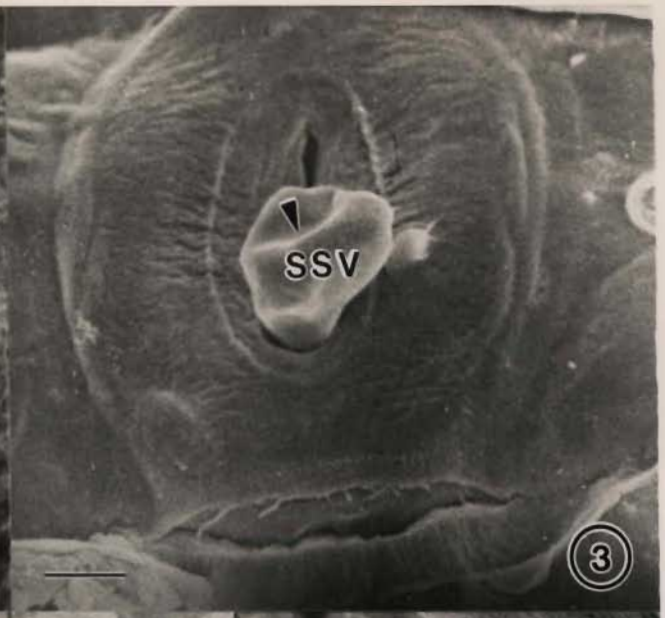
SSV
3

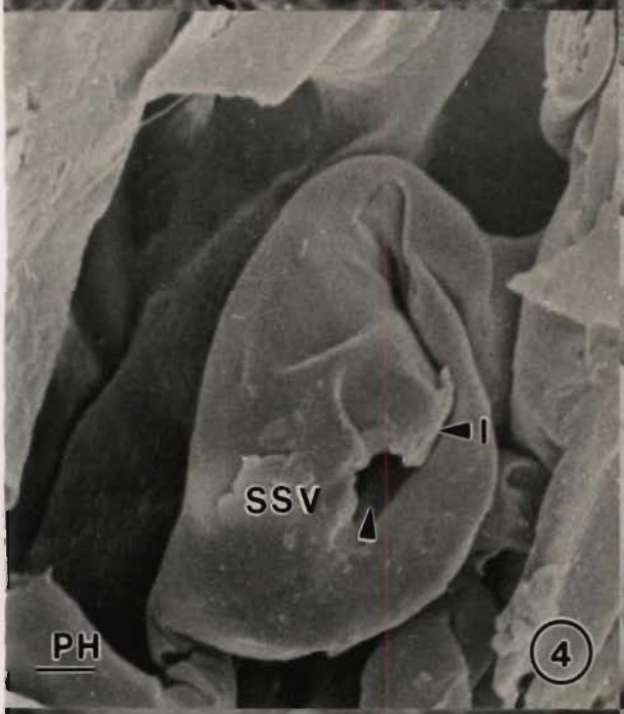
I
SSV
PH
4

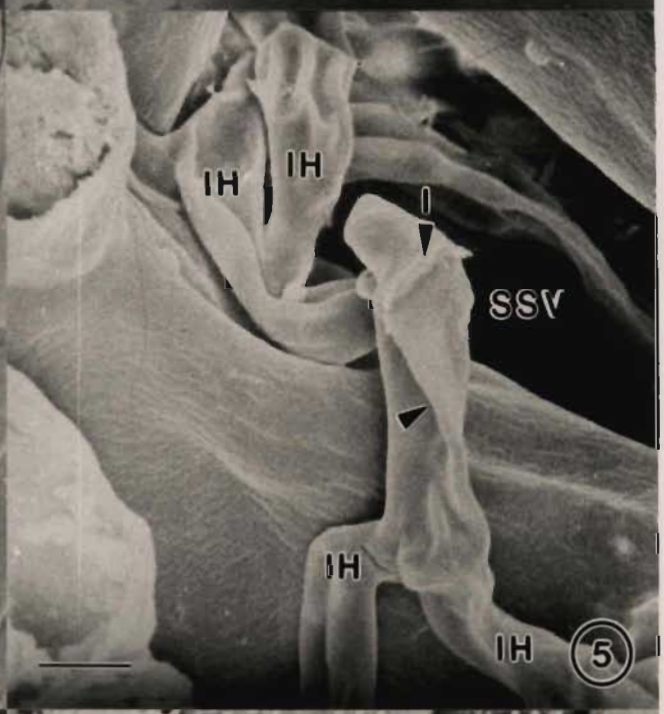
IH
IH
I
SSV
IH
IH
5

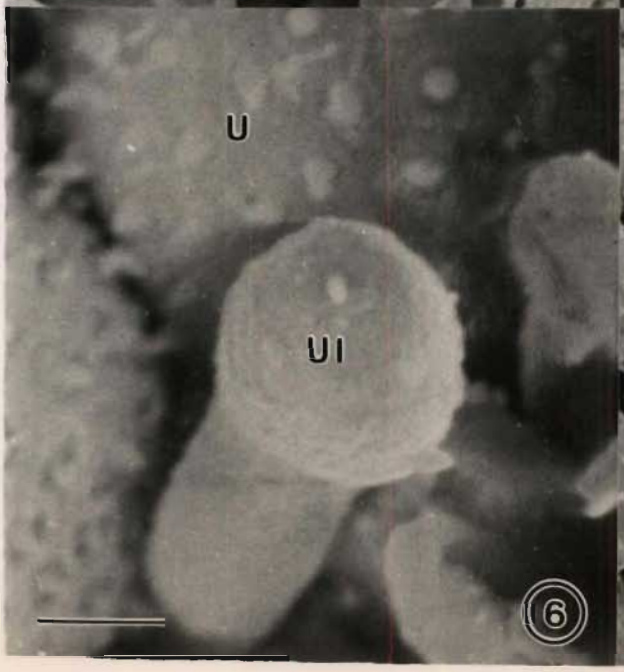
U
UI
6

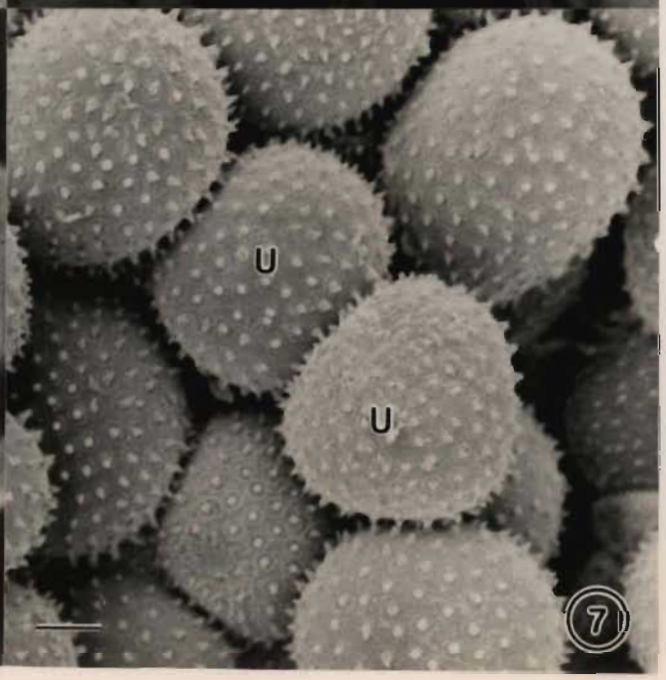
U
U
7

leaves are presented in Figure 1. On the exterior of TOD and TWS leaves there was very little difference in the percentages of germtubes that had formed appressoria. On the inside of the TWS leaf pieces there was a lower percentage of infection structures in various stages of development than on the inside of TOD leaves treated once only (Fig. 1). Very few infection structures were observed inside TWS leaves. Substomatal vesicles either failed to develop (Fig. 2) or developed and aborted prior to the development of the primary hyphae (Fig. 3). SSVs in the final stage of development showed signs of severe structural disorganization (Fig. 4). Similar disorganization was also observed in respect of intercellular hyphae (Fig. 5). Normal (no signs of structural disorganization) SSVs in their final stage were observed inside TOD leaves. The control of rust by weekly applications of bitertanol was manifested in the lack of uredia on the leaves of the TWS plants, whereas on the TOD leaf surfaces, uredia did develop. However, a number of the uredia observed on TOD leaf surfaces contained, underdeveloped urediospore initials (Fig. 6) between closely packed urediospores (Fig. 7), covered by an unruptured epidermis.

Glasshouse trials. A total of 80 mm^2 and 81 mm^2 of leaf surface treated and not treated preventatively with bitertanol, with 5778 and 4572 infection structures (including germtubes), respectively, were examined. The percentages of the various developmental categories of infection structures, 120 h post-inoculation, observed inside tissue treated and not treated with bitertanol are presented in Figure 8. The percentages of cumulative values for infection structures inside treated leaves did show differences when compared with untreated leaves (Fig. 8). There was a higher percentage of SSVs inside the treated leaves than in the not treated leaves, but SSVs with primary or secondary hyphae were virtually absent (Fig. 8). Such SSVs had aborted and showed signs of collapse (Fig. 9). Rarely did collapsed SSVs with primary hyphae (Fig. 10) or with secondary hyphae (Fig. 11) occur in the treated tissue. Normal SSVs with subtended intercellular hyphae which were often excessively branched and determinate (Fig. 12) were observed. In the treated tissue a percentage of SSVs in their final development stage either appeared normal or exhibited certain anomalies. Final stage SSVs and their intercellular hyphae clustered

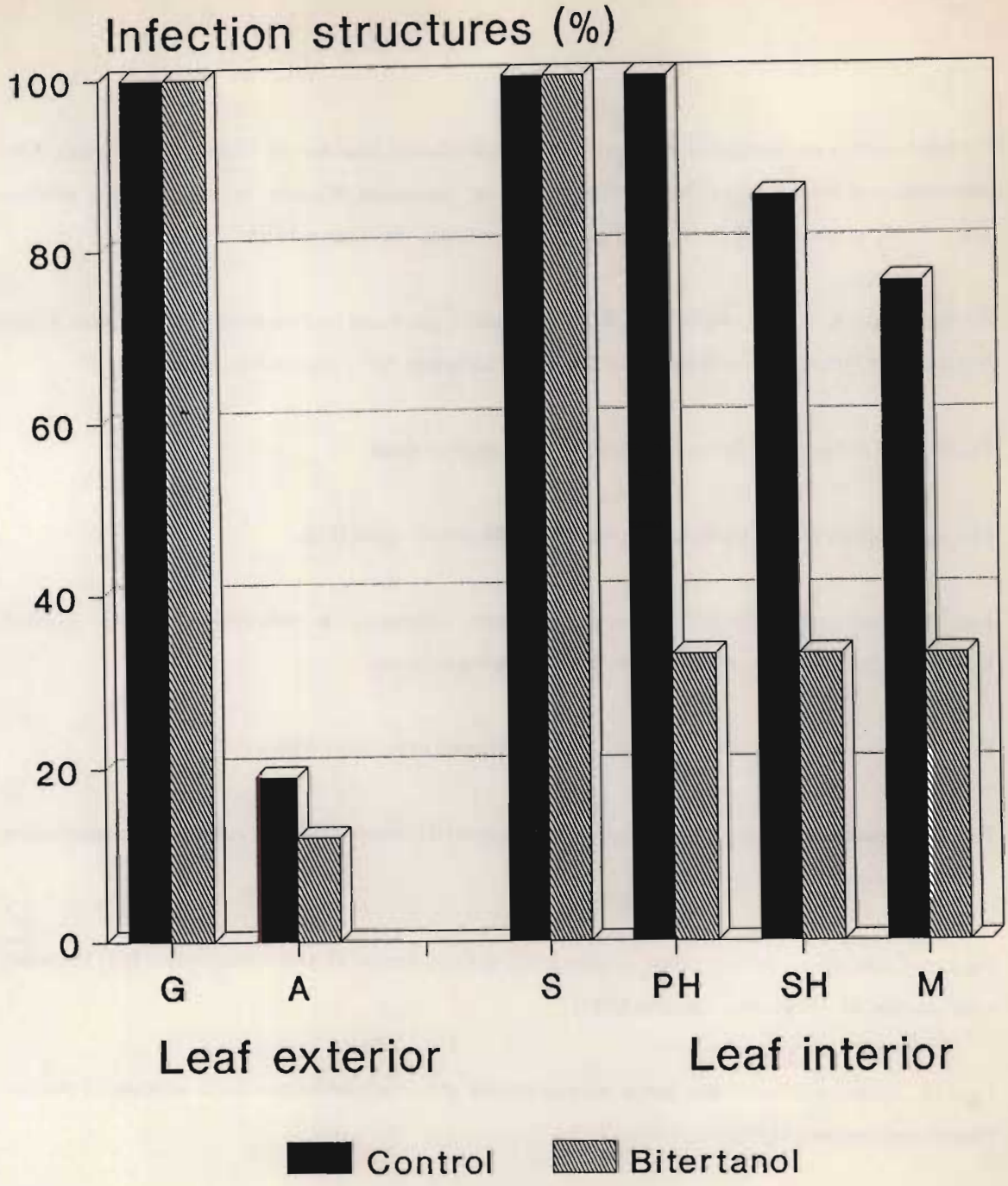

Fig. 8. A histogram of the development of infection structures of *Uromyces transversalis* interrupted at 120 h post-inoculation on and in leaves of cv. Goldfield treated with bitertanol or that remained untreated 48 h prior to inoculation under glasshouse conditions examined by scanning electron microscopy. The results are divided into infection structures on the exterior of the leaf and the intercellular infection structures in the leaf interior. On the leaf exterior the germinated urediospores that did form appressoria (A) are expressed as a percentage of all the germinated urediospores (G). The developmental stages of infection structures in the leaf interior of the treated or not treated leaves are expressed as a percentage of all infection sites within the treated and not treated leaves respectively.

Scanning electron micrographs of developed and aborted infection structures of *Uromyces transversalis*, 120 h post-inoculation inside the gladiolus cv. Goldfield leaves, pre-treated 48 h prior to inoculation with bitertanol (Figs. 9 - 15) or untreated (Fig. 16) under glasshouse conditions. Scale bar = 10 µm.

Abbreviations: I, interconnective tube; IH, intercellular hypha where no distinction is made between primary and secondary hyphae; PH, primary hypha; SH, secondary hypha; SSV, substomatal vesicle.

Fig. 9. Collapsed (arrow) substomatal vesicle (SSV) on inside of stoma.

Fig. 10. Collapsed (arrow) substomatal vesicle (SSV) with primary hypha (PH).

Fig. 11. Substomatal vesicle (SSV) showing some signs of collapse (arrow) with primary (PH) and secondary hyphae (SH), that remained attached to the epidermis during stripping.

Fig. 12. Substomatal vesicle (SSV) with apparently determinate intercellular hyphae (IH).

Fig. 13. Substomatal vesicle (SSV) with intercellular hyphae (IH) bunched together inside substomatal chamber. Note interconnective tube (I).

Fig. 14. Collapsed substomatal vesicle showing partial collapse (arrow) of intercellular hyphae (IH) inside substomatal chamber . Note interconnective tube (I).

Fig. 15. Substomatal vesicle and partial collapse (arrow) of intercellular hypha (IH) in substomatal chamber. Note interconnective tube (I).

Fig. 16. Normally developed substomatal vesicle with interconnective tube (I) and intercellular hyphae (IH) inside substomatal chamber of host.

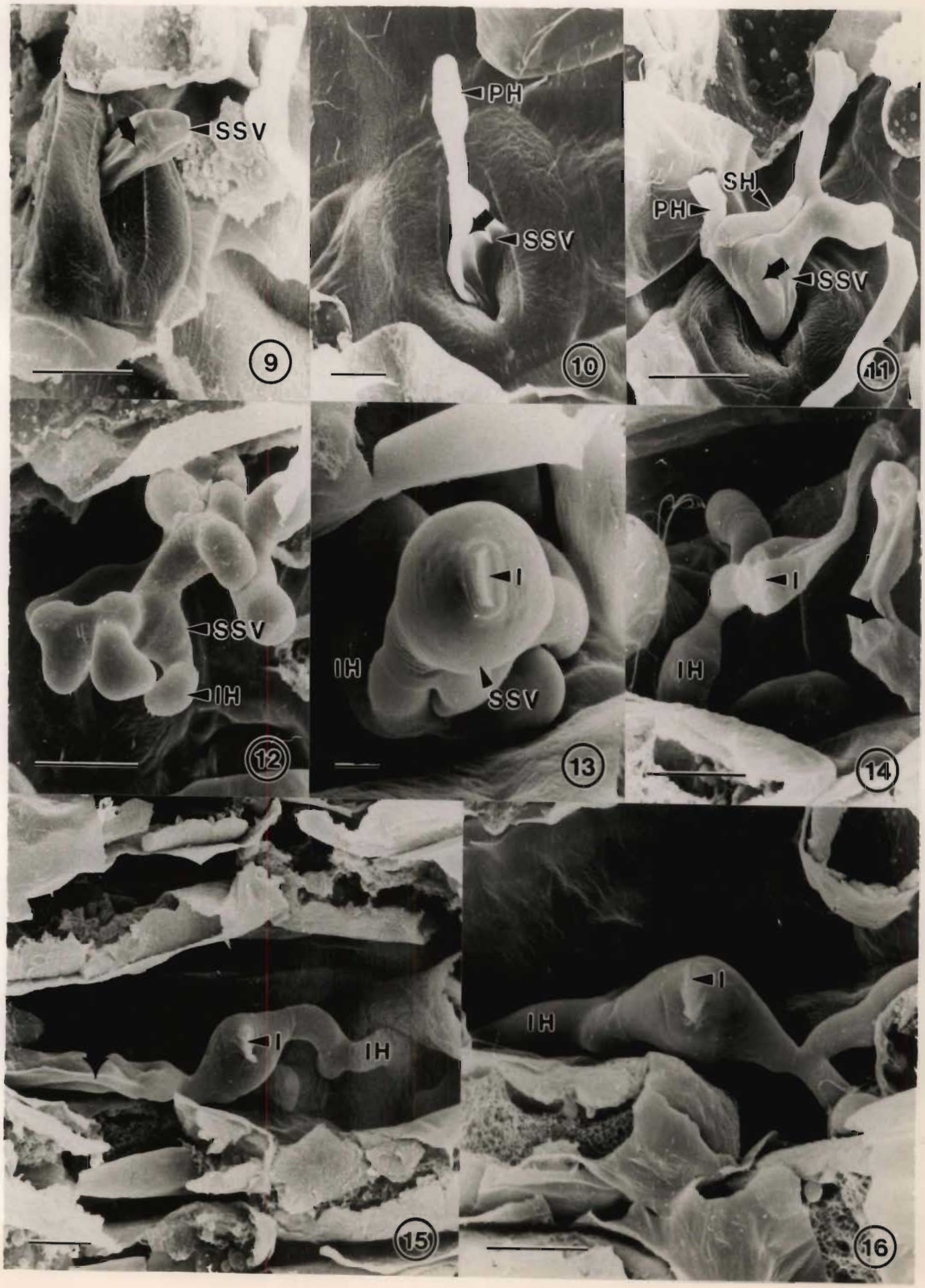
SSV
9
PH
SSV
10
SH
PH
SSV
11
SSV
IH
12
I
IH
SSV
13
I
IH
14
I
IH
15
I
IH
16

together inside a substomatal chamber (Fig. 13), although there appeared to be no physical obstruction preventing normal development (Fig. 16 and see Chapter 1) between the mesophyll cells. In other cases, substomatal vesicles appeared to have developed normally, but either an intercellular hypha and an SSV had collapsed (Fig. 14) or, for instance, a primary hypha had collapsed while the SSV appeared unaffected (Fig. 15). The normal SSV in its final stage together with its primary and secondary hyphae in the untreated tissue showed no sign of collapse or abortion (Fig. 16).

DISCUSSION

Since the percentages of germtubes of urediospores that had located stomata and formed appressoria were approximately similar for TOD and TWS leaves, the fungicidal activity of bitertanol does not appear to express itself on the leaf surface (Pring and Richmond 1976, Siegel 1981, Zobrist *et al.* 1982). The urediospores that had germinated, but had not located stomata, had been subjected to weekly applications of bitertanol which contains, because of the thick waxy cuticle, a leaf wetter. This spray mix could have washed the germinated urediospores from the leaves, especially since the gladiolus leaves have an upright posture. Some of the uredia of *U. transversalis* that had developed on gladiolus leaves which had been treated with bitertanol once before the onset of the disease in the field trials, contained tightly packed urediospores, similar to the observation by Zobrist *et al.* (1982). They found that uredia of *P. coronata* on oats, after treatment with 40% of the recommended dosage of fenpropimorph, contained tightly packed urediospores.

Between gladiolus leaves treated preventatively in the glasshouse with bitertanol and those of the not treated plants there was not much difference in the percentages of germtubes that successfully located stomata and formed appressoria. This is in accordance with the general lack of effect of triazoles on the exterior of leaves as indicated in the review by Siegel (1981), and with results obtained in studies on the effect of oxycarboxin on *U. phaseoli* in beans (Pring and Richmond 1976), and fenpropimorph on *P. coronata*

(Zobrist *et al.* 1982) on oats. Zobrist *et al.* (1982) concluded that, since there were no differences in germtube behaviour on the leaf, and because no symptoms such as yellow or necrotic spots were visible after inoculation, the inhibition of the infection structures of *P. coronata* occurred inside the leaves soon after penetration.

The present study investigated the inhibition of the development of the infection structures of *U. transversalis* after penetration by the pathogen into gladiolus leaves in glasshouse trials. A preventative treatment of gladiolus with bitertanol manifested itself in the inhibition of non-differentiated SSV development. The protective effect of oxycarboxin applied to bean leaves to control *U. phaseoli* resembled a frequently occurring form of resistance, since germination and appressorium development appeared normal (Pring and Richmond 1976). The infection of *U. phaseoli* rarely proceeded beyond infection hypha formation. In the present study the percentage of SSVs in their final stage in the treated tissue was half of that in the untreated leaf tissue. This result is misleading since some of these SSVs in the treated tissue were on one leaf piece; these appeared normal and probably escaped the fungicidal action of bitertanol. The other SSVs observed in the treated tissue either showed signs of partial collapse or abnormal development. This indicated that, although the final stage substomatal vesicles developed in the absence of bitertanol, one of the primary or one or more of the secondary hyphae came into contact with bitertanol during infection. Collapse then often extended to the SSV. The effect of the fungicide in the glasshouse trials, although applied to run-off, was not as uniform as expected, especially since a group of final stage substomatal vesicles were found in the treated gladiolus tissue that had been totally unaffected by the action of bitertanol. This, together with partial collapse, can possibly be explained on the basis of observations by Brandes *et al.* (1979). They found that the properties of bitertanol suggest that the active ingredient penetrates the plant tissue, but, unlike fully systemic fungicides, is not distributed in amounts of practical significance to untreated plant parts. This could possibly explain the results reported in Chapter 5, where triadimefon, a systemic triazole, consistently outperformed bitertanol, although the difference in performance was not statistically significant. The partial collapse

of final stage SSVs was not observed in leaf tissue from the field trials treated weekly for six weeks, since the fungicide was applied sufficiently for fungicide levels in plant tissue to be fairly uniform.

Siegel (1981) reported that triazoles cause excessive hyphal branching of fungi. In the present study normally developed SSVs were occasionally seen to be associated with excessively branched intercellular hyphae of determinate growth. Pring (1984) reported that triadimefon initially affects the intercellular hyphae of rust fungi infecting the leaves of wheat and broad bean. The action of bitertanol is similar to that of triadimefon (Kraus 1979) and it was therefore reasonable to expect an abnormality of this type.

LITERATURE CITED

BRANDES, W., H. KASPERS and W. KRAMER. 1979. Baycor, a new foliar applied fungicide of the biphenyloxy triazolyl methane group. Pflanzenschutz- Nachrichten (Bayer) 32:1-16.

KRAUS, P. 1979. Studies on the mechanism of action of Baycor. Pflanzenschutz-Nachrichten (Bayer) 32:17-30.

PRING, R. J. 1984. Effects of triadimefon on the ultrastructure of rust fungi infecting leaves of wheat and broad bean (*Vicia faba*). Pestic. Biochem. Physiol. 21:127-137.

PRING, R. J., and D. V. RICHMOND. 1976. An ultrastructural study of the effect of oxycarboxin on *Uromyces phaseoli* infecting leaves of *Phaseolus vulgaris*. Phys. Plant Pathol. 8:155-162.

SIEGEL, M. R. 1981. Sterol-inhibiting fungicides: Effects on sterol biosynthesis and sites of action. Plant Disease 65:986-989.

SIMONS, M. D. 1975. Effects of two systemic fungicides on ultrastructure of haustoria of the oat crown rust fungus. Phytopathology 65:388-392.

WHIPPS, J. M., H. W. RODERICK, B. C. CLIFFORD, and D. H. LEWIS. 1987. Effects of two carboxylic acid anilide fungicides on pustule development and carbohydrate movement and metabolism in barley leaves infected by brown rust (*Puccinia hordei* Otth.). J. Phytopathology 120:216-234.

ZOBRIST, P., V. E. COLOMBO, and K. BOHNEN. 1982. Action of fenpropimorph on exterior structures of *Puccinia coronata* on oat as revealed by electron microscopy. Phytopath. Z. 105:11-19.

APPENDIX I

General Information Regarding the Propagation of Gladiolus and the Artificial Infection with *Uromyces transversalis*

PROPAGATION OF GLADIOLUS

Gladiolus species and varieties can be categorized into two major groups, those that grow and flower in winter and those that grow and flower in summer. Since experiments were conducted year round, it was sometimes necessary to induce the winter flowering types to grow in summer and summer flowering types to grow in winter. This was done by treating the corms of summer types for two months at 4°C and those of winter types at 30°C for two months. Plants grown from treated corms developed normally and completed their life cycle without noticeable adverse effects.

Field plantings. The field preparation and planting of corms is described in Chapter 5.

Glasshouse propagation. Three gladiolus corms per 15 cm earthenware pot were planted 2 cm deep. After planting, the soil in the pots was treated with 1 g Disyston® 5G per pot for protection against thrips, and watered immediately afterwards. The pots were placed in a glasshouse in which the temperatures ranged from 15°C to 35°C. Fourteen to 18 d after planting the first leaves emerged. However, this period could be as short as 10 d if both day and night temperatures remained above 30°C. The pots were watered twice daily. Six weeks after planting the plants were ready for inoculation, each having formed five to six fully extended leaves. Plants flowered between nine and twelve weeks after planting, and corms were ready for harvest after eighteen weeks. In addition to the new corm which developed above the originally planted corm, up to 10 cormels developed around the new corm.

ARTIFICIAL INOCULATION WITH GLADIOLUS RUST

Isolates of *Uromyces transversalis*. Isolates of *U. transversalis* were collected from naturally infected commercial gladiolus plantings or field-gathered material from the following localities:

1. Rolf's Flowers, Bapsfontein, Transvaal.
2. Cedara Agricultural College, Cedara, Natal.
3. Mr Blignaut, Piet Retief, Transvaal.
4. Mrs Allan, Elandskop, Natal.

The multi-spore isolate collected at Cedara was used in experiments reported in Chapter 3 and a single-spore isolate obtained from it was used in experiments reported in Chapters 1, 2, 4 and 6. A leaf specimen with sporulating uredia from Cedara was deposited with the National Collection of Fungi, Plant Protection Research Institute, Pretoria (PREM 47693). A micro cyclone spore collector (Manufactured by E. R. I. - Shop, Iowa State University, 124 ERI Building, Ames, Iowa 50011) which collects urediospores in either a No. 00 gelatin capsule or 18 mm test tube was used.

Methods used in artificial infection.

Types of inoculation.

1. The bright orange urediospores were mixed with French chalk until a pink admixture is obtained. This mixture was dusted on, or applied to, the distal third of the leaf with a stiff camel hair brush.
2. Urediospores were applied with a stiff camel hair brush directly onto the leaf surface without an adjuvant.

3. The urediospores were suspended in a 0.1% solution in distilled water of either Biofilm® (Plaaskem), or Triton X100®, or Triton B1956®, or Tween 20®, or they were suspended in Soltrol 170® light mineral oil. The suspension medium was subsequently standardized at 0.1% Triton B1956 in distilled water.

4. A sporulating gladiolus leaf was gently tapped above a horizontally placed leaf.

Inoculating device. The inoculating device employed was essentially that described by Andres and Wilcoxson (1984). Their original design was modified by Rijkenberg (pers. comm.). Further modifications to the inoculating device were made by the author and it was manufactured by the Precision Workshop, University of Natal, Pietermaritzburg.

Dew chamber. A dew chamber was constructed to maintain the air temperature at 18°C and the relative humidity at 100%. A tubular frame was covered with galvanized sheet metal and a controlled temperature water-bath installed in the base of this chamber. The chamber was mounted on wheels and placed inside a cold room. To obtain 18°C at a 100% relative humidity the air temperature in the cold room was adjusted to 16°C and the water in the bath to 39°C. After inoculation, the plants were kept in the dew chamber for 16 h.

Disease development. Susceptible cultivars of gladiolus exhibited seedling plant resistance. Therefore, gladiolus plants in the five- or six-leaf stage had to be used in infection studies. Twelve to fifteen days after inoculation, transverse uredia appeared on the gladiolus leaves. Uredia ruptured within two days after appearance and continued to produce urediospores for up to 21 d after inoculation.

Visually detectable teliospores formed at the periphery of the uredia 5 to 7 weeks post-inoculation on susceptible cultivars. No teliospores formed on susceptible gladiolus cultivars at high inoculum densities, because the leaf tissue died, killing the rust prior to

teliospore formation. Teliospore formation was also observed 21 d post-inoculation on leaves of the rust-resistant species, *G. daleni* (infection type ; - fleck), when leaves had been subjected to high inoculum densities.

LITERATURE CITED

ANDRES, M. W., and R. D. WILCOXSON. 1984. A device for uniform distribution of liquid-suspended urediospores on seedling and adult cereal plants. Phytopathology 74: 550-552.

APPENDIX II

Brief Report on Preliminary Trials Conducted to Investigate the Effect of Free Water Period and Light on the Infection of Gladiolus with *Uromyces transversalis*

INTRODUCTION

Since the gladiolus rust regularly occurs in the mist belt areas of South Africa, and in other areas under extremely wet conditions, leaf wetness appears to be of singular importance to the infection of gladiolus by *Uromyces transversalis* (Thüm) Winter. All efforts to establish infection failed, unless free water was present.

The effects that day and night, the length of the leaf wetness period, and temperatures of 18°C and 20°C have on the of *Uromyces transversalis* infection of gladiolus were investigated. The results were a prerequisite for conducting experiments on the ultrastructure of early infection, urediosporogenesis, chemical control and resistance, and the evaluation of gladiolus germplasm to *U. transversalis*.

MATERIALS AND METHODS

The trials were conducted, before a dew chamber became available, in two walk-in Conviron® growth chambers with a 12 h day/night cycle either programmed for 18°C or 20°C. Six-week-old gladiolus cv. Goldfield plants were inoculated with a De Vilbiss® atomizer, containing 0.5 mg urediospores per 100 ml 0.1% Triton B1956® water suspension, and the entire plant, including the 15 cm clay pot, was then covered with a plastic bag and incubated. The bags were removed at hourly intervals from 1 h until 13 h post-inoculation, and after a further 12 h at 24 h post-inoculation. This procedure was repeated twice. The treatments were as follows: 18 °C (dark), 20°C (light) and 20°C (dark). The infection frequency was determined by the number of pustules 15 d after inoculation. A grid with four adjacent 1 cm^2 squares was used for these evaluations. The results were expressed as number of pustules per cm^2, and a total of 28 cm^2 per plant and three plants per variable were evaluated.

RESULTS

The inoculated plants had to be covered with a plastic bag for at least six hours to induce infection. The shortest period for a optimum infection was 9 h (Fig. 1). There was also a marked difference between uredia per cm^2 of plants subjected to 18°C compared to those at 20°C, a higher rate of infection occurring at 18°C. Exposure to light during the free water period (Fig. 1) had a negative effect on pustule development.

DISCUSSION

This study showed that optimum infection of gladiolus by *U. transversalis* occurred after 9 h at 18°C in the dark.

In previous trials conducted in the glasshouse a gradual decline in the infection frequency of maintainance cultures during successive generations of the rust was observed. The reason for the decline of infection frequency when using plastic bags was never established. The use of a dew chamber (Appendix I) resulted in no decline of infection frequency and actively sporulating rust cultures have been maintained in this manner for two years. A possible difference between plastic bags and the dew chamber may be that the temperature increased inside the plastic bags due to radiation trapped inside. According to our present study, a change of 2°C affects the infection frequency of *U. transversalis*. The plastic bags could have raised the temperature in the bag and adversely affected the infectivity of the rust urediospores in successive generations until it was too low in the sixth generation to establish any infection.

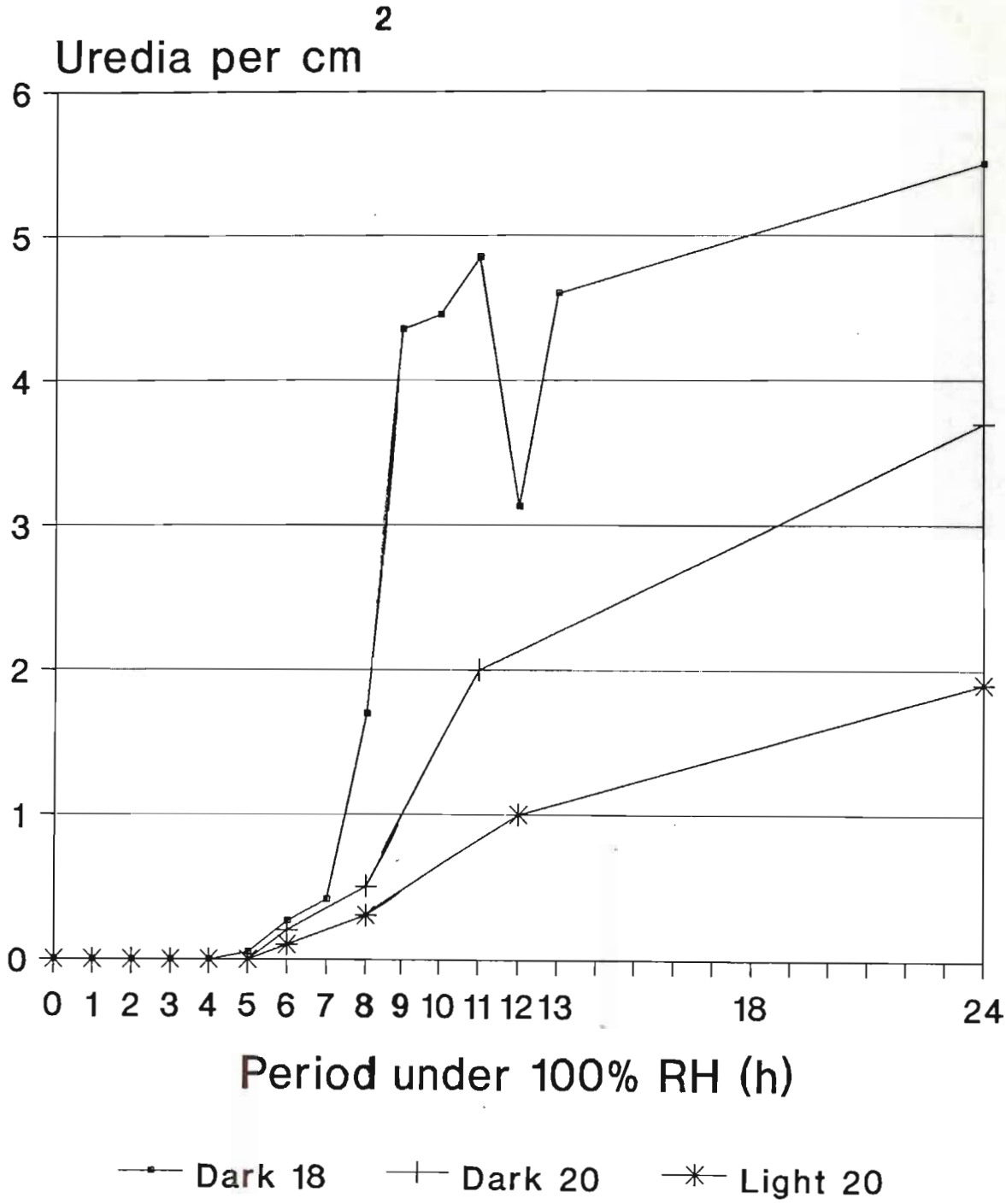

Fig. 1. A line graph of the effects of 18°C (dark) and 20°C (light) and 20°C (dark) in the presence of free water on the infection of gladiolus leaves by *Uromyces transversalis*.